

*Treating Waste with Waste – Calcined Bauxite Residue (CBR) as a Potential Wastewater Treatment Option for Oil Sands Process-affected Water (OSPW) and Municipal Wastewater*

by

Fei Cheng

A thesis submitted in partial fulfillment of the requirements for the degree of

Master of Science

in

Environmental Engineering

Department of Civil and Environmental Engineering  
University of Alberta

© Fei Cheng, 2023

## Abstract

Bauxite residue is a byproduct generated during the extraction of alumina from bauxite ore. It is highly alkaline and has the potential to release toxic substances (metals) into the surrounding environment during storage. Hence, there is a growing interest in exploring the potential for metal recovery and/or repurposing of bauxite residue to reduce the substantial accumulation of tailings, subsequently contributing to more sustainable waste management practices. This study examined the efficacy of calcined bauxite residue (CBR) as a sorbent material during wastewater treatment. Four types of wastewaters were examined, but this thesis ultimately focused on oil sands process-affected water (OSPW) and municipal wastewater treatment plant (WWTP) effluents. The applicability of CBR in the treatment of industrial wastewater polluted with organic dye (e.g., textile wastewater) and natural waters that receive treated effluents was also evaluated. The treatment performance of CBR was evaluated using a combination of analyses including **(1)** physical via characterization of CBR via imaging, elemental and crystallographic composition, and surface area/pore size distribution ; **(2)** chemical via measurement of specific pollutant removal including methylene blue, acid-extractable organics (AEOs), metals, and other general water quality parameters; **(3)** biological via evaluation of toxicity (cytotoxicity, estrogenicity, and mutagenicity) via *in vitro* bioassays and measurement of total coliform bacteria. Post-treatment neutralization with acetic acid was further implemented as the pH and the concentration of dissolved metals in water, especially aluminum (Al), increased significantly after CBR treatment. For oil sands process-affected water (OSPW), CBR effectively removed AEOs, a surrogate measurement for naphthenic acids, with an equilibrium adsorption capacity of 0.244 mg/g (pseudo-second-order adsorption kinetic model,  $R^2=0.99$ ). After applying post-treatment neutralization, the CBR-treated OSPW showed lower

estrogenicity (EC<sub>10</sub> reduced from 0.14 REF to 1.0–56.5 REF) and mutagenicity (EC<sub>IR1.5</sub> reduced from 6.7 REF to >12.5 REF) but exhibited higher cytotoxicity (IC<sub>10</sub><sub>15min</sub> increased from 0.52 REF to 0.15-0.28 REF) compared to the raw OSPW. The application of CBR for OSPW treatment was deemed effective but can be further optimized given the acceptable removals of AEOs (45%), estrogenicity, and mutagenicity achieved at 100 g/L CBR dosage. CBR treatment coupled with post-treatment neutralization considerably reduced cytotoxicity, estrogenicity, mutagenicity, coliforms, and nutrients from primary (post-biological nutrient removal [BNR]), secondary (post-secondary clarifier), and tertiary (post-UV) effluents from an operational WWTP. Furthermore, it was shown that the treatment of primary effluent with 50 g/L CBR resulted in a smaller amount of Al leached (1.5 mg/L) from CBR but still maintained good removals in comparison to 100g/L (3.2 mg/L Al was released). Although the need for further optimization of the treatment process is apparent, overall, the results showed that CBR was effective for the treatment of municipal WWTP effluents. CBR was also found to be effective for the removal of methylene blue with an equilibrium adsorption capacity ranging from 0.39 to 1.11 mg/g (pseudo-second-order adsorption kinetic model,  $R^2 = 0.98 - 1.00$ ). Finally, the application of CBR for the improvement of natural river bodies with sewage pollution was examined using diluted municipal WWTP tertiary effluent (5% tertiary effluent + 95% river water) (without post-treatment neutralization). In this case, the use of CBR was considered less attractive because it did not result in substantial removal of cytotoxicity, estrogenicity, mutagenicity, dissolved organic carbon, metals, and nutrients. Though post-treatment neutralization might be able to mitigate the toxicity and metal leaching from CBR, considering the insufficient removals of pollutants observed, the cost associated with implementing CBR will likely surpass the advantages of treating polluted water bodies at the current stage.

## **Preface**

This thesis is an original work by Fei Cheng under the supervision of Dr. Maricor Arlos. Experiments related to the treatment of municipal wastewater treatment plant effluents were run together with Jingya Pang. No part of this thesis has been previously published.

## Acknowledgments

This work would not have been accomplished without the support of many people. Words cannot express my gratitude to my supervisor Dr. Maricor Arlos for her continuous encouragement, guidance, professionalism, enthusiasm, patience, and kindness throughout my master's study. Besides helping with my personal learning and growth as a master's student, throughout this project, Dr. Maricor Arlos has dedicated her time and provided countless insightful and constructive ideas and feedback that always enlightened the next step of my experiment and guided me to think outside of the box. Secondly, I would like to thank Jingya Pang and Demi Meier for their company and help in running some of the experiments and with the ongoing *Daphnia* testing. For the ongoing *Daphnia* testing, we gratefully acknowledge the contribution of Aaron Boyd and Dr. Tamzin Blewett for their expertise and help with running the assay. I would like to acknowledge also: (1) Scott Berggren and his team for their feedback and advice on the progress of this work from an industrial and technical point of view, (2) Kia Barrow for the training and help on the *in vitro* bioassays, (3) Amy-lynn Balaberda, Petr Kuznetsov, and Dr. Ania Ulrich for the training and help on FTIR analysis, (4) the nanoFAB fabrication and characterization facility for the training and help on material characterization tools and for running the elemental and crystallographic composition analysis, (5) David Yupeng Zhao for the guidance for total coliform analysis and the help with using the equipment and tools shared by the department, (6) Pamela Chelme-Ayala, Lingling Yang, and Dr. Gamal El Din for providing the oil sands processed-affected water sample, (7) Arlos Research Lab member (Daniela Pulgarin-Zapata, Demi Meier, Jingya Pang, Jaime Hicks) for collecting the municipal wastewater samples; (8) Mitacs and GRÖN Holding Corporation for funding this project. Lastly, gratitude to my family and friends who indirectly assisted me with this work.

## Table of Contents

1. Introduction.....	1
1.1. Background .....	1
1.2. Potential Uses of Bauxite Residue .....	2
1.3. Bauxite Residue Adsorbent in Wastewater Treatment .....	5
1.3.1. Pre-treatment Methods for Bauxite Residue Adsorbent .....	9
1.4. Management loop for bauxite residue.....	11
1.5. Current Technologies for Oil Sands Process-Affected Water (OSPW) Treatment .....	14
1.6. Current Technologies for Municipal WWTP Effluent Treatment .....	16
1.7. Research Aim and Objectives .....	18
1.8. Research Hypotheses.....	19
1.9. Study Scope.....	21
2. Methodology.....	24
2.1. Overall Experiment Design.....	24
2.2. Brief Overview of Analytical Methods.....	25
2.3. Materials.....	26
2.4. Material Characterization.....	27
2.5. Water Treatment Experiments .....	29
2.5.1. Synthetic Wastewater – Methylene Blue.....	29
2.5.2. Synthetic Wastewater – Commercial Naphthenic Acids .....	31
2.5.3. Real Wastewater – Oil Sands Process-affected Water (OSPW).....	32
2.5.4. Real Wastewater – Municipal WWTP Tertiary Effluent.....	33
2.5.5. Real Wastewater – Municipal WWTP Primary, Secondary, and Tertiary Effluents (Further Evaluation and Optimization).....	34
2.5.6. Diluted Wastewater - Tertiary Effluent Diluted with River Water.....	35
2.6. Solid Phase Extraction (SPE).....	35
2.7. Chemical Analyses.....	37
2.7.1. Absorbance Measurement for Methylene Blue (MB) .....	37
2.7.2. Fourier transform infrared spectroscopy (FTIR) .....	37
2.8. Biological Analyses.....	38
2.8.1. Overview of Bioanalytical Method Selection.....	38
2.8.2. Cytotoxicity.....	39
2.8.3. Estrogenicity .....	39

2.8.4.	Mutagenicity .....	42
2.8.5.	Membrane Filtration Technique for Total Coliform.....	45
2.9.	Neutralization with Acetic Acid and Leaching Analysis .....	46
3.	Results and Discussions .....	50
3.1.	Material Characterization.....	50
3.2.	Removal of Methylene Blue (MB).....	56
3.3.	Removal of Commercial Naphthenic Acids (NAs).....	62
3.4.	Neutralization with Acetic Acid for the Control of Leaching from CBR.....	63
3.4.1.	Treatment of OSPW and Diluted Municipal Effluent Without Neutralization .....	63
3.4.2.	Comparison with the Leaching from Raw Bauxite Residue in Ultrapure Water ...	69
3.4.3.	Comparison Between Pre-treatment and Post-treatment Neutralization .....	72
3.5.	Treatment of OSPW .....	73
3.5.1.	Removal of AEOs and Toxicities on Cells After Post-Treatment Neutralization ..	73
3.5.2.	Adsorption kinetics and isotherm for AEOs.....	75
3.6.	Treatment of Municipal WWTP Wastewaters .....	80
3.6.1.	Removal and Effect of Post-treatment Neutralization on Tertiary Effluent .....	80
3.6.2.	Treatment Performance in Primary, Secondary, and Tertiary Effluents .....	83
4.	Study Limitations.....	93
5.	Conclusions and Recommendations .....	95
	References.....	100
	Appendix A. Supplementary Material to Methodology .....	111
Appendix A.1	Spectrum Scan and Calibration Curves for Methylene Blue (MB) .....	111
Appendix A.2	Calibration Curves for Sigma NAs and Cyclohexanecarboxylic Acids .....	112
Appendix A.3	YES Assay Stock Solution Preparation .....	113
	Appendix B. Supplementary Material to Results and Discussions.....	115
Appendix B.1.	SEM Images of Higher Magnifications and Raw EDX Data.....	115
Appendix B.2.	Experiment Designed to Improve the Recovery of AEOs .....	119
Appendix B.3.	More Chemical Analyses Results on Leaching/Removal of Pollutants.....	122
Appendix B.4.	CCME Guidelines and AEP Discharge Compliance for Different Samples..	131
Appendix B.5	Visual Quality of the Treatment o Tertiary Effluent by CBR.....	137

## List of Tables

<b>Table 1.</b> Outcomes of the hypotheses examined in this study .....	20
<b>Table 2.</b> Summary of analytical tools.....	25
<b>Table 3.</b> Data analysis methods adapted from Barrow et al. [85] .....	44
<b>Table 4.</b> Energy-dispersive X-ray spectroscopy (EDX) results for calcined bauxite residue (CBR) and raw bauxite residue.....	52
<b>Table 5.</b> BET surface area and total pore volume of some raw and treated bauxite residue from some literature that focused on the application of bauxite residue in water treatment ...	54
<b>Table 6.</b> Adsorption kinetic parameters obtained for the removal of methylene blue (MB) ..	58
<b>Table 7.</b> Pseudo-second-order kinetic parameters for the adsorption of methylene blue by bauxite residue adsorbents in literature.....	58
<b>Table 8.</b> Langmuir and Freundlich adsorption isotherm parameters for methylene blue (MB) removal found in literature and obtained from this study.....	61
<b>Table 9.</b> The removal of Sigma NAs and cyclohexanecarboxylic acid by 20 g/L CBR.....	62
<b>Table 10.</b> Removal of acid-extractable organics (AEOs), cytotoxicity, estrogenicity, and mutagenicity when CBR was applied on oil sands process-affected water (OSPW) and diluted municipal wastewater treatment plant tertiary effluent (5% effluent from Plant A + 95% river water) by different dosages of CBR (no neutralization) .....	65
<b>Table 11.</b> Measured water quality parameters of OSPW and diluted effluent from municipal wastewater treatment facility (5% tertiary effluent from Plant A + 95% river water) before and after the treatment with 50 g/L of CBR (without neutralization) .....	68
<b>Table 12.</b> The release of contaminants in ultrapure water by: (1) 50 g/L CBR (2) 50 g/L raw bauxite residue (3) 50 g/L CBR and pre-treatment neutralization with acetic acid (4) 50 g/L CBR and post-treatment neutralization with acetic acid .....	71
<b>Table 13.</b> The removal of AEOs from OSPW by other studies and this work .....	77
<b>Table 14.</b> The adsorption isotherm parameters for the removal of AEOs from OSPW in literature .....	79
<b>Table 15.</b> A summary of water quality parameters of untreated, 50 g/L CBR-treated, and 100 g/L CBR-treated primary effluent (after biological nutrient removal), secondary effluent (after secondary clarification), and tertiary effluent (after UV disinfection) from Plant B.....	84
<b>Table 16.</b> The concentrations of dissolved metals in municipal WWTP (Plant B) primary (after biological nutrient removal), secondary (after secondary clarifier), and tertiary (after UV disinfection) effluents after treatment with 50 g/L CBR and post-treatment neutralization with acetic acid .....	91



<b>Table 17.</b> The concentrations of dissolved metals in municipal WWTP (Plant B) primary (after biological nutrient removal), secondary (after secondary clarifier), and tertiary (after UV disinfection) effluents after treatment with 100 g/L CBR and post-treatment neutralization with acetic acid .....	92
<b>Table A.3.1.</b> Reagents for gold solution preparation adapted from Barrow et al. [85].....	113
<b>Table A.3.2.</b> Other stock solutions preparation for YES following Barrow et al. [85] .....	114
<b>Table B.1.1.</b> Unaveraged energy-dispersive X-ray spectroscopy (EDX) results and the locations on CBR particles selected for analysis .....	117
<b>Table B.1.2.</b> Energy-dispersive X-ray spectroscopy (EDX) results and the locations on raw bauxite residue particles selected for analysis .....	118
<b>Table B.2.1.</b> Recovery efficiencies of acid-extractable organics (AEOs) obtained using Oasis HLB and ENV+/C8 cartridges. OSPW = oil sands process-affected water .....	119
<b>Table B.2.2.</b> Recovery efficiencies of acid-extractable organics (AEOs) using dichloromethane for elution and directly analyzing the eluent with Fourier transform infrared spectroscopy (FTIR).....	120
<b>Table B.3.1.</b> The effect of treatment with 50 g/L CBR on nitrogen parameters in OSPW and diluted municipal WWTP (Plant A) tertiary effluent (no neutralization).....	122
<b>Table B.3.2.</b> The release of total metals and nutrients in ultrapure water by: (1) 50 g/L CBR (2) 50 g/L raw bauxite residue (3) 50 g/L CBR and pre-treatment neutralization with acetic acid (4) 50 g/L CBR and post-treatment neutralization with acetic acid .....	123
<b>Table B.3.3.</b> The concentrations of dissolved metals in untreated municipal WWTP (Plant B) primary (after biological nutrient removal), secondary (after secondary clarifier), and tertiary (after UV disinfection) effluents .....	124
<b>Table B.3.4.</b> The concentrations of total metals in untreated municipal WWTP (Plant B) primary (after biological nutrient removal [BNR]), secondary (after secondary clarifier), and tertiary (after UV disinfection) effluents.....	125
<b>Table B.3.5.</b> Additional water quality parameters measured in untreated municipal WWTP (Plant B) primary (after biological nutrient removal [BNR]), secondary (after secondary clarifier), and tertiary (after UV disinfection) effluents.....	126
<b>Table B.3.6.</b> The concentrations of total metals in municipal WWTP (Plant B) primary (after biological nutrient removal), secondary (after secondary clarifier), and tertiary (after UV disinfection) effluents after treatment with 50 g/L CBR and post-treatment neutralization with acetic acid .....	127
<b>Table B.3.7.</b> Additional water quality parameters measured in municipal WWTP (Plant B) primary (after biological nutrient removal), secondary (after secondary clarifier), and tertiary (after UV disinfection) effluents after treatment with 50 g/L CBR and post-treatment neutralization with acetic acid .....	128

<b>Table B.3.8.</b> The concentrations of total metals in municipal WWTP (Plant B) primary (after biological nutrient removal), secondary (after secondary clarifier), and tertiary (after UV disinfection) effluents after treatment with 100 g/L CBR and post-treatment neutralization with acetic acid .....	129
<b>Table B.3.9.</b> Additional water quality parameters measured in municipal WWTP (Plant B) primary (after biological nutrient removal), secondary (after secondary clarifier), and tertiary (after UV disinfection) effluents after treatment with 100 g/L CBR and post-treatment neutralization with acetic acid .....	130
<b>Table B.4.1.</b> Long-term and short-term guidelines for the protection of freshwater aquatic life for OSPW and diluted municipal WWTP effluent (5% tertiary effluent + 95% river water) before and after the treatment with 50 g/L of CBR (without neutralization) .....	131
<b>Table B.4.2.</b> Long-term and short-term guidelines for the protection of freshwater aquatic life for four Milli Q ultrapure water samples treated with (1) 50 g/L CBR (2) 50 g/L raw bauxite residue (3) 50 g/L CBR and pre-treatment neutralization with acetic acid (4) 50 g/L CBR and post-treatment neutralization with acetic acid.....	132
<b>Table B.4.3.</b> The requirement for continuous discharge, applicable to tertiary treatment with mechanical processes for a current population > 20,000 by AEP [84].....	133
<b>Table B.4.4.</b> Long-term and short-term guidelines for the protection of freshwater aquatic life for untreated municipal WWTP primary (after biological nutrient removal), secondary (after secondary clarifier), and tertiary (after UV disinfection) effluents.....	134
<b>Table B.4.5.</b> Long-term and short-term guidelines for the protection of freshwater aquatic life for municipal WWTP primary (after biological nutrient removal), secondary (after secondary clarifier), and tertiary (after UV disinfection) effluents after treatment with 50 g/L CBR and post-treatment neutralization with acetic acid .....	135
<b>Table B.4.6.</b> Long-term and short-term guidelines for the protection of freshwater aquatic life for untreated municipal WWTP primary (after biological nutrient removal), secondary (after secondary clarifier), and tertiary (after UV disinfection) effluents after the treatment with 100 g/L CBR and post-treatment neutralization with acetic acid.....	136

## List of Figures

<b>Figure 1.</b> Process chain for bauxite residue management by the industrial partner (GRÖN).	12
<b>Figure 2.</b> Images of raw bauxite residue (left) and calcined bauxite residue (CBR) (right)...	13
<b>Figure 3.</b> The four types of water matrices used in this study and the purpose of each matrix .....	21
<b>Figure 4.</b> The overall experiment flowchart, and analytical and bioanalytical methods employed in this thesis.....	24
<b>Figure 5.</b> The solid phase extraction (SPE) procedure for synthetic and real oil sands process-affected water (OSPW) with volume >50mL.....	36
<b>Figure 6.</b> Neutralization of CBR with acetic acid.....	47
<b>Figure 7.</b> Scanning electron microscope (SEM) images of inorganic and carbonaceous components of calcined bauxite residue (CBR) (a, c) and raw bauxite residue (b,d).....	51
<b>Figure 8.</b> X-ray diffraction (XRD) spectrum of the calcined bauxite residue (CBR).....	52
<b>Figure 9.</b> N <sub>2</sub> adsorption and desorption curve (left) and the corresponding Density Functional Theory (DFT) pore size distribution (right) of CBR. ....	55
<b>Figure 10.</b> Visual quality of MB removal solutions after 45 min treatment with CBR.....	56
<b>Figure 11.</b> The adsorption kinetics for methylene blue (MB) by calcined bauxite residue (CBR) (no neutralization) .....	57
<b>Figure 12.</b> The adsorption isotherms for methylene blue (MB) using different dosages of calcined bauxite residue (CBR) (no neutralization).....	60
<b>Figure 13.</b> Quality of the CBR-treated oil sands process-affected water (OSPW) with post-treatment neutralization and without neutralization .....	74
<b>Figure 14.</b> The adsorption kinetics for acid-extractable organics (AEOs) from oil sands process-affected water (OSPW) by 50 g/L calcined bauxite residue (CBR) (no neutralization) .....	76
<b>Figure 15.</b> The adsorption isotherms for acid-extractable organics (AEOs) from OSPW using different dosages of calcined bauxite residue (CBR) (no neutralization) .....	78
<b>Figure 16.</b> The effect of calcined bauxite residue (CBR) treatment and post-treatment neutralization on municipal WWTP (Plant A) tertiary effluent.....	81
<b>Figure A.1.1.</b> Absorbance pattern for 20 mg/L methylene blue (MB) .....	111

<b>Figure A.1.2.</b> Sample calibration curve for determining MB concentration in water samples.....	111
<b>Figure A.2.1.</b> Sample calibration curve for determining the concentration of Sigma NAs....	112
<b>Figure A.2.2.</b> Sample calibration curve for determining the concentration of cyclohexanecarboxylic acids .....	112
<b>Figure B.1.1.</b> SEM images of CBR at higher magnifications.....	115
<b>Figure B.1.2.</b> SEM images of raw bauxite residue at higher magnifications .....	116
<b>Figure B.2.1.</b> Pictures of the FTIR cell before experiment (left) and after experiment (right) .....	121
<b>Figure B.5.1.</b> From left to right: filtered untreated municipal WWTP tertiary effluent, filtered 20g/L-, 50g/L-, and 100g/L-CBR-treated municipal WWTP tertiary effluent .....	137
<b>Figure B.5.2.</b> From left to right: the SPE extracts of untreated, 20g/L-CBR-treated, 50g/L-CBR-treated, and 100g/L-CBR-treated municipal WWTP effluents .....	137

# **1. Introduction**

## **1.1. Background**

Bauxite residue, or red mud, is a highly basic (pH ranges between ~12 to 13) waste product generated from the Bayer process, a widely used technique for the extraction of alumina from bauxite ore [1], [2]. Typically, bauxite ore is heated and mixed with sodium hydroxide solution in a pressure vessel. As a result of the digestion process, the aluminum component dissolves as sodium aluminate, which is further extracted, while the undissolved solids (bauxite residue) are separated and discharged as waste [3]. Production of one tonne of alumina leads to the generation of 0.4 to 2 tonnes of bauxite residue depending on the ore quality [4]. The current global storage of bauxite residue waste is estimated to be approximately 4.6 billion tonnes with an annual production rate of 150 million tonnes [4]. Similar to other mining and refinery wastes, the current management practice for the bauxite residue produced is stockpiling in constructed tailings [3].

The dried bauxite residue solid is composed primarily of fine-grained mineral oxides including  $\text{Fe}_2\text{O}_3$  (30-60% by weight),  $\text{Al}_2\text{O}_3$  (10-20%),  $\text{SiO}_2$  (3-50%),  $\text{Na}_2\text{O}$  (2-10%),  $\text{CaO}$  (2-8%), and  $\text{TiO}_2$  (up to 2.5%) and trace amounts of other minerals [1], [5]. Given its iron (III) oxide composition, bauxite residue has a characteristic red color, hence the name “red mud”. The primary environmental concern of bauxite residue is mainly from its high alkalinity (i.e., from sodium hydroxide digestion) and its potential of metal leaching into the surrounding environment [6]. In addition, the tailings dam can pose severe geo-stability hazards as a result of inappropriate design and maintenance protocols. In October 2010, the biggest incident of bauxite residue dam failure ever reported (Ajka dam failure in western Hungary) led to the spill of nearly one million  $\text{m}^3$  of bauxite residue sludge which flooded the nearby villages and towns, causing 10 human

lives [6]–[8]. The immediate environmental effects were mainly related to the caustic and saline nature of the slurry, while long-term effects were associated with salinity and the leaching and cycling of hazardous metals in the water-soil system [6]. Considering the massive storage of bauxite residue and the environmental and geological hazards with tailings ponds, it is beneficial to assess alternatives to treating and reusing bauxite residue effectively.

## **1.2. Potential Uses of Bauxite Residue**

A decent amount of research has been conducted to explore the potential uses of bauxite residue including in construction, metallurgy, and environmental remediation fields [4], [9]. The application of bauxite residue as bulk construction material or as additives to building material is one of the most popular and relatively mature technologies for reuse. This option allows large and quick consumption of bauxite residue while acquiring a relatively small cost for preparing and enhancing the physical and chemical properties of bauxite residue for use. For road construction, bauxite residue can be used as a pavement foundation material or can be incorporated into weak subgrade soil to improve its strength for corrosion prevention [10]. For landfill management, bauxite residue can be added as landfill cover to enhance the water-holding capacity of the subsoil [7]. Moreover, bauxite residue can be exploited as a low-permeability and sorptive layer as part of the landfill liner [11], [12]. For building materials, bauxite residue can be used for the synthesis of heat- and fire-retarding geopolymers and for the production of cement as it has compositions similar to Portland cement [9], [13]. According to the International Aluminium Institute, among the 3 million tonnes of bauxite residue being utilized worldwide each year (less than 2% of bauxite residue being produced), cement production is the primary contributor to bauxite residue consumption [4], [14]. The main limitation to reusing bauxite residue in the construction industry is associated with its highly caustic nature – bauxite residue

contains large amounts of soluble alkali and chemical-binding alkali compounds which can lead to a pH increase when exposed to moisture [9]. As the alkalinity content in cement is strictly controlled to prevent the infrastructure from deforming and cracking, the amount of bauxite residue that can be utilized is also restricted [9].

The recovery of valuable metals from bauxite residue has gained popularity over recent years due to the rapid consumption of raw natural ores. Bauxite residue can be a source of iron (Fe), aluminum (Al), titanium (Ti), and rare earth metals such as vanadium (V), scandium (Sc), and gallium (Ga) [14]–[16]. Depending on the Bayer process and the bauxite ore, bauxite residue possesses up to 4–16% of unextracted alumina which can be recovered with additional acid and heat supply [4]. With currently developed metal-separation technologies such as magnetism, smelting, and hydrometallurgy, bauxite residue can be utilized as a source of low-grade Fe due to its abundant Fe content [4]. Although Ti and rare earth metals are not major components of bauxite residues, the recovery of these metals from bauxite residue is also considered a profitable option due to the increasingly high cost, demand, and scarcity of natural ore [16]. As the recovery of Ti and rare earth metals can be enhanced after the removal of base metals such as Fe and Al, the extraction of multiple metals in a process chain is promoted [15], [16]. This chained extraction further allows for better recycling of reagents in the process, thus reducing chemical and waste generation [15]. However, because of the presence of abundant metal oxides, the recovery of metals from bauxite residue needs to be carried out in multiple steps to first separate out the interfering metals – these processes require high energy and chemical input and can contribute to further waste generation [15], [16].

With growing public awareness of environmental protection, the application of bauxite residue in environmental remediation has become quite appealing. Having relatively good

porosity and a specific surface area ranging from about 10 to 30 m<sup>2</sup>/g, bauxite residue can be utilized as an adsorbent to capture contaminants from wastewater and air [1], [17]. Due to its high alkalinity, bauxite residue can also be used for the amendment of acidic tailings and soil as well as for the removal of sulfur from flue gas [17], [18]. Furthermore, the rich metal oxide composition, especially Fe and Ti oxides, allows for the use of bauxite residue as a catalyst for reactions in wastewater treatment (i.e., Fenton process and photocatalysis for the degradation of organic pollutants) as well as in air pollution control (the catalytic reduction of nitrogen oxides and catalytic oxidation of carbon monoxide and volatile organic compounds) [19]–[21]. Bauxite residue can be manufactured into coagulants or flocculants for removing colloidal materials from wastewater due to its polyvalent cations content, mainly Fe and Al.

Although there are several potential uses for bauxite residue, current environmental remediation uses are insufficient to utilize the vast amounts currently stored in tailings ponds. To better manage this waste, it is important to explore options for further processing and optimization for its effective use in wastewater treatment [14]. Given that the bauxite residue on itself contains toxic substances, it is critical that any such use be approached with caution and subject to rigorous research and testing to ensure it is environmentally safe [14]. The subsequent sections describe the potential for bauxite residue as a sorbent material for wastewater treatment and outline ways that have been completed thus far to improve its sorbent capacity.



### **1.3. Bauxite Residue Adsorbent in Wastewater Treatment**

Industrial and municipal wastewater can contain organic contaminants that are present in varying amounts. They can range from sub-ppb to ppt levels (e.g., pharmaceuticals and personal care products present in domestic wastewater) level [22] to ppm (mg/L) such as naphthenic acids [NAs] in oil sands processed affected water in northern Alberta [23]. Depending on the organic contaminants, they can illicit toxic effects on exposed aquatic organisms [24]. Over the years, several treatment technologies have been assessed and evaluated for their efficient removal of organic chemicals [25]. The technologies range from physicochemical treatment approaches to biological treatment, including reverse osmosis, electrodialysis, chemical oxidation, adsorption, and microbial degradation [25]. Among these technologies, microbial degradation can be limited if the organic pollution presents high toxicity, and advanced technologies like chemical oxidation and reverse osmosis are usually associated with higher capital and operating costs [25].

By contrast, adsorption technology is a more economical and flexible approach and is applicable to the removal of a wide range of organic contaminants [24]. More specifically, activated carbon is a common and effective adsorbent used for organics removal due to its excellent microporosity and high specific surface area. Research has shown that the addition of powdered activated carbon to conventional wastewater treatment processes effectively improved the removal of trace organic pollutants such as pharmaceutical compounds [26]. Although activated carbon is well utilized for organic contaminants and taste/odour compound removal for drinking water treatment, large-scale application of commercial activated carbon in wastewater treatment is still scarce [25]. Only in the recent decade that the use of activated carbon in municipal WWTP effluent treatment for trace organics removal has been pioneered in some

European countries (particularly Switzerland and Germany) to meet government mandates in reducing trace organic chemical pollution[27].

Bauxite residue is one of the more cost-effective adsorbents due to its large availability across the globe [25]. More specifically in Canada, the annual production rate of bauxite residue is estimated at ~1.5 million tonnes and the total reserve was ~40 million tonnes, occupying 2.2 km<sup>2</sup> of land resource [28]. Wang et al. [29] further suggested that in addition to being an excellent adsorbent for organics, bauxite residue can also be used for inorganics pollutants including metal ions (chromium, lead, copper, and cadmium) and non-metallic ions (fluorine, arsenic, and phosphorous). In addition to possessing a good specific surface area, bauxite residue contains metal ions like Ca<sup>2+</sup> and Mg<sup>2+</sup> which can form precipitates with the presence of carbonate species, yielding new adsorption sites for contaminants binding and improving the overall adsorption efficiency [29].

Dyes are major contaminants of concern in wastewater produced from industries such as textile, paper, leather, and printing [24]. Most dyes are toxic and resistant to light and biological degradation [24]. If released into the aquatic system, dyes can prevent light penetration to the plants, leading to eutrophic pollution [24]. Studies have shown that bauxite residue can achieve excellent removal of many dye compounds such as procion orange, Congo red, acid violet, indigo carmine, rhodamine B, fast green, and methylene blue, suggesting bauxite residue as a promising adsorbent for color removal in wastewaters [30]–[34].

Phenolic compounds are commonly used in the synthesis of plastics, pharmaceuticals, pesticides, dyes, and a variety of products [29]. As phenols are extremely hazardous to the ecosystem even at low concentrations, the presence of phenols in final effluents from industries is strictly regulated [24]. Gupta et al. [35] showed the effectiveness of bauxite residue in

removing phenolic compounds including phenol, 2-chlorophenol, 4-chlorophenol, and 2,4-dichlorophenol, indicating that bauxite residue could be applicable to the treatment of phenols-polluted wastewater.

Aydin et al. [36] demonstrated the potential application of bauxite residue adsorbent in removing psychiatric drugs from wastewater. Pharmaceuticals are emerging pollutants in waters and their presence in aquatic environments is growing drastically with the globally increasing population and the increasing use of medicines [36]. Pharmaceuticals in water pose long-term effects on both animals and humans [36]. Many pharmaceutical compounds are not easily degradable and cannot be removed sufficiently by conventional wastewater treatment processes [36]. Aydin et al. [36] synthesized a composite named magnetic red mud nanoparticles with bauxite residue for the treatment of effluent from a wastewater treatment plant, and as a result, they found that the composite adsorbent was effective in the removal of pharmaceuticals including antidepressants (fluoxetine, paroxetine), antiepileptic (carbamazepine) and anti-anxiety medications (diazepam, lorazepam). Given the efficacy of bauxite residue adsorbent in removing organic pollutants including dyes, phenols, and pharmaceuticals, bauxite residue is potentially also effective in the removal of other toxic organic chemicals and applicable to the treatment of other organic wastewaters.

Besides organic pollutants, bauxite residue can also be used for the removal of inorganic pollutants such as heavy metals including copper, lead, cadmium, nickel, and arsenic as well as nutrients including nitrogen and phosphorus [37]–[40]. Heavy metals can cause detrimental consequences on the growth and development of aquatic species and are very persistent in the environment [41]. Apak et al. [39] found that bauxite residue is effective in the removal of copper, lead, and cadmium (the order of decreasing sorption capacity) and also in relation to the

increasing solubility of the metal hydroxides formed. Similarly, Zouboulis and Kydros [40] showed that the alkalinity from bauxite residue promoted the precipitation and sedimentation of nickel from water by forming insoluble hydroxides. The discharge of nitrogen- and phosphorus-rich wastewater can lead to eutrophication of the receiving of water bodies [38] and Huang et al. [42] achieved an effective removal of phosphate using bauxite residue, potentially due to the chemical interaction with the surface functional groups of bauxite residue. Zhao et al. [38] were able to recover nitrogen and phosphorus from wastewater using bauxite residue-modified biochar and demonstrated potential utilization of the nutrients-loaded bauxite residue-modified biochar for plant growth.

Although bauxite residue is an inexpensive option for contaminants removal from wastewater, there are still challenges to be addressed for the efficient and safe utilization of bauxite residue. Firstly, the direct use of raw bauxite residue has limited treatment performance and improvement of the bauxite residue material might be needed to increase its adsorption capacity relative to activated carbon [29]. Secondly, settling by gravity is insufficient to separate raw bauxite residue from treated wastewater, and advanced separation processes such as centrifugation or filtration are required but can amount to higher capital and operational costs [36]. Thirdly, bauxite residue can release metals into the wastewater, and the intensity and effect of this leaching need to be considered and minimized [29]. Lastly, the bauxite residue sludge that remained after adsorption might become more toxic. Additional management practices (e.g., regeneration and reuse) of the sludge are essential for environmental protection and for the effective utilization of bauxite residue waste [29].

### 1.3.1. Pre-treatment Methods for Bauxite Residue Adsorbent

In wastewater treatment applications, pre-treatment of bauxite residue is necessary to (1) improve the adsorption performance of bauxite residue and (2) minimize the leaching of toxic metals into the water during treatment. The most common preparation methods for bauxite residue adsorbent include neutralization, acid/surfactant treatment, thermal treatment, and composite synthesis with other materials [43].

Understanding the structure and properties of the bauxite residue material is critical to the selection of proper improvement methods to minimize metals release and increase adsorption capacity. Ren et al. [44] investigated the general physical and chemical properties of bauxite residue for management and reuse purposes. It was determined that the primary solid phases in bauxite residue include katoite, sodalite, calcite, and hematite and among them, katoite, sodalite, and calcite are alkaline phases that can leach alkaline slowly and continuously into the water, resulting in the strong acid-neutralizing capacity of bauxite residue. Except for vanadium (V), chromium (Cr), and copper (Cu), most metal species in bauxite residue are in residual forms, suggesting they have low mobility in natural environments [44]. The leaching of V, Cr, and Cu could increase extensively under acidic conditions, but this may not be a concern because the total bauxite residue contains very small amounts of V, Cr, and Cu, and bauxite residue has high alkalinity [44]. The release of metals at different pH conditions was also examined and the results showed that the leaching of metals, especially Al, V, and Cr, from bauxite residue, is minimal at neutral pH but can increase substantially in highly acidic or highly alkaline environments [44].

Besides suppressing the release of metal ions, neutralization of bauxite residue is essential as the treated wastewater must have acceptable pH – between 6.5 and 9 according to the

guideline for the protection of freshwater aquatic life by the Canadian Council of Ministers of the Environment (CCME) [45]. Furthermore, the neutralization of bauxite residue could also reduce the interparticle repulsion between bauxite residue particles, promoting the separation of bauxite residue from water [46]. Acid addition and salt precipitation (mainly  $\text{Ca}^{2+}$  and  $\text{Mg}^{2+}$ ) are two approaches to reducing the alkalinity of bauxite residue [2]. Mineral acids are effective for the neutralization of bauxite residue but are not favourable for large-scale applications because of the high cost [2]. Less expensive alternatives include the use of acidic gases such as carbon dioxide and sulfur dioxide from flue gas, neutralization with acid mine drainage or acid rain, and production of organic acids by growing microorganisms in bauxite residue [2], [47]. However, the former two options can contribute additional toxicants to the bauxite residue while the latter has a high demand for nutrients [2]. Due to their rich  $\text{Ca}^{2+}$  and/or  $\text{Mg}^{2+}$  content, seawater, salts such as gypsum and lime, and potentially industrial waste brines can also be utilized to neutralize bauxite residue by precipitating out the alkaline species [46], [48], [49].

Activation with acid, surfactant, and heat are common approaches to improve the sorption capacity of adsorbent material. It was reported that treatment with dilute acid can develop new cavities and increase the surface area of bauxite residue by dissolving some metallic compositions on the surface [50], [51]. Enlarging the surface area, however, may not always lead to better removal as some chemicals are removed mainly due to chemisorption, not physisorption. For example, Li et al. [50] showed the removal of phosphate was reduced for bauxite residue with acid treatment, potentially because the removal of metallic components decreased the surface attraction to phosphate. Surfactants enhance adsorption by modifying the surface charge of bauxite residue [52]. Deihimi et al. [51] showed the removal of ferricyanide ions was improved by treating bauxite residue with cetyltrimethylammonium bromide, which

converted the charge of the bauxite residue surface from negative to positive. In addition, the treatment with cetyltrimethylammonium bromide greatly reduced the release of metals from bauxite residue [52]. Heat treatment releases volatile or oxidizable substances from the surface, creating porous structures in the adsorbent. Calcination at the right temperature can increase the surface area of bauxite residue due to the evaporation of water molecules but overheating can cause pore shrinkage [50]. Furthermore, excessive thermal treatment can remove hydroxyls and minerals like calcite, reducing the sorption capacity for some organics and inorganics contaminants [50], [53]. Thermal treatment can lead to phase transformation in bauxite residue, which can alter the interaction between adsorbate and adsorbent and ultimately affect the removal efficiency of pollutants [50], [54].

Depending on the pollutant types, composition with other materials can be an effective method to improve the adsorption performance of bauxite residue. Kazak et al. [53] synthesized bauxite residue with sucrose-based carbon and Cao et al. [55] synthesized bauxite residue with polystyrene microspheres. They both found that the composite material has a much higher specific surface area and total pore volume compared to the raw bauxite residue and both composites significantly improved the removal of dyes. Yet, compositing with other materials can be expensive due to the additional material and energy requirement.

#### **1.4. Management loop for bauxite residue**

Partnering with GRÖN Holding Corp. (Canada), this thesis focuses on a profitable and environmentally friendly process chain for the reuse of bauxite residue, as well as for the treatment of wastewater, as illustrated in Figure 1.

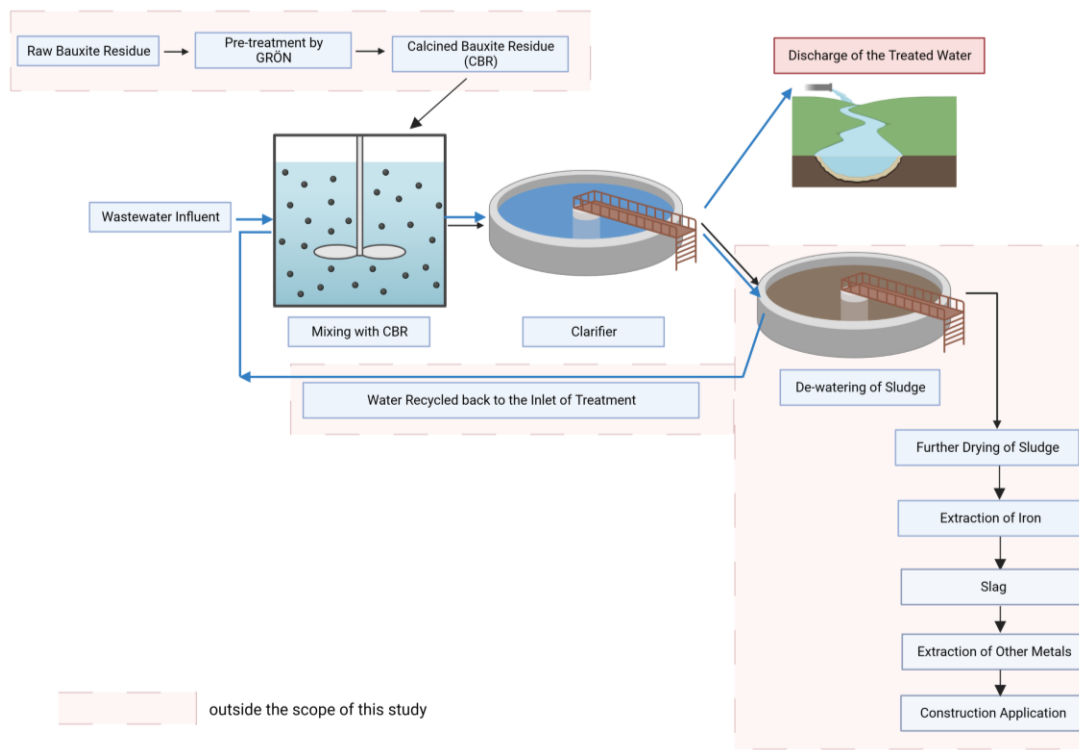


**Figure 1.** Process chain for bauxite residue management by the industrial partner (GRÖN). Note that this thesis is focused on the wastewater treatment (aqueous phase) aspect of the diagram. The image is drawn with BioRender.

First, raw bauxite residue undergoes a pre-treatment process (patented by GRÖN) that primarily removes impurities and moisture from bauxite residue through calcination and converts hematite ( $\text{Fe}_2\text{O}_3$ ) in bauxite residue to magnetite ( $\text{Fe}_3\text{O}_4$ ). This calcined material is called reduced calcined bauxite mineral residue, or simply **calcined bauxite residue (CBR)**, and is ready for use in wastewater treatment. Due to the reduction of iron species, the CBR adsorbent transforms from red to black in color, and its particles are very fine and powdery, as shown in Figure 2.





**Figure 2.** Images of raw bauxite residue (left) and calcined bauxite residue (CBR) (right)

As a general overview, CBR is first mixed with target wastewater, and the solution is neutralized with acid to reach a neutral pH for discharge purposes. The wastewater then enters the clarifier where the separation of CBR from the treated wastewater will take place via sedimentation (additional coagulants/flocculants may be required depending on the treatment needs). The clean supernatant from the clarifier will be discharged into natural water bodies while the sludge will be sent for further de-watering. The water separated from the sludge during the de-watering process will be returned to the inlet of the wastewater treatment tank, and the thickened sludge is used for iron extraction. After drying, iron (Fe) is extracted from the metal oxides in the solid waste in a reducing furnace and the adsorbed organic pollutants are detached in gaseous forms and collected for treatment. The solid waste remaining after the extraction of iron becomes “slag”. There are two management options for this solid waste product: (1) further extraction of the valuable metals from slag and (2) using slag as aggregate for roadbeds or for other construction applications. If successfully implemented, this process chain can accomplish

the treatment of two wastes – bauxite residue and wastewater at one time, as well as achieve the extraction of Fe and other valuable metals, thus generating higher revenue.

The subsequent Sections 1.5 and 1.6 provide a brief overview of the treatment technologies used for OSPW (focused on naphthenic acids [NAs]) and municipal wastewater treatment plant (WWTP) effluent (focused on ecotoxicological impacts from trace organic compounds in municipal WWTP effluent). These sections also provide a rationale for why CBR is an attractive option for use in these wastewaters.

### **1.5. Current Technologies for Oil Sands Process-Affected Water (OSPW) Treatment**

Oil sands mining is one of the major industries in Alberta and the process produces a significant volume of wastewater named oil sands process-affected water (OSPW) [23]. For many organisms, exposure to OSPW can lead to detrimental effects such as suppressed immune system, endocrine disruption, impaired reproduction and growth, and histological modification [23]. Due to the high toxicity of OSPW, the zero-discharge policy has been enforced, forbidding the discharge of OSPW in natural waters [56]. In general, OSPW contains toxic organic pollutants including naphthenic acids, PAHs, BTEX, and phenolic compounds, as well as inorganic pollutants including heavy metals and other ions [23]. Among them, naphthenic acids (NAs) are considered a prime pollutant in OSPW treatment [23], [56], [57]. NAs consist of a group of complex and distinct carboxylic acids and are very difficult to degrade [56]. NAs can cause both acute and chronic toxicity in mammals and aquatic species [57]. In aged tailings ponds, the average concentration of NAs ranges from 40 to 70 mg/L [57]. Quinlan and Tam [57] reviewed the current technologies for the removal of NAs from OSPW, which include advanced oxidation, biodegradation, coagulation, membrane filtration, and adsorption.

Advanced oxidation involves the generation of hydroxyl radicals which in turn break down the NAs through oxidation [57]. Effective reduction of NAs was achieved by implementing advanced oxidation processes including ozonation, UV/H<sub>2</sub>O<sub>2</sub>, O<sub>3</sub>/H<sub>2</sub>O<sub>2</sub>, microwave/TiO<sub>2</sub>, UV/chlorine, etc. [58]–[62]. Despite the good removal, advanced oxidation processes are very expensive due to high material and/or energy requirements [57]. Another concern is that advanced oxidation can result in the formation of byproducts that are more hazardous than the original NAs if the chemical reactants are not fully degraded [57].

Biodegradation relies on the ability of microorganisms to metabolize NAs [57]. Organisms originating from the tailings are often selected for the NA degradation because they are less susceptible to the toxicity of OSPW [63]. Removal of NAs can be achieved with nutrients supplied to the OSPW to facilitate microbial growth [63]. There are two main limitations to removing NA by biodegradation: (1) the cost increase due to the additional food source required and (2) some NAs are not prone to biodegradation, with some recalcitrant fractions could take months to years to remove [57].

Coagulants such as alum and iron oxide remove NAs from OSPW by forming precipitates with positively charged surfaces, which then trigger the binding of negatively charged NAs onto the precipitates [64]. Similarly, electrocoagulation can generate multivalent metal cations, which then remove NAs by coagulation [65]. Achieving an efficient removal of NAs, however, consumes large amounts of coagulants as well as results in the production of sludge, which requires additional post-treatment [57].

Membrane filtration can produce high-quality effluent which can potentially be recycled and reused in the process [57]. Membrane filtration eliminates NAs by size exclusion and electrostatic interaction [66]. While membrane technologies like nanofiltration are effective for

NA reduction, issues such as fouling, costs, and the need for replacement and treatment of membranes used are all important factors to be considered before application [57], [67].

Adsorption involves the partitioning of NAs from OSPW onto the surface of the adsorbent through physical and/or chemical interactions [57]. Adsorbents including commercial activated carbons as well as activated carbons derived from waste products such as petroleum coke and sawdust have good adsorption efficiency for NAs [68]–[70]. However, purchasing commercial activated carbon for OSPW treatment may not be economically feasible, and the activation process can also be very expensive depending on the precursors [57]. To date, CBR has never been applied to assess removal of NAs and this study is the first to show its potential in OSPW treatment.

#### **1.6. Current Technologies for Municipal WWTP Effluent Treatment**

In recent years, due to the rising population and insufficient removal by conventional sewage treatment, the occurrence of micropollutants such as personal care products, pharmaceuticals, endocrine-disrupting compounds, and disinfection by-products has been notably increasing in natural water bodies [71], [72]. Although not yet regulated, long-term exposure to micropollutants even at trace levels, can present significant health risks to both the ecosystem and humans [71], [73]. Thomaidi et al. [72] examined the risk of discharging domestic effluent with secondary treatment in aquatic systems in Greece and found that even for rivers with large dilution capacity (up to 2388), a potential ecological threat cannot be eliminated because of the existence of the micropollutants. More recently, in some WWTPs in Switzerland, advanced treatment by ozonation or activated carbon adsorption was implemented for micropollutants removal [27]. With concern and attention growing on the presence of

micropollutants in the natural environment, more countries may need to upgrade their WWTP processes soon to improve the removal of these emerging pollutants.

Technologies available for the removal of micropollutants can be divided into three categories including physical processes (nanofiltration, reverse osmosis, adsorption, and coagulation), chemical processes (advanced oxidation processes, ozonation, photo-Fenton and Fenton, photocatalysis, sonochemical), and biological processes (activated sludge, algal reactors, constructed wetlands, and trickling filters) [73]. Similar to OSPW treatment, despite chemical processes being very effective in mineralizing organic contaminants, large-scale application of chemical oxidation processes for domestic wastewater treatment might be hindered by high cost of chemicals [57], [73]. The application of biological treatment is also restricted if the target pollutants are persistent or toxic to the microorganisms [73]. Membrane filtration technologies such as nanofiltration and reverse osmosis can remove a diverse range of emerging pollutants from wastewater. In fact, nanofiltration and reverse osmosis have been employed for drinking water treatment [73]. However, these advanced membrane technologies are expensive for wastewater treatment, and the process generates a concentrated liquid waste stream which can be more difficult to treat and dispose of [73].

Having multiple advantages such as low initial cost, easy operation, less sensitivity to toxic chemicals, and high removal efficiency, adsorption is one of the available approaches for the removal of emerging contaminants in wastewater [73], [74]. Extensive studies have been conducted exploring the adsorption capacity of different adsorbents for reducing emerging pollutants in wastewater, such as activated carbon, modified biochar, carbon nanotube, graphene, mesoporous carbon, and other novel adsorbents [74]–[78]. As mentioned earlier, Aydin et al. [36] removed psychiatric pharmaceuticals from wastewater treatment plant effluent successfully

using a modified bauxite residue adsorbent named magnetite red mud nanoparticles, demonstrating the potential applicability of bauxite residue adsorbent for the treatment of emerging contaminants in wastewater. Though the pre-treatment methods are different, the CBR used in this thesis might also be capable of improving the water quality of the municipal WWTP effluent.

### 1.7. Research Aim and Objectives

Although many studies have explored the adsorption capacity of bauxite residue, the CBR potentially possesses different performance in wastewater treatment due to its unique preparation method (i.e., calcination) and the source of raw bauxite residue. Therefore, the applications of this CBR material in wastewater treatment are yet to be explored and optimized. The main purpose of this thesis is to assess the feasibility of the calcined bauxite residue (CBR) as an adsorbent for wastewater treatment. The assessment consists of four parts:

- (1) **Material characterization** based on its microscopic image, elemental composition, phase composition, specific surface area, pore volume, and pore size distribution to understand the structure, properties, and possible removal mechanisms of CBR as an adsorbent.
- (2) **Cell toxicity pathway evaluation** via the cytotoxicity, estrogenicity, and mutagenicity in oil sands process-affected water (OSPW) and municipal wastewater treatment plant (WWTP) effluents using *in vitro* bioassays. Additionally, the inactivation of total coliform bacteria in municipal WWTP effluents was also evaluated.
- (3) **Analysis of adsorption kinetics and isotherm** for the removal of methylene blue in synthetic solution and AEOs in OSPW to understand the adsorption mechanism between organics and CBR and evaluate optimal treatment conditions.

- (4) **Assessment of the metal and anion leaching** before and after CBR neutralization with acetic acid to determine if neutralization can be used to control the release of secondary pollutants from CBR during treatment.

## 1.8. Research Hypotheses

The work performed in this study, including material characterization, water treatment experiments, and comparison with literature (described in Section 2 Methodology), were designed primarily to test the following set of hypotheses:

**Hypothesis 1.** CBR will possess similar removal efficiencies for organic compounds such as methylene blue as their material in comparison to the raw bauxite residue based on published literature.

**Hypothesis 2a.** If CBR can remove methylene blue (organic), it will also be able to remove other organic pollutants such as naphthenic acids.

**Hypothesis 2b.** If CBR can remove naphthenic acids from synthetic wastewater (simple matrix consisting naphthenic acid mixture and ultrapure water), it will also be able to remove naphthenic acids from real wastewater (complex matrix) such as OSPW.

**Hypothesis 2c.** If priority pollutants (e.g., naphthenic acids in OSPW) of the wastewater were removed by CBR, the toxicities (cytotoxicity, estrogenicity, and mutagenicity) of the wastewater will also be reduced.

**Hypothesis 2d.** If CBR treatment can reduce the toxicities of OSPW, it can also reduce the toxicities of other wastewater such as diluted and undiluted municipal WWTP effluents, because of the removal of organic and inorganic pollutants.

**Hypothesis 2e.** Because CBR is highly caustic, adding CBR to municipal WWTP effluents will cause the inactivation/removal of coliform bacteria.

**Hypothesis 3a.** Given that bauxite residue can leach metals to surrounding environments and that the calcination pre-treatment did not result in significant alteration of physical properties of bauxite residue, without additional mitigation measures, CBR will also release metals into water during treatment similar to untreated bauxite residue.

**Hypothesis 3b.** If the CBR solution (the CBR slurry prior to treatment or the wastewater containing CBR after treatment, described in Section 2.9) is neutralized, the release of metals (especially aluminum) from CBR will be reduced because the solubility of metals is pH-dependant and the solubility of aluminum is lower at neutral pHs.

**Hypothesis 3c.** As the leaching of metals from CBR can be reduced by neutralization, if neutralization were implemented as part of the water-treatment-by-CBR process, it will positively impact the removal of toxicities from wastewater.

These hypotheses were tested using the four water matrices described in Section 1.9 and the outcomes were explained in different sections of Section 3 (Table 1).

**Table 1.** Outcomes of the hypotheses examined in this study.

<b>Proposition</b>	<b>Outcome</b>
Hypothesis 1	Sections 3.1 and 3.2
Hypothesis 2a	Section 3.3
Hypothesis 2b	Sections 3.4.1, 3.5.1, and 3.5.2
Hypothesis 2c	Sections 3.4.1 and 3.5.1
Hypothesis 2d	Sections 3.4.1, 3.6.1, and 3.6.2
Hypothesis 2e	Sections 3.6.1 and 3.6.2
Hypothesis 3a	Sections 3.1, 3.4.1, and 3.4.2
Hypothesis 3b	Sections 3.4.3
Hypothesis 3c	Sections 3.5.1 and 3.6.1



## 1.9. Study Scope

This study involves the use of four water matrices: (1) synthetically made wastewater, (2) real industrial and municipal WWTP wastewater, (3) ultrapure water, and (4) diluted tertiary municipal WWTP wastewater. The four matrices as well as the purpose of each of the water types are summarized and shown in Figure 3.

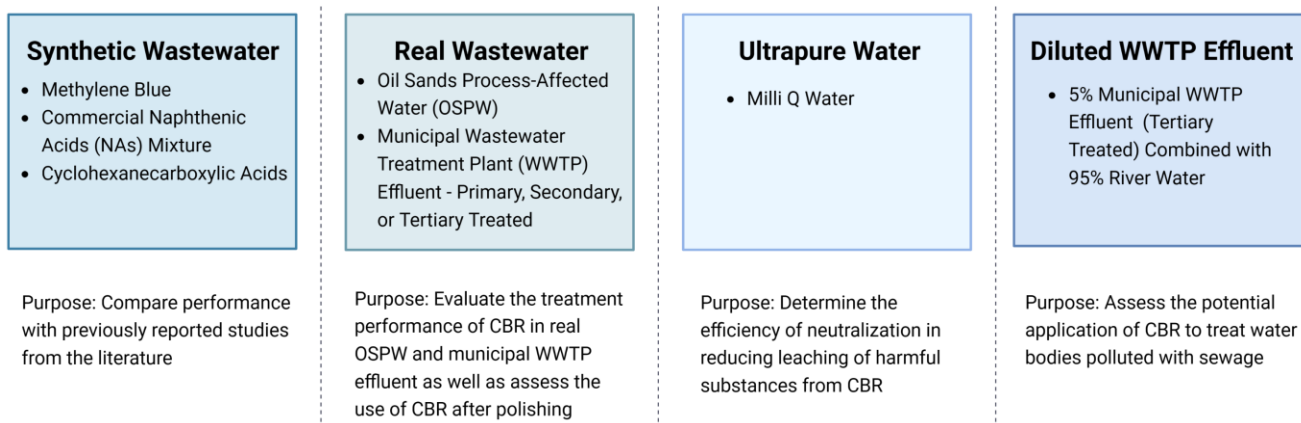


**Figure 3.** The four types of water matrices used in this study and the purpose of each matrix in addressing research objectives related to this thesis. The image is drawn with BioRender.

Three synthetic solutions were made by mixing target concentrations of the specific organic chemical with water. First, methylene blue was used as a representative organic dye as the removal of methylene blue by bauxite residue is well-studied and the adsorption parameters such as dosage, removal, kinetics, and isotherm are available in the literature for comparison [34], [53], [79], [80]. This experiment was also intended to provide insights into the potential application of CBR for treating wastewater polluted with organic dyes such as that used in textile and food industries. Sigma NAs are commercially available naphthenic acids mixture and a synthetic OSPW was made following the method described by Iranmanesh et al. [70], who investigated the removal of commercial NAs using sawdust-activated carbon. Similarly, an experiment measuring the removal of commercial NAs by CBR was carried out in this study in

an attempt to compare the adsorption capacity of CBR with the activated carbon adsorbent prepared from sawdust by Iranmanesh et al. [70]. Having a shorter carbon-chain structure and higher solubility in water, cyclohexane carboxylic acid can be an alternative compound for making synthetic OSPW [81]. It was suggested that if the adsorbent can remove cyclohexane carboxylic acid from water, then it is likely also capable of removing other longer carbon-chain fractions of NAs which have lower affinity to water [81].

Two real wastewaters: (1) OSPW samples from an oil sands operator in northern Alberta and (2) primary, secondary, and tertiary effluents from the municipal WWTP were used in this study. For both wastewaters, the removal of potentially toxic effects (i.e., cytotoxicity, estrogenicity, and mutagenicity) with CBR was analyzed via *in-vitro* bioassays. Since NAs are identified as one of the primary pollutants in OSPW, the adsorption kinetics and isotherm for the removal of NAs (using its surrogate measurement AEOs) were also determined as another parameter to assess the efficacy of CBR for OSPW treatment.

Additionally, some of our preliminary testing showed a substantial reduction in turbidity after mixing with CBR, indicating CBR might have the ability to enhance the removal of suspended or colloidal particles besides soluble organic pollutants. Hence, it is hypothesized that the treatment with CBR can also improve the reduction of pathogenic species alongside the removal of turbidity. This hypothesis was assessed by determining the concentration of total and fecal coliform bacteria, commonly-used indicators for the presence of harmful pathogens.

Besides adsorption efficiency, the leaching of secondary pollutants such as metal ions from bauxite residue adsorbent must also be monitored and minimized for the effective implementation of CBR in wastewater treatment. This thesis also tested the effectiveness of neutralization with acetic acid, an environmentally friendly organic acid, in reducing the leaching

of contaminants from CBR. The leaching test was conducted in both clean/ultrapure water and the target wastewaters (i.e., OSPW and municipal WWTP effluents). The treated wastewater samples before and after neutralization with acetic acid were analyzed with *in vitro* bioassays to determine the change in cytotoxicity, estrogenicity, and mutagenicity. Also, a set of clean/ultrapure water samples treated with CBR were submitted for chemical analysis to compare the release of metal cations and anions before and after neutralizing with acetic acid.

Finally, the cytotoxicity, estrogenicity, and mutagenicity of a diluted WWTP effluent – 5% tertiary-treated municipal WWTP effluent combined with 95% river water - after treatment with CBR were analyzed. This water matrix was used to provide insights into the applicability of CBR in the remediation of water bodies polluted with sewage.

## 2. Methodology

### 2.1. Overall Experiment Design

The overview of the experiments and general methods completed in this thesis are shown in Figure 4. Briefly, CBR was mixed with the wastewater in a jar tester, a wrist shaker, or an orbital shaker depending on the experiment. Next, the treated wastewater was separated from the CBR sludge by filtration, centrifugation, or settling. For most analyses, the supernatant or the filtered water samples were analyzed directly or sent for analysis, except for Fourier transform infrared spectroscopy (FTIR) and *in-vitro* bioassays that require additional sample cleanup via solid phase extraction (SPE) (Section 2.6). SPE removes interfering compounds from the sample matrix and concentrates the samples to improve chemical and bioanalytical detection.

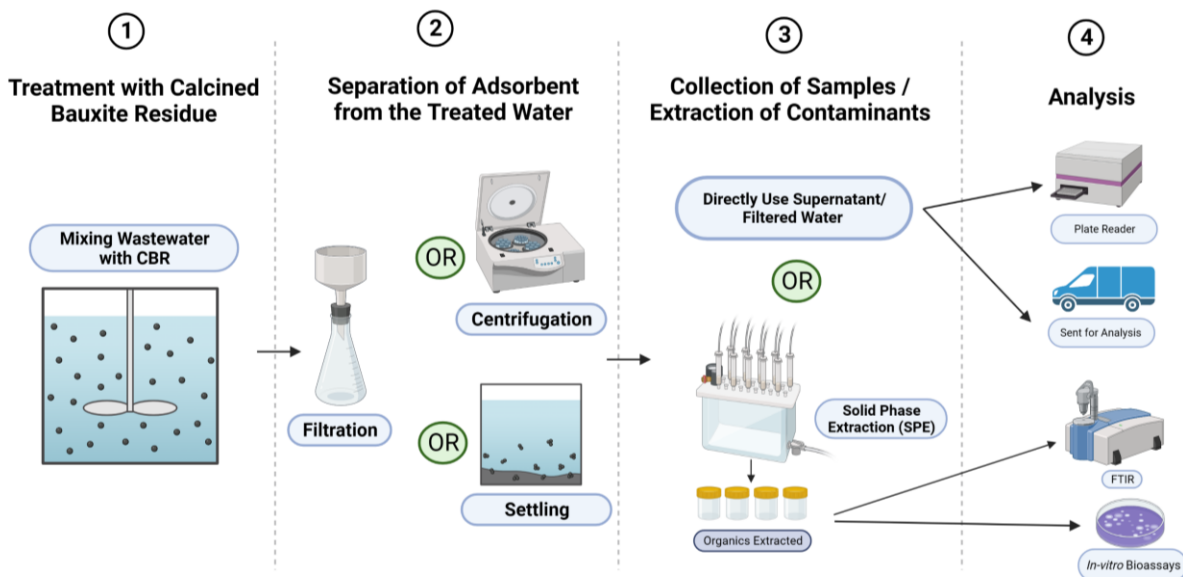


**Figure 4.** The overall experiment flowchart, and analytical and bioanalytical methods employed in this thesis. CBR = calcined bauxite residue. The image is drawn with BioRender.

## 2.2. Brief Overview of Analytical Methods

Table 2 summarizes all the analytical tools used in this study. For the characterization of the CBR adsorbent, microscopic images were taken with scanning electron microscopy (SEM). The elemental composition was obtained with the energy dispersive X-ray (EDX) analysis. The solid phases were determined with the X-ray diffraction (XRD) technique. The Brunauer-Emmett-Teller (BET) surface area, total pore volume, and pore size distribution were estimated using the gas (N<sub>2</sub>) adsorption method.

**Table 2.** Summary of analytical tools. SEM = Scanning Electron Microscope, EDX = Energy Dispersive X-ray, XRD = X-ray Diffraction, FTIR = Fourier Transform Infrared Spectroscopy, YES= Yeast Estrogen Screen.

<b>Material Characterization</b>	<b>Adsorption Kinetics and Isotherm</b>	<b>Cell Toxicity Pathway</b>	<b>Metal and Anion Leaching</b>
Microscopic Properties Analysis (SEM)	Methylene Blue (Absorbance@665nm)	Cytotoxicity (BioTox-LumoPlate)	Samples were sent to an accredited laboratory for analysis (Bureau Veritas – Edmonton)
Elemental Analysis (SEM-EDX)	Commercial Naphthenic Acids (FTIR)	Estrogenicity (YES)	
Phase Identification (XRD)	Cyclohexane Carboxylic Acids (FTIR)	Mutagenicity (Umu-Chromo (gene) Test)	
BET Surface Area, Total Pore Volume, and Pore Size Distribution (Adsorption of N <sub>2</sub> )	Acid Extractable Organics (FTIR)	Total Coliform (Membrane Filtration Method)	

For adsorption kinetics and isotherm studies, the concentration of methylene blue was determined with spectrophotometry (absorbance of light at a wavelength of 665nm) (Section 2.7.1). The concentration of commercial NAs, cyclohexane carboxylic acids, and acid-

extractable organics (Section 2.7.2) were all measured with FTIR based on the C=O bond of carboxylic functional groups. The effect of CBR treatment on cell toxicity pathways was evaluated using *in-vitro* bioassays (Sections 2.8.2 to 2.8.4): cytotoxicity was determined based on the inhibition of the *Aliivibrio fischeri* bacteria; estrogenicity and mutagenicity removals were determined using the Yeast Estrogen Screen (YES) assay and the UMU-ChromoTest procedure respectively. Finally, the concentration of total coliform bacteria was determined using the membrane filtration method (Section 2.8.5). For leaching studies (Section 2.9), water samples were sent to an accredited laboratory (Bureau Veritas Laboratory, Edmonton) for determination of more water quality parameters such as metals, dissolved organic carbon (DOC), and anions including fluoride, chloride, sulfate, and nutrients.

### **2.3. Materials**

The raw bauxite residue (BR) and calcined bauxite residue (CBR) used in this study were prepared and provided by GRÖN Holding Corp. (Canada). The OSPW sample was obtained from an oil sands tailings pond operator in northern Alberta. The municipal WWTP effluent samples were taken from two WWTPs (Plant A and Plant B) with tertiary treatment. All wastewater samples were stored in amber glass bottles at 4°C before use. All SPE extracts were stored at -20°C prior to analysis. Commercial NAs (technical grade), cyclohexanecarboxylic acid (98%), acetic acid (glacial grade, ≥99.7%), ethyl acetate (≥99.5%), dichloromethane (≥99.8%), and estradiol were purchased from Sigma-Aldrich, Canada. Hydrochloric acid (10N), sodium hydroxide (10N), methanol (≥99.9%), dimethyl sulfoxide (≥99.9%), sodium chloride (≥99.0%), methylene blue (1% w/v), 3,5-dichlorophenol (99%), and ethanol (70%) were purchased from Fisher Scientific, Canada. Ultrapure water was obtained from a MilliQ IQ 7000 purification system with a resistivity 18.2 MΩ-cm (25°C) and total organic carbon (TOC) ≤ 5 ppb.

For cytotoxicity and mutagenicity testing, the BioTox-LumoPlate and the UMU-ChromoTest kits were purchased directly from Environmental Bio-detection Products Inc. (EBPI). For estrogenicity testing, the yeast strain *Saccharomyces Cerevisiae* for the YES assay was provided by the Servos Lab at the University of Waterloo. Reagents for YES including adenine hydrochloride hydrate, L-histidine-HCl, L-arginine-HCl, L-methionine, L-tyrosine, L-isoleucine, L-lysine-HCl, L-phenylalanine, L-glutamic acid, L-aspartic acid, L-valine, L-threonine, L-serine, L-leucine, L-tryptophan, uracil, glycerol, D-(+)-Glucose, copper sulfate pentahydrate, yeast nitrogen base (YNB) without amino acids were obtained from Sigma-Aldrich, Canada. Bacto agar and the yeast  $\beta$ -galactosidase assay kit (including 2X  $\beta$ -galactosidase assay buffer and Y-PER yeast protein extraction reagent, and  $\beta$ -galactosidase assay stop solution) were obtained from ThermoFisher Scientific, Canada. For coliform testing, the mLES Endo agar was purchased from Fisher Scientific, Canada.

#### **2.4. Material Characterization**

Scanning electron microscopy (SEM) functions by exciting the sample with a beam of electrons, and the secondary electrons emitted from the sample are received by a detector and transcribed into images, allowing for the microscale visual analysis of the material [82]. In this study, the SEM technique was employed for visual inspection of the particle shape, size, and porosity, which are all characteristics important for the physisorption of CBR [82]. Prior to SEM analysis (Zeiss EVO MA 10 SEM), the samples were mounted on carbon-taped stubs and coated with gold for 100 seconds under a pressure of about 150 mT with the Denton Gold Sputter Unit. The structure of untreated bauxite residue was also observed using SEM to investigate the structural modifications to the bauxite residue via calcination.

The energy-dispersive X-ray (EDX) operates by exciting the sample with an X-ray beam. As a result, different elements in the sample will be excited and release energy in the form of an X-ray with wavelengths unique to the element, which can then be collected to determine the elemental composition of the sample [82]. Besides microscopic imaging, the Zeiss EVO M10 SEM was also used to perform EDX analysis of the sample at 20 kV. Elemental analysis with EDX was included in this study for multiple purposes: (1) to examine the change in chemical composition after the pre-treatment via calcination; (2) to identify the metal species and their content to optimize the use of CBR; (3) to compare with the leaching of metals from CBR in treated wastewater to determine if there is a correlation.

The Brunauer-Emmett-Teller (BET) surface area, total pore volume, and the Density Functional Theory (DFT) pore size distribution were derived based on the N<sub>2</sub> adsorption/desorption curve of the sample at 77°K [82] using Autosorb-iQ (Anton-Paar GmbH). Prior to analysis with N<sub>2</sub>, the sample was outgassed for 4 hours at 200°C. These parameters were intended to provide a quantitative measure of available binding sites and porosity of CBR.

X-ray diffraction (XRD) was conducted to identify the solid phase composition of CBR. A beam of X-rays is introduced to the sample at a range of angles. The atoms in a crystal can cause scattering of X-rays due to their periodic nature and produce a constructive signal at certain angles of incidence [82], [83]. From there, the crystal structures of the sample can be determined as crystals produce their distinctive diffraction peaks at certain angles of incidence [82]. The sample was scanned by the Bruker XRD D8 Discover, with a copper source and an X-ray throughput of 40 kV and 30 mA ( $2\theta = 4^\circ - 80^\circ$ ). The XRD data were analyzed using the JADE software to determine the different phases present in the CBR and to identify the phases that could potentially interact with the contaminants in wastewater during adsorption.



## **2.5. Water Treatment Experiments**

### **2.5.1. Synthetic Wastewater – Methylene Blue**

A preliminary removal experiment was carried out by mixing different doses of CBR with 45 mL of 20 mg/L of methylene blue (MB) solution in 50 mL conical tubes for 45 min with a wrist shaker (Burrell Scientific Model 75). After mixing, the tubes were allowed to settle overnight, and the concentration of MB remaining was determined based on the absorbance measurement at 665 nm of the supernatant. In general, both the dosage of adsorbent applied and the initial concentration of adsorbate have an impact on the interaction between the adsorbent and adsorbate, which could ultimately affect the time required for effective removal or lead to changes in adsorption efficiency. Therefore for the kinetic studies, four sets of experiments, 20 mg/L MB treated with 20 g/L CBR, 20 mg/L MB treated with 50 g/L CBR, 50 mg/L MB treated with 20 g/L CBR, and 50 mg/L MB treated with 50 g/L CBR, were included to account for the difference in adsorption performance by varying CBR dosages and initial MB concentrations.

For the adsorption kinetic study, CBR was added to the 500 mL of MB solution (containing either 20 mg/L or 50 mg/L MB) in a 1 L beaker to achieve an adsorbent dosage of either 20 g/L or 50 g/L. Then the solution was mixed continuously at 120 rpm using the jar tester (VELP FC 4S Flocculation Stirrer). Water samples of 2 mL were taken at different time points (total volume of samples taken  $\leq$  10% total water volume) and were centrifuged at 5000 rpm for 10 min for solid-liquid separation. After centrifugation, 300  $\mu$ L of the sample supernatant was transferred to a 96-well plate with transparent background (Falcon 96-Well, Cell Culture Treated, Flat-Bottom Microplate) and the absorbance of the sample at 665 nm was measured using the plate reader (Synergy LX plate reader with Gen5 Software). After calculating the MB concentration in samples via a standard curve consisting of 16 points (ranging from 0 to 20

mg/L), the amount of adsorbate, MB, adsorbed onto the CBR adsorbent at a specific time  $t$ ,  $q_t$  (mg/g), was calculated according to Equation 2 (EQN 1) and fitted with the Lagergren pseudo-first-order kinetic model (EQN 2) as well as the pseudo-second-order kinetic model (EQN 3) as described by Sahoo and Prelot [24].

$$q_t = \frac{(C_0 - C_t)V}{M} \quad (\text{EQN 1})$$

$$\frac{dq_t}{dt} = k_1(q_e - q_t) \quad (\text{EQN 2})$$

$$\frac{dq_t}{dt} = k_2(q_e - q_t)^2 \quad (\text{EQN 3})$$

where,  $C_0$  (mg/L) is the initial concentration of adsorbate,  $C_t$  (mg/L) is the concentration of the adsorbate at  $t$  (min),  $V$  (L) is the water volume,  $M$  (g) is the mass of adsorbent (CBR) added,  $q_e$  (mg/g) is the amount of adsorbate adsorbed at equilibrium,  $k_1$  (/min) is the equilibrium rate constant for the pseudo-first-order kinetic model and  $k_2$  (g/mg/min) is the equilibrium rate constant for the pseudo-second-order kinetic model.

For the adsorption isotherm study, different doses of CBR were added to 40 mL of MB solution (containing either 20 mg/L or 50 mg/L MB) in 50 mL plastic conical tubes. The solutions were mixed at 150 rpm by shaking horizontally in an incubator for at least 12 hours to ensure adsorption equilibrium has been obtained before analysis. After mixing, 2mL of water samples were taken from each of the 50 mL treated MB solutions and centrifuged for 10 min at 5000 rpm. Absorbance at 665 nm of the sample was then measured for the calculation of MB. For isotherm models fitting,  $q_e$ , the amount of MB adsorbed at equilibrium was calculated based on  $C_e$ , the concentration of MB at equilibrium, as shown in EQN 4. The obtained data were fitted to two common adsorption isotherm models – Langmuir (EQN 5) and Freundlich (EQN 6) [24].

$$q_e = \frac{(C_0 - C_e)V}{M} \quad (EQN 4)$$

$$q_e = \frac{K_L Q_m C_e}{1 + K_L C_e} \quad (EQN 5)$$

$$q_e = K_F C_e^{1/n} \quad (EQN 6)$$

where  $K_L$  and  $Q_m$  are constants for the Langmuir isotherm model:  $Q_m$  is the maximum adsorption capacity and  $K_L$  is the adsorption affinity coefficient.  $K_F$  and  $n$  are Freundlich isotherm constants:  $K_F$  is the adsorption affinity coefficient and  $n$  is the nonlinear index.

### 2.5.2. Synthetic Wastewater – Commercial Naphthenic Acids

Two synthetic OSPW solutions, either with Sigma NAs (20 mg/L) or with cyclohexane carboxylic acids (80 mg/L), were made following a procedure similar to that described in Iranmanesh et al. [70]. Firstly, Sigma NAs or cyclohexanecarboxylic acids were weighed and added to Milli Q ultrapure water in a capped glass bottle. One or two drops of 10N NaOH were added to raise the initial solution pH to around 8 or 9 to promote the dissolution of chemicals. The solution was sonicated (Branson M5800H) for 3 min [70]. Then the bottle was wrapped with tin foil to prevent light degradation, and the solution was mixed overnight with the magnetic stir plate (for at least 12 h prior to the adsorption experiment). The next day before removing the lid, the bottle was shaken for 15 sec to re-dissolve any chemicals partitioned into the upper air space overnight. To simulate the pH of the actual OSPW (average pH is 8.5) [64], the solution pH was adjusted to approximately 8.5 by adding drops of 10N or 1N NaOH. Prior to the treatment experiment, the solution was mixed for another 30 min using the magnetic stir plate to dissipate the bubbles formed during shaking. The synthetic OSPW solutions prepared were then distributed into smaller aliquots in 100 mL glass bottles. CBR was added to the bottle at a dosage of 20 g/L. The solution was mixed for 30 min using the wrist shaker. After adsorption, the

solution was centrifuged at 5000 rpm for 10 min followed by filtration with the 0.45 $\mu$ m-pore nylon syringe filters (Basix Syringe Filters, PVDF, Sterile). The AEOs in the solution were extracted via SPE (Section 2.6) and estimated via FTIR (Section 2.7.2).

### **2.5.3. Real Wastewater – Oil Sands Process-affected Water (OSPW)**

OSPW (500 mL) and four different doses of CBR (0, 20, 50, and 100 g/L) were mixed in a 1 L glass beaker at 120 rpm for 24 h using the jar tester. Toward the end of the 24 h mixing, the solution pH was lowered to neutral using concentrated acetic acid. Once the pH stabilized within the neutral pH range (6.5 to 9), the mixing was stopped, and the solution was left to sit for 30 min. After settling, the supernatant was filtered with the 1 $\mu$ m-pore hydrophilic glass fiber filter (Sigma APFB04700) and acidified to a pH of about 2 using 10 N HCl. The supernatant was divided into smaller aliquots for extraction and analyses separately: approximately 50-100 mL for FTIR and 100 mL for *in vitro* bioassays. The aliquots were extracted following the SPE procedure described in Section 2.6. The removal of AEOs in the treated OSPW extracts was obtained using the FTIR procedure described in Section 2.7.2. The AEOs concentration was calculated based on the calibration curve derived for the commercial NAs mixture (Sigma NAs), assuming that the composition of NAs in OSPW is more comparable to the Sigma NAs mixture. The analyses for cytotoxicity, estrogenicity, and mutagenicity followed the procedure described in Sections 2.8.2 to 2.8.4.

The adsorption kinetics study was carried out by mixing 1800 mL of OSPW with 50 g/L CBR continuously at 120 rpm using the jar tester. In total, 20 water samples of 10 mL were taken at different time points from 0 to 72 h. Upon collection, the samples were filtered using the 0.45  $\mu$ m syringe filters and acidified to a pH of about 2 by adding two drops of 10N HCl. The filtrate (7.1 to 9.5 mL) was extracted following the SPE procedure described in Section 2.6 except the

Oasis HLB 6cc/150mg cartridges were used instead because of the smaller sample volume. The concentration of AEOs at different time points was determined with FTIR, and the data obtained were fitted to the pseudo-first and pseudo-second kinetic models described in Section 2.5.1.

The isotherm experiment was started with the addition of CBR of different dosages, ranging from 0 to 100g/L into 40 mL of OSPW in 50 mL glass conical tubes. The tubes were placed horizontally inside the incubator and shaken for 2 days at 150 rpm. After mixing, the solution was settled for 2 h. The supernatant was filtered using the 0.45  $\mu\text{m}$  syringe filters and acidified to a pH of 2 using 10N HCl. The filtrate (32 – 38 mL) was extracted using the SPE described in Section 2.6. The equilibrium concentration of AEOs with different CBR dosages was determined using FTIR, and the data were fitted to the Langmuir and Freundlich isotherm models previously described in Section 2.5.1.

#### **2.5.4. Real Wastewater – Municipal WWTP Tertiary Effluent**

Municipal WWTP tertiary effluent (1.8 L) (from Plant A) and four different doses of CBR (0, 20, 50, and 100 g/L) were mixed in a 2 L glass beaker at 120 rpm for 24 h using the jar tester. At the end of the mixing, the solution was either neutralized using concentrated acetic acid to within the neutral pH range (6.5 to 9) or not neutralized, and the solution was left to settle for 30 min. Depending on the CBR dosage applied, about 960 mL (for 100 g/L CBR dose) to 1550 mL (for 20 g/L) of supernatant was collected from each treatment; the volumes of supernatant and sludge formed are related to the dosage of CBR – the higher dosage, the less volume of supernatant. The supernatant was then filtered with 1  $\mu\text{m}$  glass fiber filters and acidified to a pH of about 2 using 10 N HCl. The water samples were extracted following the SPE procedure described in Section 2.6 and reconstituted with 1 mL methanol for *in-vitro* bioanalyses (the extraction factors ranged from 960 to 1550).

The removal of cytotoxicity, mutagenicity, and estrogenicity was analyzed following the same procedure for *in vitro* bioassays described in Sections 2.8.2 to 2.8.4. Besides toxicity, the removal of a common indicator bacteria for pathogens in municipal wastewater – total coliform was also examined using the membrane filtration technique (Section 2.8.5).

#### **2.5.5. Real Wastewater – Municipal WWTP Primary, Secondary, and Tertiary Effluents (Further Evaluation and Optimization)**

This experiment utilized the effluent samples taken from Plant B. Here, primary, secondary, and tertiary effluents refer to the effluents following the biological nutrient removal unit, the secondary clarifier, and the UV disinfection unit respectively. The water treatment procedure was similar to the previous for the tertiary effluent experiment collected from Plant A, except (1) only 50 g/L and 100 g/L CBR were tested; (2) the solutions were all neutralized with acetic acid after treatment. The raw and treated water samples were extracted and analyzed using *in-vitro* bioassays and total coliform determination described in Sections 2.6 and Sections 2.8.2 to 2.8.5 or sent to Bureau Veritas for analyses including the following: pH, alkalinity, total suspended solids, total metals, dissolved metals, total organic carbon, dissolved organic carbon, biochemical oxygen demand (BOD), anions including fluoride, sulphate, chloride, and nutrients, and fecal coliform. The commonly regulated water quality parameters of CBR-treated effluents were compared with the discharge requirements set by the Alberta Environment and Parks (AEP) for Plant B as part of the “approval to operate” [84]. The concentrations of dissolved metals in the treated samples were compared with the CCME guidelines for the protection of freshwater aquatic lives [45] whenever available to determine the environmental significance of the concentrations of metals leached.

### **2.5.6. Diluted Wastewater - Tertiary Effluent Diluted with River Water**

The water treatment (without neutralization with acetic acid), extraction, and bioanalytical procedures were the same as that for the municipal WWTP tertiary effluent experiment (Section 2.5.4), except only 900 mL of water sample was used for treatment each time and the samples were mixed in a 1 L beaker. The extraction factors of the diluted effluent samples ranged from 375 to 850, Section 2.6. The concentration of total coliform after treatment was not evaluated because the sample was expected to have relatively low coliform concentrations to begin with.

### **2.6. Solid Phase Extraction (SPE)**

The SPE procedure followed Barrow et al. [85] with some minor modifications, as illustrated in Figure 5. First, the SPE cartridges (Oasis HLB 6cc/500mg, Waters Corporation) were placed onto either the 12-position (for sample volume >50 mL) or the 24-position (for sample volume <50 mL) vacuum manifold (Supelco Visiprep) and pre-conditioned with 5 mL of methanol followed by 10 mL of Milli Q ultrapure water. Samples with volumes >50mL were introduced to the cartridges at a controlled flow rate of approximately 1 mL/min by turning on and off the pump (GAST Model DOA-P704-AA) and adjusting the pressure valve on the vacuum manifold. Samples with volume <50mL were loaded into the cartridges via pipetting and were let to pass down the cartridges by gravity. After sample introduction, the cartridges were rinsed with 10 mL ultrapure water (pH adjusted to 2 with HCl) to remove some impurities attached. Then the cartridges were dried under vacuum for at least 45 min. Following vacuum drying, the cartridges were eluted with 5 mL of methanol and then 5 mL of 1:1 methanol: ethyl acetate by volume. The eluents were evaporated to complete dryness by blowing with a gentle stream of nitrogen and water bathing at 30 to 35°C. For samples to be analyzed by FTIR, the dried extracts were stored

directly in the -20°C freezer directly until analysis. For samples to be analyzed using *in-vitro* bioassays, the dried extracts were reconstituted with 1 mL of methanol and the extraction factor (EF) was calculated following EQN 7. Finally, the reconstituted extracts were wrapped in parafilm and stored at -20°C until analysis.

$$\text{Extraction Factor (EF)} = \frac{\text{Sample Volume before SPE (mL)}}{\text{Sample Volume after Reconstitution (mL)}} \quad (\text{EQN 7})$$

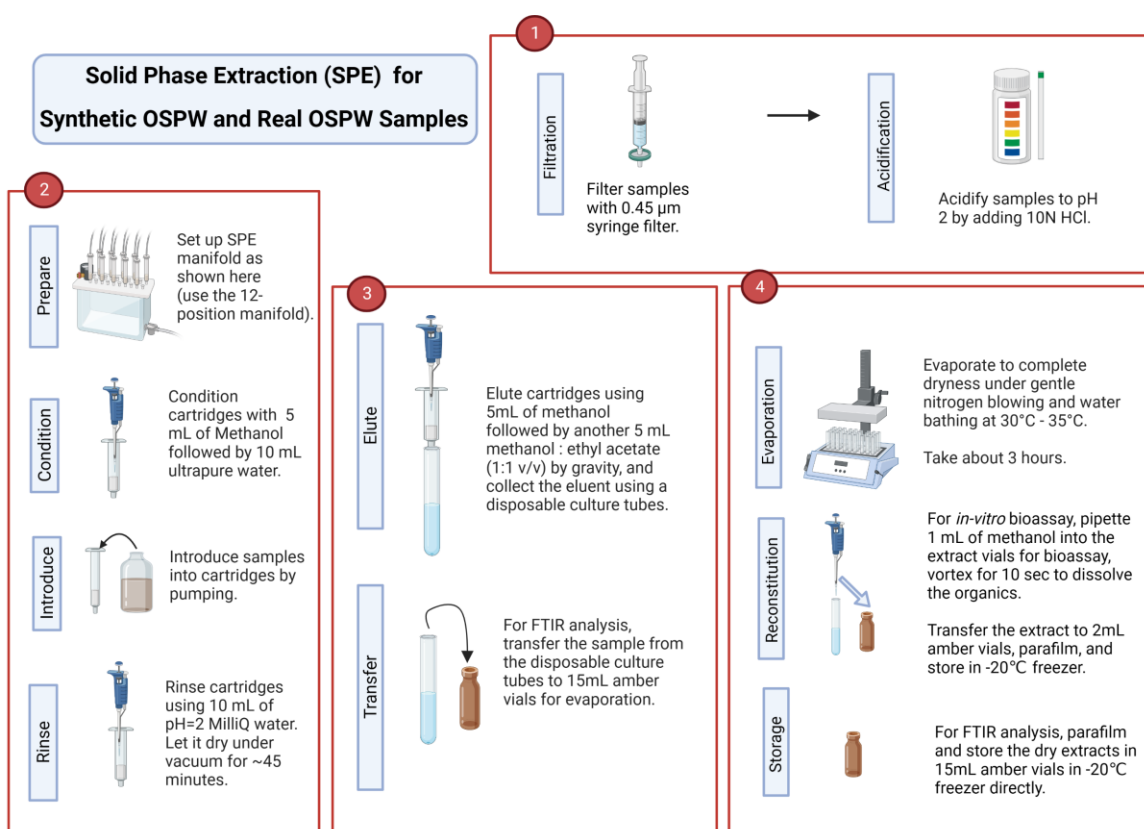


**Figure 5.** The solid phase extraction (SPE) procedure for synthetic and real oil sands process-affected water (OSPW) with volume >50mL. The figure was taken and slightly modified from Barrow et al. [85].



## **2.7. Chemical Analyses**

### **2.7.1. Absorbance Measurement for Methylene Blue (MB)**

The concentrations of methylene blue (MB) was determined via absorbance. To confirm the absorbance peak for anticipated MB concentrations in the treated water samples, the absorbance pattern for wavelengths ranging from 500 nm to 700 nm was measured for the 20 mg/L MB stock solution. A volume of 300 uL of 20 mg/L MB solution was transferred into a well in a clear 96-well plate, and the spectrum scanning was completed using the plate reader. The absorbance spectrum for 20 mg/L MB obtained is shown in Appendix A.1 – the absorbance peak was observed at the wavelength of 665 nm. From there, the calibration curve for determining the MB concentration in water samples was obtained – the MB concentration is linearly related to the absorbance at 665 nm ( $R^2 = 0.995$ ), as shown in Appendix A.1. For samples that were expected to have a concentration greater than 25 mg/L (above which the peak absorbance was no longer at 665nm), the samples were diluted by two or more times prior to measurement with the plate reader.

### **2.7.2. Fourier transform infrared spectroscopy (FTIR)**

Fourier transform infrared spectroscopy (FTIR) has been a common analytical technique for evaluating the NAs content in wastewater [86]. Following extraction (as described above), the synthetic OSPW and real OSPW samples were analyzed with FTIR, and its NAs fraction is quantified by the absorbance at 1743 and 1706  $\text{cm}^{-1}$  based on the C=O stretching of the carboxylic groups [86]. For the Sigma NAs and cyclohexane carboxylic acids used in this study, however, the peaks shifted slightly due to the different nature of NAs compounds. Based on the FTIR spectrum obtained from this experiment, it was observed that the absorbance peaks for Sigma NAs were  $\sim 1739$  and  $1701 \text{ cm}^{-1}$  while the peaks for cyclohexane carboxylic acids were

observed  $\sim 1742$  and  $1704\text{ cm}^{-1}$ . Standards calibration curves were therefore obtained separately for Sigma NAs and cyclohexane carboxylic acids, as described in detail in Appendix A.2. The concentration in the extract was then measured and calculated based on the calibration curve equation derived.

## **2.8. Biological Analyses**

### **2.8.1. Overview of Bioanalytical Method Selection**

While chemical analysis focuses on the detection of individual known pollutants, bioanalytical methods compensate for the unknown pollutants as well as the pollutants below the detection limit as the bioactivity of the entire sample is being evaluated [87]. Additionally, when various chemicals are mixed, they can interact with each other and together they may lead to more harmful effects, which cannot be quantified by chemical analysis but can be captured using bioanalytical tools [87], [88]. Without the need to harm animals, *in vitro* bioassays are cell-based toxicity testing carried out under controlled conditions in a test tube or microtitre plate [87]. Three *in-vitro* bioassays that represent non-specific, specific, and reactive toxicities were employed to assess the efficiency of CBR to remove biological activity (cytotoxicity, estrogenicity, mutagenicity). Barrow et al. [89] recently showed the utility of 7 bioassays (including the ones employed here) to assess the baseline conditions in the Athabasca River prior to the potential release of treated OSPW, and found that these bioassays are representative in assessing the potential cell toxicity pathways elicited by OSPW and domestic wastewaters.

The membrane filtration technique was employed to measure the removal/inactivation of total coliform bacteria, a commonly used indicator bacteria for the presence of pathogens, in municipal WWTP effluent. As some of the preliminary experiments showed the potential of CBR in removing turbidity from municipal WWTP effluent and high alkalinity was released

from CBR into the wastewater during treatment, it was hypothesized that CBR could potentially remove microorganisms via sweep-floc precipitation or directly inactivate microorganisms due to its caustic nature.

### **2.8.2. Cytotoxicity**

Depending on the sample matrix and its extraction factor, a volume of 40-400  $\mu\text{L}$  of SPE extract was taken and evaporated to dryness by blowing under a gentle stream of  $\text{N}_2$ . The dried extract was reconstituted with water containing 2% salinity [90]. The pH of the reconstituted sample was raised to between 6 and 8.5 using 1N NaOH. The *Aliivibrio fischeri* bacterial reagent was reconstituted and first stabilized at 4°C for at least 30 min, then stabilized at 15°C for 30 min before exposure. After adding the sample to the 96-well plate for luminescence measurement, two-fold serial dilutions by rows were performed for all wells except for the first row such that 7 concentrations of each sample were analyzed (analysis run in duplicate). The luminescence of the cell solution was measured using the plate reader after exposing it to the sample for 0, 5, 10, 15, and 30 min [85]. The sample temperature was controlled at 15°C using a cooling rack (Torrey Pines Chilling/Heating Dry Bath) throughout the duration of the analysis. For validation of the assay, 3,5-dichlorophenol was employed for positive control. Lastly, the concentration caused 10% light inhibition after 15min of exposure ( $\text{IC}_{10_{15\text{min}}}$ ) for the sample was determined following the data analysis procedure analysis described by Barrow et al. [85] in Table 3.

### **2.8.3. Estrogenicity**

Prior to the assay, the stock solutions for yeast culturing were prepared by mixing and dissolving the chemicals in Milli Q ultrapure water at specified concentrations as listed in Appendix A.3. Appendix A.3 also includes the sterilization methods through autoclaving or filtration with 0.2  $\mu\text{m}$  filter unit (Nalgene Rapid-Flow disposable bottle top filters with PES

membrane), and storage temperatures for the stock solutions prepared. Agar plates for the inoculation of yeast were prepared by firstly mixing 78 mL ultrapure water, 10 mL YNB without amino acids solution and 2 g of bactoagar in a 250 mL round glass bottle. The mixture was autoclaved, and after cooling to touch, 10 mL of 20% dextrose, 1 mL of histidine, and 1 mL of lysine solution were added and mixed. The agar solution was then poured onto the Petri dishes, and the agar plates were stored at 4°C upside down until use.

To prepare the cell solution for the assay, the yeast cell stock solution was taken out from the -80°C freezer and was thawed at 4°C. After thawing, 50 µL of the cell solution was pipetted onto a corner of the agar plate and dried for 30 min in the biosafety cabinet. Following drying, plate streaking was performed to distribute the yeast cells across the plate for the formation of isolated colonies. The plate was incubated at 30°C upside down for 3-4 d for colonies to develop and was stored in the 4°C fridge for no longer than 2 weeks for use.

The YES assay can be divided into four parts. The first part involves the inoculation of yeast in an aqueous media. Firstly, to two 15 mL conical tubes 1 mL of gold media is added. Then, 1 colony-forming unit (CFU) of yeast was transferred from the petri dish into each tube. Lastly, the tubes were incubated at 30°C with orbital shaking at 300 rpm for 18–24 h.

After the first day of incubation, one cultured tube was used for checking cell growth, while the other one was refreshed for later use in the assay. Firstly, the spectrophotometer was blank by reading the absorbance at 660 nm of 3.6 mL fresh gold media in a cuvette. Following this, the optical density was checked by reading the absorbance at 660 nm of the mixture combining 0.9 mL of cell solution from the cultured tube and 2.7 mL of gold media – the assay was continued only if the reading was around or slightly greater than 1 (ranged from 1 to 1.3 in the experiment). After optical density checking, 9 mL of minimal media was combined with 1

mL of cell solution from the other cultured tube in a flat bottom flask, which was expected to have similar cell density as the one inspected using the spectrophotometer. The flask was incubated at 30°C at 300 rpm for 18-24 h.

The third part involves the storage of yeast cells, preparation of the seeding solution, as well as exposure of cells to samples. To start with, after the second day of incubation, 100  $\mu$ L of cells were mixed with 100  $\mu$ L of 30% glycerol in a microcentrifuge tube and stored at -80°C for future YES assays. For the remaining cell solution, another 10 mL of minimal media was added, and the flask was incubated at 30°C at 300 rpm for another 4-6 h. To prepare the seeding media, 20 mL minimal media was mixed with 100  $\mu$ L of 10 mM CuSO<sub>4</sub> pentahydrate in a 50 mL glass beaker, and 3.6 mL of this mixture was taken to blank the spectrophotometer (absorbance at 660 nm). Cells from the flat bottom flask were added to the mixture in small increments until the absorbance reading reached around 0.03. To prepare the sample for exposure, a pre-determined amount of sample (40-200  $\mu$ L), was pipetted into the 96-well plate. Two-fold dilutions by row were performed such that 8 concentrations of each sample were analyzed, and the analysis was run in duplicates. Next, the diluted extracts were transferred into 2 mL amber vials where methanol in the extracts were left to evaporate to complete dryness inside a biosafety cabinet. In this experiment, estradiol (E2) was implemented as the positive control compound for validation of the assay. Finally, 200  $\mu$ L of the seeding media prepared previously was added to all the sample vials, and the vials were capped and incubated at 30°C at 300 rpm for 18-24 hrs. Also at this time, the  $\beta$ -gal reagent (2X  $\beta$ -galactosidase assay buffer) was transferred from the -20°C freezer to the 4°C fridge for thawing.

Following exposure to samples for 18-24 h, 25  $\mu$ L solution from each 2 mL amber vial was transferred into a clear 96-well plate, and to each well 75  $\mu$ L of minimal media was added.

The absorbance at 660 nm of the plate was measured in the plate reader for the quantification of cell growth. Then to quantify the estrogenic response, the absorbance at 420 nm was read after adding 100  $\mu$ L of a combined mixture of 5 mL  $\beta$ -gal and 5 mL Y-PER to each well. Finally, the concentration that caused a 10% effect (EC10) and the E2 equivalence (E2EQ) were calculated for each sample following the data analysis method by Barrow et al. [85], as shown in Table 3.

#### **2.8.4. Mutagenicity**

The mutagenicity assay performed in this study followed the procedure without S9 activation provided in the UMU-ChromoTest kit from EBPI with minor modifications to the plate arrangement following Barrow et al [85], [91]. Prior to analysis, the dried bacteria were rehydrated in growth media with nutrients added and incubated at 37°C and 100 rpm for 16-18 h to achieve the ideal growth. A pre-determined amount of SPE extract (40-500  $\mu$ L) was taken and evaporated to dryness under N<sub>2</sub> blowing. The dried extract was reconstituted with 0.85% sterile saline water containing 10% dimethyl sulfoxide (DMSO). The pH of the reconstituted sample was adjusted to  $7.0 \pm 0.2$  using 1N NaOH. In the 96-well plate, the sample was diluted by two-fold five times such that 6 different concentrations were analyzed, and each sample was analyzed in duplicates. For validation of the assay, 4-Nitroquinoline 1-oxide (4-NQO) was employed as the positive control chemical. Glucose and growth media solution was added to the wells to provide nutrients for cells.

The growth of the incubated bacteria was evaluated by the absorbance at 600 nm. Once the ideal cell density was obtained, the bacteria were combined with fresh growth media and incubated for another 1.5 h at 37°C and 100 rpm. The absorbance at 600 nm of the reinoculated bacteria was inspected again, and the bacteria were added to the microplate containing the prepared samples. The plate was incubated for 2 h at 37°C and 100 rpm. Following this, samples

were transferred to a second microplate that contains growth media and glucose in the wells, and the absorbance at 600 nm of the second plate was read. The second plate was incubated for 2 hrs at 37°C and 100 rpm, and after that, the absorbance at 600 nm was measured once again to determine the cell growth/inhibition during this 2-h incubation period. Then, samples from the second plate were transferred to a third plate that contains a mixture of 2-mercaptoethanol and B-Buffer reagent. ONPG reagent was added to all the wells in the third plate and the plate was incubated for 30 min at 37°C and 100 rpm to allow for any color development. The mutagenic response was measured by the absorbance at 420 nm. Finally, the sample concentration that caused an induction ratio of 1.5,  $EC_{IR1.5}$  were determined using the data analysis method described by Barrow et al. [85] in Table 3.

**Table 3.** Data analysis methods adapted from Barrow et al. [85]. RLU = relative light units, OD = optical density, IR = induction ratio, A = absorbance.

Assay Type	Validation	Data Analysis
<i>Aliivibrio Fischeri</i> toxicity assay	Positive control is 3,5-dichlorophenol.  In this study, IC10 <sub>15min</sub> =8.3±0.3mg/L	<ol style="list-style-type: none"> <li>Calculate % Inhibition from the raw RLU using the equation below:  <math display="block">\% \text{ Inhibition} = 1 - \frac{\text{RLU}_{\text{sample,t min}}}{\text{RLU}_{\text{sample,0}} * \frac{\text{RLU}_{\text{blank,t min}}}{\text{RLU}_{\text{blank,0}}}}</math> </li> <li>Normalize % Inhibition from 0 - 100%</li> <li>Complete a Ligand Binding-Sigmoidal Dose response regression using log concentration and average normalized % Inhibition (on Sigmaplot)</li> <li>Calculate IC<sub>10</sub> using parameters obtained from regression fitting</li> </ol>
YES assay	Positive control and reference compound is 17β-estradiol (E2).  In this study, EC10=52.8±48.0ng/L	<ol style="list-style-type: none"> <li>Calculate the β-Galactosidase (β-Gal) response using the raw cell density (OD<sub>660</sub>) and raw β-Gal data (OD<sub>420</sub>). Note that at OD<sub>420</sub> only absorbance values between 0.2 to 1.0 were included in the analysis.  <math display="block">\text{BGal response} = \frac{1000 * \text{slope}(\text{raw Bgal data})}{\text{volume of cells plated (mL)} * \text{average OD}_{660}}</math> </li> <li>Normalize β-Gal response from 0 – 100%</li> <li>Remove cytotoxicity interferences at higher concentrations from the data set</li> <li>Model the data using a 4-Parametric Logistic Equation using concentration and average normalized β-Gal response (on Sigmaplot)</li> <li>Calculate EC<sub>10</sub> using parameters obtained from regression fitting</li> <li>Calculate the E2-EQ of each sample using the EC<sub>10</sub> of E2</li> </ol>
UMU-ChromoTest assay	Reference compound and positive control is 4-nitroquinoline 1-oxide (4-NQO).  For validation, the IR of 4-NQO at 5.26 μM must be at least 2.  In this study, IR <sub>5.26μM</sub> =5.8±1.7, EC <sub>IR1.5</sub> =118.4±43.6μg/L	<ol style="list-style-type: none"> <li>Determine the β-Galactosidase (β-Gal) activity using the following equation:  <math display="block">\beta - \text{Galactosidase activity} = \frac{A_{420\text{sample}} - A_{420\text{blank}}}{A_{420\text{negative control}} - A_{420\text{blank}}}</math> </li> <li>Determine the growth factor (G) using the following equation:  <math display="block">\text{Growth factor} = \frac{A_{600\text{sample}} - A_{600\text{blank}}}{A_{600\text{negative control}} - A_{600\text{blank}}}</math> <p>Note: G must be greater than 0.5 for results to be considered valid</p> </li> <li>Find the IR by dividing the β-Gal by G.  <p>Note: For a sample to be considered mutagenic, IR must be &gt; 1.5</p> </li> <li>Find the slope by fitting the data to a linear trendline with a y-intercept of 1</li> <li>Find the EC<sub>IR1.5</sub> for each sample using the following equation:  <math display="block">\text{EC}_{\text{IR1.5}} = \frac{0.5}{\text{slope}}</math> <p>Calculate the 4-NQO-EQ using the EC<sub>IR1.5</sub> of 4-NQO</p> </li> </ol>



### 2.8.5. Membrane Filtration Technique for Total Coliform

To prepare for the total coliform test, 51 g of mLES Endo agar and 27 mL of 70% ethanol were added to 1 L of deionized water. The solution was heated to boiling to dissolve the agar. Once boiled, the solution was cooled to around 50°C and poured onto the 47 mm-diameter polystyrene Petri dishes (Fisherbrand). Once the agar solidified, the plates were stored at 4°C in dark upsides down for no more than two weeks prior to being used.

Prior to membrane filtration, the sample was mixed with water to make up a total volume of at least 30 mL such that the bacteria can spread out more evenly on the filter. The samples were each run through the Whatman mixed cellulose ester membrane filter with 0.45µm pores and 47mm diameter. The filter paper was transferred to the premade agar plate, and the plate was incubated at 35°C for 24 h (Corning LSE Benchtop Shaking Incubator). The next day, the number of total coliform colonies grown (with green- and gold-sheen reflection) were counted and converted to colony-forming units (CFU) per 100 mL of the sample using *EQN 8*:

$$\frac{CFU}{100 \text{ mL}} = \frac{CFU \text{ counted}}{\text{Volume of the original sample filtered (mL)}} \times 100 \text{ mL} \quad (EQN 8)$$

## 2.9. Neutralization with Acetic Acid and Leaching Analysis

Acetic acid, an organic acid, was selected for the neutralization of CBR or CBR-treated wastewater to prevent the introduction of hazardous anions such as chlorine and sulfate when using inorganic acids. As illustrated in Figure 6, two neutralization methods – pre-treatment neutralization (neutralization of CBR before water treatment) and post-treatment neutralization (neutralization of the CBR-treated water) were explored and their efficiencies to reduce leaching of metal ions and anions from CBR in treatment were compared. This leaching test was performed in Milli Q ultrapure water.

In the pre-treatment neutralization method, 30g of CBR was first made into a concentrated slurry by mixing it with a small amount of ultrapure water (~50 mL) in a 1L beaker. Then concentrated acetic acid (~0.8 mL) and a very small amount of 10N NaOH (~0.2 mL) were added to neutralize the slurry until the pH reached about 6. At this point, neutralization of the CBR slurry was finished and the CBR slurry was ready for treating water – more water (~550 mL) was added to the CBR slurry until an adsorbent dosage of 50 g/L was reached. The solution was left mixed in a jar tester at 120 rpm for 24 hours. The 24-h duration was chosen to ensure that maximum adsorption and leaching were achieved at the time of water sample collection. At this stage, the optimal operating conditions including the reactor type, mixing intensity, and retention time had not yet been determined. At the end of the mixing, it was observed that the pH of the solution raised to ~8.5. After settling by gravity for 30 min, the supernatant was filtered with the 1 $\mu$ m-pore glass fiber filter. The filtered sample was sent for the analysis of dissolved metals and anions at Bureau Veritas, Edmonton. Because it was unknown if an advanced separation process would need to be in place after gravity sedimentation in the real application

scenario, an unfiltered supernatant sample was collected and sent for the analysis of total metals (accounting for both particulate and dissolved fractions).

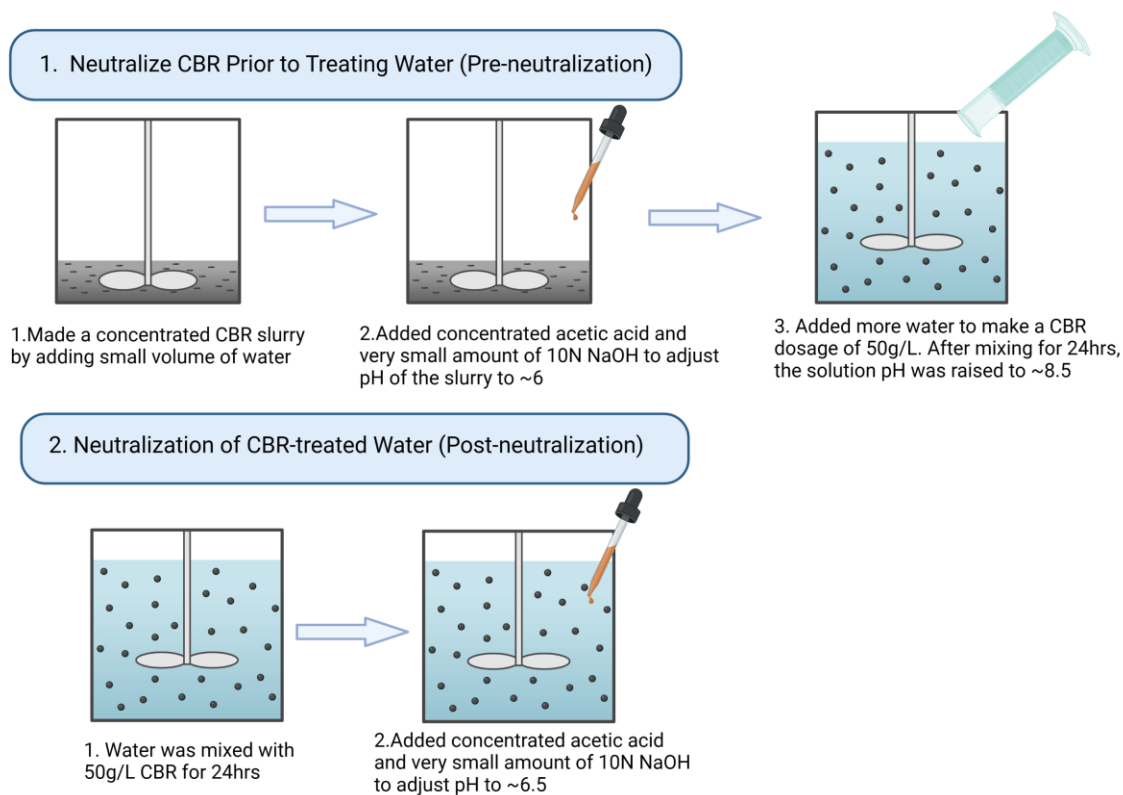


**Figure 6.** Neutralization of CBR with acetic acid. The image is drawn with BioRender.

In the post-treatment neutralization method, CBR was directly applied to the water at the dosage of 50 g/L (to 900 mL Milli Q ultrapure water added 45g of CBR). The solution was left stirring in the jar tester at 120 rpm for 24 h. Toward the end of the 24-h mixing, the solution pH was lowered using concentrated acetic acid (~1 mL) and a small amount of 10N NaOH (~0.1 mL) in total until a pH of about 6.5 was reached. It was noted that this pH adjustment was not completed in one go – the solution pH kept rising back up a few minutes after the pH adjustment. Therefore, each time acetic acid was added to neutralize the pH, the solution would be left to stir for another 5 min. After 5 min, the solution pH was measured and adjusted again with acetic

acid. This pH adjustment and waiting process was repeated about three to four times until the final solution pH was stabilized within a neutral pH range. After 30 min sedimentation, the supernatant was filtered with the 1 µm glass fiber filter and sent for chemical analysis. Likewise, an unfiltered supernatant was also analyzed for total metals after post-treatment neutralization.

Similarly, a non-neutralized sample was prepared by mixing 50g/L CBR or raw bauxite residue with ultrapure water at 120 rpm for 24 h (to 600 mL ultrapure added 30g CBR/raw bauxite residue). The raw bauxite residue was included here to compare the impact of calcination pretreatment on leaching from bauxite residue. In addition, to determine the significance of the concentration leached out, the results of dissolved metals and anions in the non-neutralized, pre-neutralized, and post-neutralized samples were compared with the guideline values for the protection of freshwater aquatic lives by CCME [45] whenever available. Noted that the guideline is not for end-of-pipe discharge compliance but rather for assessing qualities of the water bodies, hence it might be more stringent than discharge limits (conditions of the receiving water body such as dilution capacity will be taken into consideration).

With few exceptions, most guidelines target total concentration rather than the dissolved fraction to take into consideration different exposure pathways and the particulate fraction becoming more bioavailable over time [92]. In this study, however, the concentration of total metals was analyzed but was not compared to the guidelines for any exceedances because the concentration of total metals in the final effluent for discharge was expected to be different from the ones obtained. In real wastewater treatment applications, the particulates will need to be further removed via separation processes, meaning metals that bind to the particulates would also be eliminated. Thus, the total concentrations obtained for the unfiltered supernatant would not be representative of the final effluent that is usually obtained in practice.

Lastly, unlike in most other studies where neutralization of bauxite residue was completed as a stand-alone pretreatment process, neutralization was carried out together with wastewater treatment and directly utilized the wastewater as the aqueous medium for the dilution concentrated acid and for the contact between CBR and acids in this study. This approach was employed to prevent additional generation of wastewater, the cost with separating and drying the neutralized solids, and the cost required to build the facility for a stand-alone process.

### 3. Results and Discussions

#### 3.1. Material Characterization

The SEM images (Figure 7) show that the particles of both raw bauxite residue and CBR vary in size (ranging from ~10 to 100  $\mu\text{m}$ ) and morphology. The EDX results further suggest that the particles found in raw bauxite residue and CBR can be divided into two categories: (1) carbonaceous (containing >70% carbon by weight and <10% metals) and (2) inorganic (containing <20% carbon content). The CBR inorganic particles appeared to have rougher surfaces and they are highly rich in metals with a distribution of 23.0% Fe, 8.6% Al, 7.1% Na, 2.4% Ti, 0.63% Ca, and 0.13% Cr on average (Table 4). The inorganic raw bauxite residue particle has a similar composition to that of CBR indicating that the calcination pretreatment process did not significantly alter the elemental composition by weight of the bauxite residue material. The agglomerates formed at the surface of the inorganic particles potentially enlarged the surface area of bauxite residue and provided more sites for adsorption. Lastly, macropores were observed on the carbonaceous particle of raw bauxite residue but not on that for CBR, possibly due to the oxidation of carbon during calcination pretreatment.

Phase search was conducted based on the elements identified previously from EDX and the assumption that after calcination pretreatment, most of the mineral phases would be converted to mineral oxides. The XRD results (Figure 8) show that CBR consists of both amorphous and crystalline phases. The major crystalline phases of CBR include magnetite ( $\text{Fe}^{+2}\text{Fe}^{2+3}\text{O}_4$ ), hematite ( $\text{Fe}_2\text{O}_3$ ), anatase ( $\text{TiO}_2$ ), quartz ( $\text{SiO}_2$ ), silicon oxide ( $\text{SiO}_2$ ), aluminum oxide ( $\text{Al}_2\text{O}_3$ ), and lime ( $\text{CaO}$ ). Calcite ( $\text{CaCO}_3$ ) was also a common phase in bauxite residue [42], [44], [79], [93] but it was not present in CBR as a major phase, potentially because the high temperature applied during the calcination pretreatment decomposed  $\text{CaCO}_3$  into  $\text{CaO}$  [94].

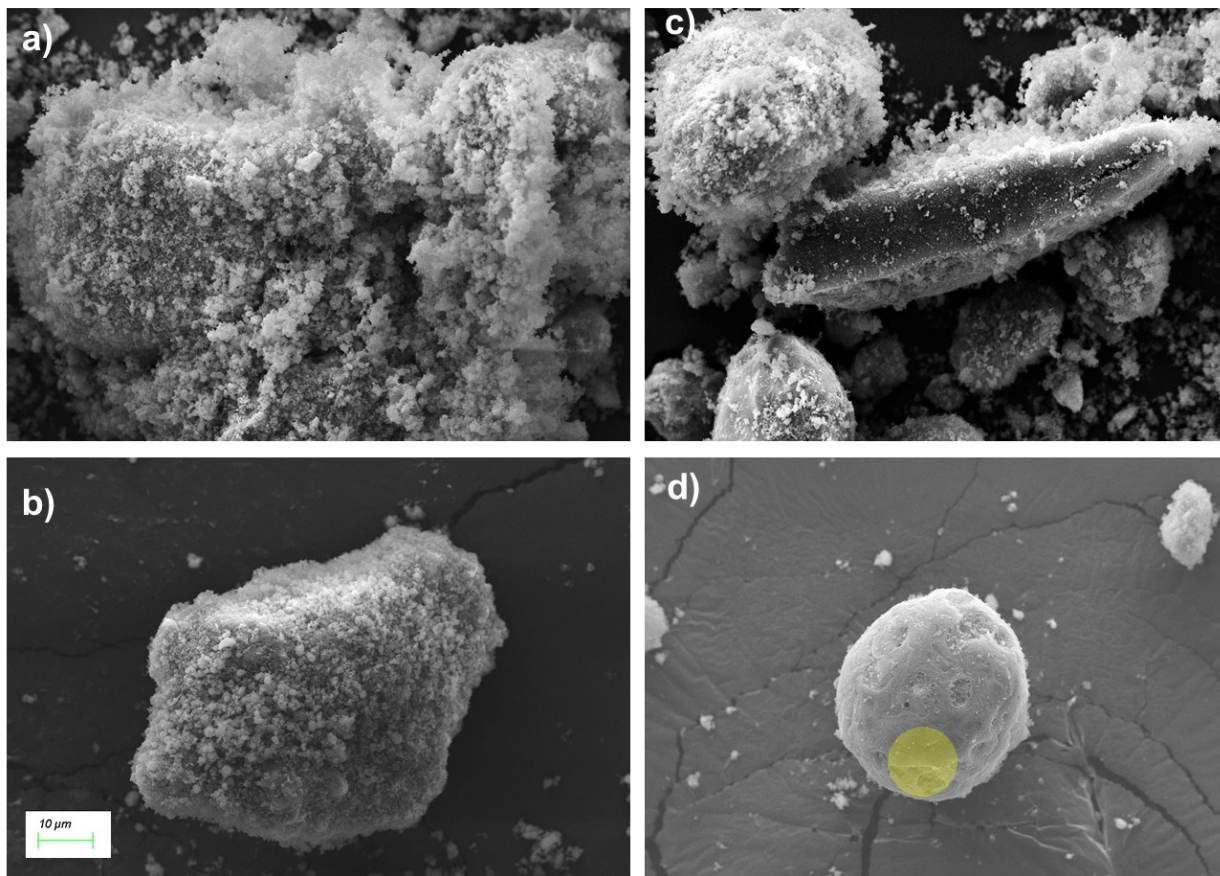


**Figure 7.** Scanning electron microscope (SEM) images of inorganic and carbonaceous components of calcined bauxite residue (CBR) (a, c) and raw bauxite residue (b,d). See Table 4 for the elemental analysis of each component via Energy-dispersive X-ray spectroscopy (EDX). These images were taken at a magnification of 1000x and a working distance of 7.3mm. The yellow highlighted region is a pore observed on the carbonaceous raw bauxite residue particle.

**Table 4.** Energy-dispersive X-ray spectroscopy (EDX) results for calcined bauxite residue (CBR) and raw bauxite residue. \*The spectrum chosen for EDX analysis was shown in Appendix B.1. \*\*The values shown were the average of 2 spectra. Appendix B.1 also displays SEM images of the particles taken at higher magnifications – 2k, 5k, 10k, and 20k)

Percent by Weight	CBR (Inorganic)**	CBR (Carbonaceous)*	Raw Bauxite Residue (Inorganic)*	Raw Bauxite Residue (Carbonaceous)*
C	16.25	76.86	19.53	74.34
O	36.76	13.77	36.68	13.75
Na	7.09	1.25	5.87	0.27
Mg	-	0.20	-	-
Al	8.61	2.03	10.42	3.66
Si	4.86	0.20	5.72	0.54
S	0.25	1.60	0.37	2.40
Cl	0.08	-	0.14	-
K	-	0.07	-	-
Ca	0.63	0.70	0.56	0.11
Ti	2.42	0.23	2.92	0.66
Cr	0.13	-	-	-
V	-	-	-	0.15
Fe	23.02	3.09	17.79	4.11

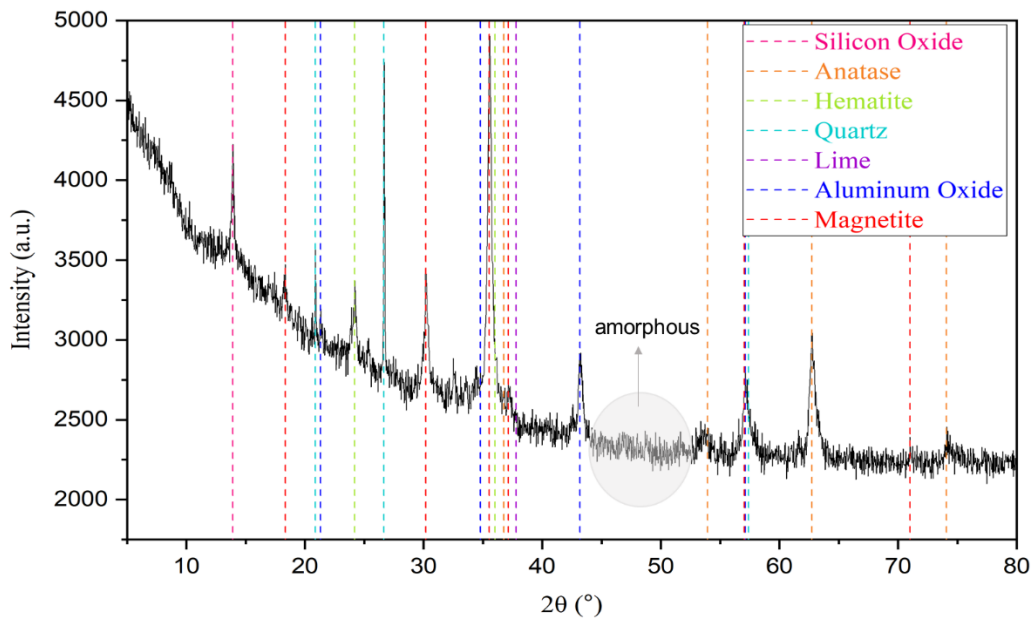


**Figure 8.** X-ray diffraction (XRD) spectrum of the calcined bauxite residue (CBR). The spectrum shows that CBR is semi-crystalline material as shown by the broad features that are typical of the amorphous pattern and XRD peak suggesting crystalline phases.



The BET surface area of CBR is 25.1 m<sup>2</sup>/g and the total pore volume is 0.137 cm<sup>3</sup>/g. Compared to the literature values for some untreated bauxite residue and pre-treated bauxite residue (via neutralization, acid activation, and/or calcination) (Table 5), the BET surface area of the CBR adsorbent is similar to treated bauxite residue adsorbents from other studies, except with the material prepared by Hu et al. [80]. In terms of total pore volume, CBR was much superior compared to most treated bauxite residue adsorbents, again with the exception of the material by Hu et al. [80], indicating that CBR might have a higher capacity for physisorption.

Bauxite residues that were composited with other materials (e.g., sucrose-based carbon and polystyrene microspheres) are about 4-9 times higher in BET surface area and about 2 times higher in total pore volume, but this production process may require additional material and energy costs. The pre-treatment process by Hu et al. [80] that incorporates HCl and ammonium hydroxide treatment followed by heating at 200°C appears to be the most effective among the studies reviewed (their BET surface area and total pore volume were comparable to activated carbon adsorbents) [70]. Hence, it might be attractive to optimize the pre-treatment of CBR to improve water treatment potential. However, the current process for CBR production was designed with the potential recovery of valuable metals from the “spent” CBR. More specifically, the process converts Fe<sub>2</sub>O<sub>3</sub> to Fe<sub>3</sub>O<sub>4</sub> which enables the sufficient recovery of iron from sludge following water treatment. Hence pre-treatment procedures currently explored in the literature may not be amenable for the metal recovery process. Considering that the removal of wastewater pollutants is an added value to the CBR product, this study focused only on evaluating the performance of CBR produced from the already-established pretreatment method.

**Table 5.** BET surface area and total pore volume of some raw and treated bauxite residue from some literature that focused on the application of bauxite residue in water treatment. \*: not included in the calculation for the average BET surface area or total pore volume. \*\*: the bauxite residue was dried at 105 °C for 24 hours for moisture removal.

Treatment Type	BET Surface Area (m <sup>2</sup> /g)	Total Pore Volume (cm <sup>3</sup> /g)	Reference
Raw	8	0.02	[55]
Raw	18.11	0.013	[53]
Raw	11.73	0.03	[48]
Raw	22.7	0.057	[42]
Raw	13.15	0.063	[95]
Raw	28.8	0.129	[96]
Raw	21.0	0.058	[97]
Raw*	56	0.08	[80]
Raw**	22.93	0.047	[79]
<b>Mean ± std. dev</b>	<b>18.3 ± 6.9</b>	<b>0.05 ± 0.04</b>	-
Treated with Gypsum	12.77	0.03	[48]
Treated with Seawater	13.82	0.03	[48]
Treated with HCl	28.48	0.078	[42]
Treated with HCl	23.80	0.109	[95]
Treated with HNO <sub>3</sub>	38.15	0.066	[42]
Treated with HNO <sub>3</sub>	31.9	0.056	[97]
Treated with heat (300 °C)	18.01	0.017	[79]
Treated with heat (800 °C)	10.1	0.033	[97]
Treated with HCl and heat (700 °C)	33.78	0.093	[42]
Treated with HCl and heat (900 °C)	26.46	0.111	[95]
Treated with HNO <sub>3</sub> and heat (700 °C)	33.33	0.097	[42]
Treated with HCl and ammonium hydroxide and dried at 105 °C*	207	0.31	[80]
Treated with HCl and ammonium hydroxide, dried at 105 °C, and annealed at 200 °C*	381	0.90	[80]
<b>Mean ± std. dev</b>	<b>24.6 ± 9.6</b>	<b>0.07 ± 0.03</b>	-
Composited with sucrose-based carbon	105.090	0.219	[53]
Synthesized with polystyrene microspheres	232	0.27	[55]

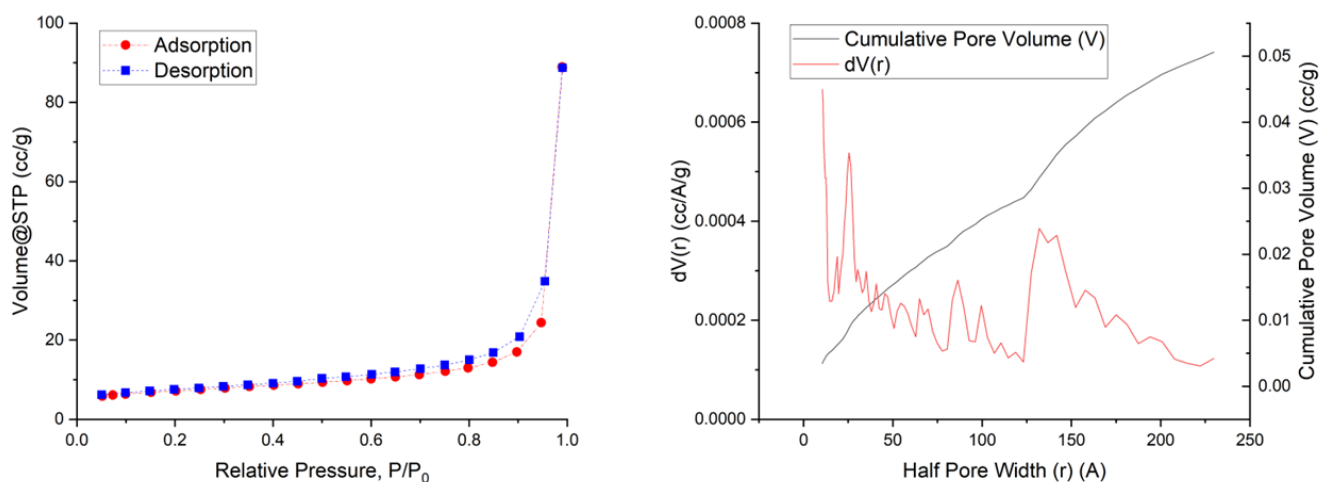


**Figure 9.** *N<sub>2</sub> adsorption and desorption curve (left) and the corresponding Density Functional Theory (DFT) pore size distribution (right) of CBR. The y-axis of the pore size distribution curve  $dV(r)$  refers to the volume of pores with radii between  $r$  and  $r + dr$  [98].  $1 \text{ \AA} = 0.1 \text{ nm}$ .*

According to the classification of physisorption isotherm by the International Union of Pure and Applied Chemistry (IUPAC), the adsorption and desorption curve of  $N_2$  by CBR (Figure 9 left) follows type V isotherm the most closely, such that, at lower pressures, there is negligible monolayer formation and little adsorption occurs as the interaction between the absorbent (the surface of CBR) and the adsorbate ( $N_2$ ) is relatively weak. At higher pressures, adsorption increases due to the clustering of adsorbate ( $N_2$ ) molecules and the filling of pores [99]. The hysteresis between the adsorption and desorption curves suggests the presence of pores in CBR [99]. Based on the DFT pore size distribution plot (Figure 9 right), the sizes of pores present in CBR are not homogenous. The width of pores ranges from 2 to 46 nm, indicating that the pores in CBR were mostly mesopores (pores with diameters between 2 and 50 nm) [99].

Regardless of the physical characteristics of CBR such as pore volume and BET surface area obtained, it is essential to assess the treatment efficacy of CBR in adsorption experiments designed for the targeted pollutants. The study by Huang et al. [42] showed an example in which

the BET surface area and pore volume of bauxite residue was enlarged after pretreatment, the adsorption capacity was reduced as some surface functional groups that can attract the target pollutants were removed during pretreatment.

### 3.2. Removal of Methylene Blue (MB)

Given the potential for CBR as an adsorbent material as per the characterization results above, experiments via the removal of MB were first completed to establish preliminary outcomes that can direct further water treatment experiments related to CBR (i.e., dosage, equilibrium, kinetics, isotherm). The results (Figure 10) showed that CBR 60 g/L CBR was able to reduce 20 mg/L MB by 94% within 45 min, indicating that CBR has the potential for the removal of organic dyes from textile wastewater and other industrial wastewaters contaminated by organic dyes. Additional CBR doses evaluated include 5 g/L (15% removal), 10 g/L (25% removal), 20 g/L (46% removal), and 40 g/L (78% removal).

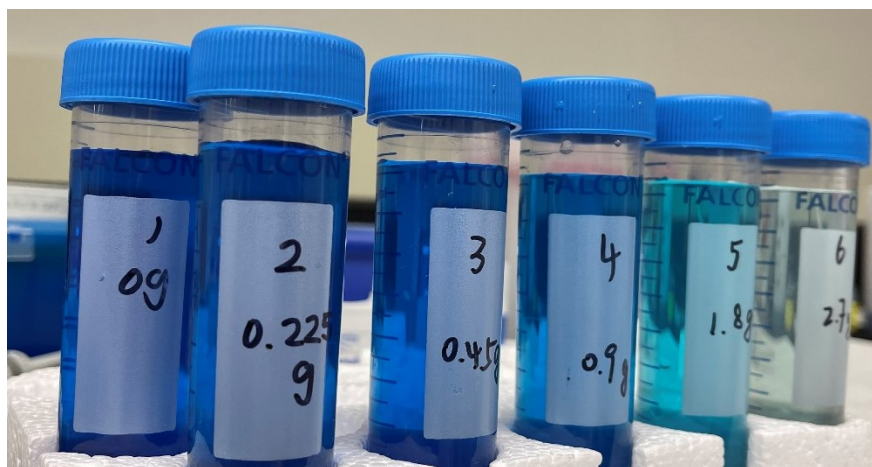


**Figure 10.** Visual quality of MB removal solutions after 45 min treatment with CBR.

The kinetic study results (Table 6 and Figure 11) showed that the adsorption of MB by CBR poorly fitted the pseudo-first-order kinetic model ( $R^2$  range from 0.842 to 0.949 and the calculated  $q_e$  were far from the experimentally determined  $q_e$ ). Instead, adsorption kinetics

followed the pseudo-second-order model ( $R^2$  range from 0.984 to 1.000 and the calculated  $q_e$  were close to the experimentally determined  $q_e$ ), suggesting chemisorption is the rate-limiting step [24]. This result is consistent with the findings by [53], [79], [80] that the pseudo-second-order model described the removal of MB by bauxite residue better compared to the pseudo-first-order kinetic model. Therefore, if sufficient contact time was provided for the adsorption to reach equilibrium, complete removal of 1 mg of MB from water will require  $\sim 1.0$ – $1.1$  g of CBR. The rate of adsorption  $k_2$  and the amount adsorbed at equilibrium ( $q_e$ ) varied with CBR adsorbent dosages (Table 6) and initial MB concentrations. When CBR is applied in excessive amounts (higher than the dosage needed to remove MB), adsorption will occur faster (shorter contact time), but still leaving plenty of adsorption sites for other adsorbates.

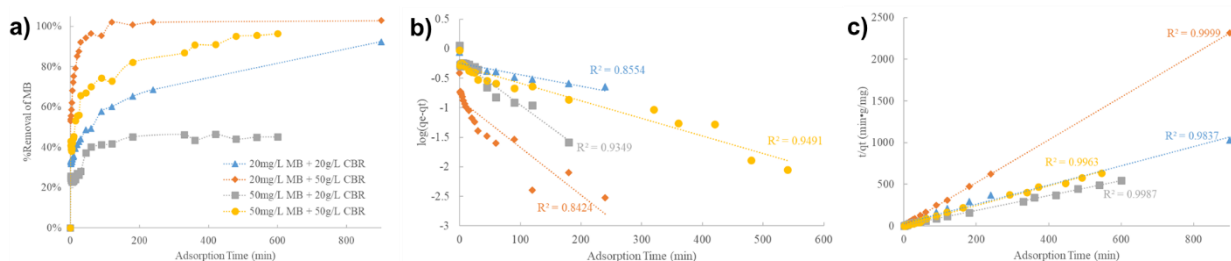


**Figure 11.** The adsorption kinetics for methylene blue (MB) by calcined bauxite residue (CBR) (no neutralization). (a) %Removal of MB at different times. (b) Fitting of the data to pseudo-first-order kinetic model. (c) Fitting of data to pseudo-second-order kinetic model. The adsorption kinetic data were fitted following the method described in [23].

**Table 6.** Adsorption kinetic parameters obtained for the removal of methylene blue (MB).  $t_e$  (min) = time to reach equilibrium (determined experimentally).  $q_e$  (mg/g) = the amount of adsorbate adsorbed at equilibrium.  $k_1$  (/min) = the equilibrium rate constant for the pseudo-first-order kinetic model.  $k_2$  (g/mg/min) = the equilibrium rate constant for the pseudo-second-order kinetic model.

Initial MB (mg/L)	CBR Dosage (g/L)	Observations		Pseudo-first-order Kinetic Parameters				Pseudo-second-order Kinetic Parameters		
		Maximum Removal	$t_e$ (min)	$k_1$ (/min)	Experimental $q_e$ (mg/g)	Calculated $q_e$ (mg/g)	$R^2$	$k_2$ (g/mg/min)	$q_e$ (mg/g)	$R^2$
20	20	92%	<900	0.0044	0.874	0.563	0.855	0.0446	0.867	0.984
20	50	100%	120	0.0186	0.389	0.137	0.842	0.802	0.390	1.000
50	20	46%	330	0.0173	1.129	0.630	0.935	0.118	1.114	0.999
50	50	96%	540	0.0068	0.943	0.521	0.949	0.0817	0.939	0.996

**Table 7.** Pseudo-second-order kinetic parameters for the adsorption of methylene blue by bauxite residue adsorbents in literature.

MB Concentration (mg/L)	Treatment of Bauxite Residue	Bauxite Residue Dosage (g/L)	$k_2$ (g/mg/min)	$q_e$ (mg/g)	$R^2$	Reference
500	Dried at 105°C to remove moisture	5	1.915	1.222	0.998	[79]
25	Composited with sucrose-based carbon	1	0.030	22.51	0.999	[53]
50	Composited with sucrose-based carbon	1	0.019	47.86	0.999	[53]
100	Treated with HCl and ammonium hydroxide and dried at 105°C	1	0.011	95.2	1.000	[80]
100	Treated with HCl and ammonium hydroxide, dried at 105°C, and annealed at 200°C	1	0.011	90.8	1.000	[80]

The adsorption rate ( $k_2$ ) and adsorption capacity ( $q_e$ ) derived from the pseudo-second-order kinetic model of CBR are similar to the moisture-free bauxite residue [79] (Table 7). However, the adsorption capacity of CBR is much smaller compared to bauxite residue composited with sucrose-based carbon [53] and the bauxite residue prepared by Hu et al. [80], possibly owing to the superior specific surface area and porosity.

The MB removal curve from the adsorption isotherm study confirms the finding from prior kinetic studies, i.e., at equilibrium conditions, ~1 g of CBR is needed per mg of MB to achieve complete removal of MB (Figure 12a). The adsorption capacity generally increases with higher residual MB concentration (Figure 12b). Furthermore, adsorption isotherms studies have indicated the MB adsorption by CBR follow either Langmuir or Freundlich isotherm models with good correlations ( $R^2 > 0.85$ ) (Table 8). However, this study found the adsorption by CBR did not fit the Langmuir model ( $R^2 < 0.5$ ) (assumes monolayer adsorption and homogenous adsorption sites) and only fitted slightly better with the Freundlich model ( $0.39 < R^2 < 0.68$ ) (multi-layer adsorption and heterogeneous adsorption sites), as shown in Figure 12c,d.

The poor fit with the Langmuir and Freundlich isotherm models could be caused by (1) the inhomogeneity of particles in the CBR adsorbent (2) the change in pH by different dosages of CBR. Firstly, as mentioned earlier in Section 3.1, the CBR used in this study consists of two types of particles (inorganic and carbonaceous), suggesting that multiple adsorption mechanisms might be at play. Although exploring the differences between two particle types might be ideal, it is currently difficult to separate these materials from the bulk CBR. Secondly, the increase in CBR dosage would have led to an increase in pH of the MB solution during treatment, but studies have shown that the adsorption of MB by bauxite residue is pH-dependent [79]. Other isotherms suggesting adsorption mechanisms different than the conventional Freundlich and

Langmuir models might be worth exploring (e.g., Redlich Peterson, Langmuir-Freundlich, Dubinin-Radushkevich, etc.) [24]. Alternatively, it might be desirable to attempt starting with the determination of optimal dosage of adsorbent and pH for the removal of MB and then proceed with the adsorption isotherm experiment by varying initial concentration of the MB adsorbate as a next step, but this is currently out of scope of this thesis.

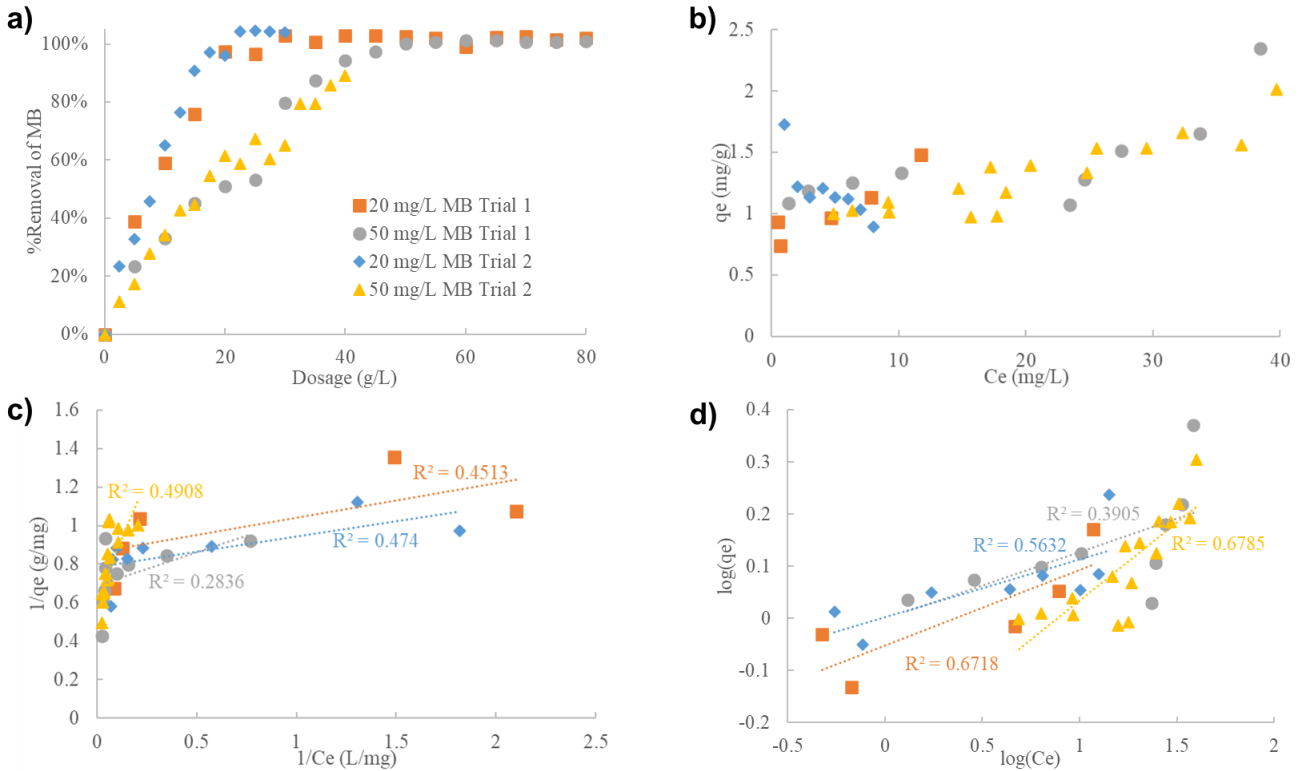


**Figure 12.** The adsorption isotherms for methylene blue (MB) using different dosages of calcined bauxite residue (CBR) (no neutralization). (a) Removal (%) of methylene blue (MB) at different doses of CBR at equilibrium. (b) Adsorption capacity at different equilibrium MB concentrations. (c) Fitting of data to Langmuir adsorption isotherm model. (d) Fitting of data to Freundlich adsorption isotherm model. The adsorption isotherm data were plotted following the method described in [23]. The concentration shown in the legend refers to the initial concentration of MB.



**Table 8.** Langmuir and Freundlich adsorption isotherm parameters for methylene blue (MB) removal found in literature and obtained from this study. \*the corresponding water temperature was 30 °C (in this study the water temperature was at room temperature around 20 °C); \*\*: values were converted from mol-based unit to mg-based using the molecular weight of methylene blue (319.85 g/mol); \*\*\*: isotherm parameters calculated for this study considered only data from the second trial - the second trial of the experiment used smaller increments of dosages from 0 g/L to roughly the dosage added was expected to be just enough to reach 100% MB removal; \*\*\*\*: the unit displayed in the original paper was L/mg.

Reference	[33]*	[53]	[79]	[80]	This Study***		
Adsorbent (g/L)	10	1	Not Specified	1	0-20	0-40	
Initial MB (mg/L)	32-352**	10-500	10-60	100-300	20	50	
Langmuir Adsorption Isotherm Model							
$K_L$ (L/mg)	0.000560**	0.250	0.057	0.056	0.032	4.956	0.268
$Q_m$ (mg/g)	0.167**	76.923	6.541	232.2	274	1.272	1.571
$R^2$	$\geq 0.9534$	0.998	0.993	0.99	0.86	0.474	0.491
Freundlich Adsorption Isotherm Model							
$K_F$ (mg/g)·(L/mg) <sup>1/n</sup>	$4.57 \cdot 10^{-5}$	27.797	0.747	38.70****	28.68****	1.005	0.546
$n$	0.24	5.102	2.012	2.24	1.38	8.977	3.362
$R^2$	$\geq 0.9135$	0.851	0.989	0.96	0.98	0.563	0.679
Treatment of Bauxite Residue	hydrogen peroxide and heat (500 °C)	composited with sucrose-based carbon	Dried at 105 °C	HCl and ammonium hydroxide then dried at 105 °C	HCl and ammonium hydroxide, dried at 105 °C, and annealed at 200 °C	Calcination Pretreatment by GRÖN	

### 3.3. Removal of Commercial Naphthenic Acids (NAs)

CBR can remove both Sigma NAs and cyclohexanecarboxylic acids from the aqueous phase as displayed in Table 9. At a dosage of 20 g/L, CBR removes Sigma NAs and cyclohexanecarboxylic acid by 33.4% and 48.8%, respectively. Additionally, the IC<sub>10</sub><sub>15min</sub> of the untreated sample (spiked with cyclohexanecarboxylic acids) was  $2.45 \pm 0.79$  REF (relative enrichment factor) and  $4.89 \pm 1.71$  REF for the treated sample, indicating cytotoxicity was reduced after treatment. Hence, there is a potential for CBR as a treatment option for oil sands process-affected water (OSPW). However, the plan to optimize the CBR dose and subsequent bench-scale operation did not proceed due to the low recovery of chemicals measured via FTIR analysis (Table 9). The recovery obtained for Sigma NAs was similar to the recovery value reported in Samanipour et al. [100] where a similar SPE process was employed (an average recovery of 44.7% was obtained over a wide range of NAs tested). The recoveries of the same chemical for experiments performed on different days were also not consistent during preliminary testing (results not shown).

**Table 9.** *The removal of Sigma NAs and cyclohexanecarboxylic acid by 20 g/L CBR.*

	Initial Concentration (mg/L)	Recovered from Untreated (mg/L)	Recovered from Treated (mg/L)	Average Removal* (%)	Average Recovery** (%)
<b>Sigma NAs</b>	20	$9.72 \pm 0.61$	$6.47 \pm 0.90$	33.4	48.6
<b>Cyclohexane carboxylic Acid</b>	80	$49.53 \pm 10.48$	$25.34 \pm 0.95$	48.8	61.9

$$*: \text{Removal} = \frac{\text{Recovered from Untreated} - \text{Recovered from Treated}}{\text{Recovered from Untreated}} \times 100\%$$

$$**: \text{Recovery} = \frac{\text{Nominal Spiked Concentration} - \text{Recovered from Untreated}}{\text{Initial Concentration}} \times 100\%$$

As it was assumed that the major loss of chemicals likely occurred during the sample extraction process (SPE), an attempt to improve the recovery were completed via the use of a different SPE cartridge (ISOLUTE C8/ENV+ 400mg/6mL from Biotage, US) as in Samanipour et al. [100]. An assessment of dichloromethane as the elution solvent for SPE was also completed (instead of methanol and ethyl acetate as described in Section 2.6). Given that dichloromethane is the solvent used in FTIR analysis, employing the same solvent during SPE allowed for the immediate storage and analysis of extracts without undergoing evaporation and reconstitution (i.e., minimizing the loss of volatile chemicals). The complete procedure and results for this experiment are described in Appendix B.2. Overall, the recoveries obtained from both cartridges (Oasis HLB vs ISOLUTE ENV+/C8) were low, ranging from 15% to 61%. The Oasis HLB cartridge showed slightly higher recovery of two synthetic OSPWs made of Sigma NAs and cyclohexanecarboxylic acid compared to the ENV+/C8 cartridge. Eluting the cartridges with dichloromethane and analyzing this eluent directly had a notable improvement in the extraction efficiencies, especially for the ENV+/C8 cartridge (improved from 15% to 57%). However, this method brought a slight contamination to the FTIR cell, with a white stain that could not be removed after rinsing with clean dichloromethane. Therefore, it was deemed more appropriate to proceed testing with real wastewater samples due to more consistent results as described in the subsequent sections.

### **3.4. Neutralization with Acetic Acid for the Control of Leaching from CBR**

#### **3.4.1. Treatment of OSPW and Diluted Municipal Effluent Without Neutralization**

Preliminary experiments with real wastewater were conducted, where 100% OSPW and diluted effluent from a tertiary WWTP (5% tertiary treated effluent + 95% river water to represent receiving aquatic environment) were treated with several doses of CBR. It was

observed that the removals of AEOs increased with higher CBR dosage (Table 10), with AEO removals of ~55% at 100 g/L CBR dose. The study by Qin et al. [101] demonstrated that the organic fraction of OSPW, composed primarily of NAs, exhibited significant cytotoxicity (via RAW 264.7 mouse macrophage cell lines) whereas the inorganic fraction of OSPW and whole OSPW were relatively non-cytotoxic. However, despite the removal of AEOs observed in this study, the cytotoxicity, estrogenicity, and mutagenicity did not change substantially after treatment, with some treatment showing increase in toxicities (e.g., 100 g/L CBR, Table 10). This result suggests that there is a possibility of toxic substances leaching from CBR, or more hazardous transformation products forming during the treatment process [87].

The results from the 5% tertiary-treated effluent experiments revealed a similar trend. Here, cytotoxicity increased at all dosages; estrogenicity decreased at 20 g/L and 50 g/L but increased at 100 g/L; and mutagenicity increased at 50 g/L (Table 10). As the leaching of metals from bauxite residue is a known problem [28], [101], it is possible that metals were also leaching from CBR during the treatment of OSPW and diluted municipal WWTP effluent, and the metals released might then react with the organic compounds and produce complexes that have higher cytotoxicity, estrogenicity, and mutagenicity. A similar observation was reported by Domingues et al. [19] that showed an increase in cytotoxicity in treated wastewater despite the high degradation efficiency of phenolic acids obtained. This further supports the choice of *in-vitro* bioassays in assessing treatment efficiency as it does not only look at the chemical compositions but the overall toxicity of the effluent.

**Table 10.** Removal of acid-extractable organics (AEOs), cytotoxicity, estrogenicity, and mutagenicity when CBR was applied on oil sands process-affected water (OSPW) and diluted municipal wastewater treatment plant tertiary effluent (5% effluent from Plant A + 95% river water) by different dosages of CBR (no neutralization). a: IC10<sub>15min</sub> = the concentration that causes 10% inhibition at 15min; b: REF = relative enrichment factor; c: EC10: the concentration that causes 10% effect; d: EC<sub>IR1.5</sub> = the concentration that causes an induction ratio of 1.5.

<b>CBR Dosage (g/L)</b>	<b>AEOs (mg/L)</b>	<b>Cytotoxicity IC10<sub>15min</sub><sup>a</sup> (REF<sup>b</sup>)</b>	<b>Estrogenicity EC10<sup>c</sup> (REF)</b>	<b>Mutagenicity EC<sub>IR1.5</sub><sup>d</sup> (REF)</b>
Untreated OSPW	37.7 ± 2.9	0.52 ± 0.26	0.14 ± 0.00	6.7
20	31.2 ± 0.1	0.58 ± 0.35	0.20 ± 0.05	5.9 ± 3.2
50	24.0 ± 3.2	0.90 ± 0.27	0.49 ± 0.14	3.8
100	16.9 ± 0.0	0.35	0.08	6.0
Untreated Diluted Effluent	-	53 ± 14	41	>142
20	-	28 ± 12	80	53
50	-	27 ± 6	151	>381
100	-	50 ± 7	19	>343

The chemical analysis results verified the hypothesis that metals were leaching from CBR at potentially harmful concentrations during treatment (Table 11). For OSPW, the concentration of dissolved aluminum (Al) increased remarkably from 0.0082 mg/L to 100 mg/L after the treatment with 50 g/L of CBR. In Alberta, the Alberta Environment and Protected Areas (A-EPA) set industrial release limits based on ambient environmental quality guidelines to ensure industries comply with the release limits, and appropriate technologies are employed to protect the environment and human health. Given that this procedure is site-specific (i.e., A-EPA develops limits based on the receiving environment), there are currently no limits nor regulations related to OSPW release due to the zero-discharge policy set by the Alberta and Federal

governments. For the purposes of this thesis, the concentrations were compared against the CCME guidelines for the protection of freshwater aquatic life from long-term effects. Although the industrial effluents treated with CBR will not comprise nearly 100% of the total receiving environment by volume, this approach is conservative and more stringent.

The aluminum concentrations that leached out of the bench-scale test far exceeded the guideline of 100 µg/L by 1000 times [44]. Dissolved boron (B), molybdenum (Mo), selenium (Se), chloride (Cl), fluoride (F), and pH also increased after treatment and exceeded the guideline for long-term effects. Antimony (Sb), cadmium (Cd), chromium (Cr), potassium (K), sodium (Na), sulphur (S), vanadium (V), and sulphate (SO<sub>4</sub>) increased but were considered less concerning as they either did not exceed the guidelines or the guideline values were not available for these substances. Similarly for 5% tertiary-treated effluent, parameters including Al (increased from <0.003 mg/L to 110 mg/L), Mo, Se, F, and pH exceeded the guidelines for long-term effects after treatment by 1.3-1100 times. Sb, B, S, V, Cl, SO<sub>4</sub>, and ammonia increased but they either did not exceed the guidelines or the guideline values were not available for comparison. Additionally, the hardness values for both water samples were notably higher after treatment, primarily contributed by the dissolution of aluminum from CBR.

In addition to the increase in pH and the leaching of some metals and anions, this experiment also showed poor removals of contaminants by CBR. For example, the dissolved organic carbon (DOC) only decreased from 1.8 mg/L to 1 mg/L in diluted municipal WWTP effluent (Table 11) and small reductions in orthophosphate were observed (from 0.0045 mg/L to below 0.0030 mg/L). Metals including arsenic (As), barium (Ba), copper (Cu), lithium (Li), magnesium (Mg), nickel (Ni), silicon (Si), strontium (Sr), uranium (U), and zinc (Zn) also decreased slightly after treatment without neutralization.

Since CBR demonstrated promising removal in AEOs from OSPW, the treatment experiment for OSPW was continued with an additional neutralization step to assess the quality of the final effluent after pH adjustment (results discussed in Section 3.5.1). However, the 5% municipal effluent was relatively clean prior to CBR treatment (and had already achieved compliance testing), hence the release of metals, especially aluminum, and the increase in pH from CBR were considered more problematic than its potential to remove contaminants in 5% effluent. Though the metal leaching and the basic pH might be mitigated by neutralization, the cost for calcination pre-treatment of the CBR material, neutralization, and the operational and sludge handling for using CBR is not economical. However, it was deemed more appropriate to test the removal after the primary and secondary effluents) to determine the applicability of CBR as a supplemental treatment step within an operational WWTP (discussed in Section 3.6.2). For this reason, the applicability of CBR for the treatment of diluted municipal WWTP effluent, which was used in this study to simulate natural water bodies polluted with sewage, was not assessed further.

Overall, the leaching of metal ions, especially aluminum, and the basic pH appeared to be priority concerns for CBR usability during wastewater treatment (especially for OSPW). Thus, a neutralization step with acid was implemented to remediate both the basic pH and the release of metals in future experiments. Furthermore, acetic acid was selected for this neutralization to prevent additional release of anions such as Cl and SO<sub>4</sub> from the use of common inorganic acids.

**Table 11.** Measured water quality parameters of OSPW and diluted effluent from municipal wastewater treatment facility (5% tertiary effluent from Plant A + 95% river water) before and after the treatment with 50 g/L of CBR (without neutralization). The values **highlighted in green** exceeded the **long-term** guideline for the protection of freshwater aquatic life by CCME [44]. Results were not compared with the guidelines if not available. \*: Hardness was not measured but estimated based on the concentrations of dissolved calcium, magnesium, and aluminum. \*\*: pH value displayed was measured for the supernatant after sedimentation and filtration; it was expected to be close to the pH of the sample at the time of chemical analysis. Refer to Appendix B.3 Table B.3.1 for the concentration of more nitrogen parameters (not shown here as the releases were insignificant). Refer to Appendix B.4 Table B.4.1 for short- and long-term guideline values for each water sample.

Parameters	Unit	OSPW	OSPW + 50g/L CBR	Diluted Effluent	Diluted Effluent + 50g/L CBR
<b>Dissolved Metal Ions</b>					
Dissolved Cadmium (Cd)	ug/L	0.027	0.036	<0.020	<0.020
Dissolved Aluminum (Al)	mg/L	0.0082	100	<0.0030	110
Dissolved Antimony (Sb)	mg/L	0.0014	0.011	<0.00060	0.0038
Dissolved Arsenic (As)	mg/L	0.0018	0.0014	0.00024	0.00024
Dissolved Barium (Ba)	mg/L	0.10	0.063	0.078	0.044
Dissolved Beryllium (Be)	mg/L	<0.0010	<0.0010	<0.0010	<0.0010
Dissolved Boron (B)	mg/L	1.1	1.8	0.025	0.35
Dissolved Calcium (Ca)	mg/L	47	18	37	37
Dissolved Chromium (Cr)	mg/L	<0.0010	0.0021	<0.0010	<0.0010
Dissolved Cobalt (Co)	mg/L	<0.00030	<0.00030	<0.00030	<0.00030
Dissolved Copper (Cu)	mg/L	0.013	0.0028	0.0070	0.0021
Dissolved Iron (Fe)	mg/L	<0.060	<0.060	<0.060	<0.060
Dissolved Lead (Pb)	mg/L	<0.00020	<0.00020	<0.00020	<0.00020
Dissolved Lithium (Li)	mg/L	0.11	<0.020	<0.020	<0.020
Dissolved Magnesium (Mg)	mg/L	24	<0.20	16	<0.20
Dissolved Manganese (Mn)	mg/L	<0.0040	<0.0040	<0.0040	<0.0040
Dissolved Molybdenum (Mo)	mg/L	0.058	0.16	0.0011	0.095
Dissolved Nickel (Ni)	mg/L	0.0069	0.0032	0.0015	<0.00050
Dissolved Phosphorus (P)	mg/L	<0.10	<0.10	<0.10	<0.10
Dissolved Potassium (K)	mg/L	13	28	1.8	1.2
Dissolved Selenium (Se)	mg/L	0.0011	0.041	0.0010	0.026
Dissolved Silicon (Si)	mg/L	4.5	<0.50	<0.50	<0.50
Dissolved Silver (Ag)	mg/L	<0.00010	<0.00010	<0.00010	<0.00010
Dissolved Sodium (Na)	mg/L	220	440	14	210
Dissolved Strontium (Sr)	mg/L	0.91	0.072	0.19	0.051
Dissolved Sulphur (S)	mg/L	130	220	15	70
Dissolved Thallium (Tl)	mg/L	<0.00020	<0.00020	<0.00020	<0.00020
Dissolved Tin (Sn)	mg/L	<0.0010	0.0010	<0.0010	<0.0010
Dissolved Titanium (Ti)	mg/L	<0.0010	<0.0010	<0.0010	<0.0010
Dissolved Uranium (U)	mg/L	0.0025	<0.00010	0.00050	<0.00010
Dissolved Vanadium (V)	mg/L	0.0054	0.12	<0.0010	0.013
Dissolved Zinc (Zn)	mg/L	0.019	<0.0030	0.023	<0.0030
<b>Anions</b>					
Fluoride (F)	mg/L	3.2	16	0.16	2.1
Chloride (Cl)	mg/L	33	120	16	42
Sulphate (SO <sub>4</sub> )	mg/L	390	530	52	110
<b>Organics</b>					
Dissolved Organic Carbon (DOC)	mg/L	20	16	1.8	1.0
<b>Nutrients</b>					
Dissolved Ammonia (N)	mg/L	0.034	0.019	<0.015	0.017
Orthophosphate (P)	mg/L	0.0078	<0.0030	0.0045	<0.0030
<b>General</b>					
Hardness Estimated*	mg/L	216	601	158	704
pH**		8	11	8	11



### 3.4.2. Comparison with the Leaching from Raw Bauxite Residue in Ultrapure Water

Given that CBR can release potentially toxic substances, a leaching test was carried out in ultrapure water to examine the background toxicities of CBR and raw bauxite residue for a better understanding of the effect of the calcination pretreatment on the material. A dosage of 100 g/L was used for the determination of background cytotoxicity, estrogenicity, and mutagenicity induced by CBR and raw bauxite residue (without neutralization). Cytotoxicity, measured by  $IC_{10_{15min}}$ , was 3.7 REF after CBR treatment, similar to that for the raw bauxite residue (3.6 REF). Estrogenicity, measured by  $EC_{10}$ , was 17 REF for CBR and 888 REF for raw bauxite residue, suggesting the calcination pretreatment likely led to the release of some estrogenic chemicals (i.e., low  $EC_{10}$  values suggest higher toxicity). Mutagenicity, expressed by  $EC_{IRI.5}$ , was 14 REF for CBR and 11 REF for raw bauxite residue, showing the calcination pretreatment very mildly decreased the release of mutagens from bauxite residue.

The metal leaching results (Table 12 Samples [1] and [2]) agreed with the *in-vitro* bioassays results. This leaching experiment was conducted with 50 g/L of CBR and raw bauxite residue. For CBR, the substances released included dissolved Al, As, Mo, Se, F, and the pH after contact exceeded the limits for long-term effects. For raw bauxite residue, dissolved Al, As, Cu, Fe, phosphorus (P), Se, F, and pH surpassed the limits. After calcination pretreatment, the leaching of chemicals including Al, Sb, B, Ca, Mo, Se, Sr, S, and hardness increased, while the leaching of chemicals including As, Ba, chromium, Cu, Fe, P, K, Si, Na, titanium (Ti), U, V, Zn, F, Cl, and  $SO_4$  decreased. With the background toxicities confirmed, it is evident that without further optimization (i.e., neutralization), CBR and raw bauxite residue will likely elevate the toxicity of wastewater.

It was observed that the cytotoxicity, estrogenicity, and mutagenicity of the CBR-contacted ultrapure water were much higher than the CBR-treated diluted effluent (Table 10). One possible reason was that the organic contents present in diluted municipal WWTP effluent provided additional nutrients to the microorganisms used for *in-vitro* bioassays, thus cell growth was being encouraged instead of being inhibited as in the case of cytotoxicity. Another possible explanation was the leaching of some metal species from CBR was higher in ultrapure water than in wastewater, and this extra release contributed to the increase in toxicities. For example, the release of Al was 110 mg/L in diluted effluent but 190 mg/L in ultrapure water, and the release of As in diluted effluent was 0.00024 mg/L (below the long-term guideline) but was 0.007 mg/L in ultrapure water (above the long-term guideline). Regardless of the result and background matrix, CBR produced background toxicity that must be dealt with prior to its potential for pilot- or full-scaling. Here, neutralization by the addition of acetic acid was explored as discussed subsequently below.

**Table 12.** The release of contaminants in ultrapure water by: (1) 50 g/L CBR (2) 50 g/L raw bauxite residue (3) 50 g/L CBR and pre-treatment neutralization with acetic acid (4) 50 g/L CBR and post-treatment neutralization with acetic acid. The values **highlighted in green** exceeded the **long-term** guideline for the protection of freshwater aquatic life by CCME [44]. Results were not compared with the guidelines if not available. \*: Hardness was not measured but estimated based on the concentrations of dissolved calcium, magnesium, and aluminum. \*\*: pH value displayed was measured for the supernatant after sedimentation and filtration; it was expected to be close to the pH of the sample at the time of chemical analysis. Refer to Appendix B.3 Table B.3.2 for the concentration of total metals in the unfiltered supernatant and some nutrient parameters analyzed. Refer to Appendix B.4 Table B.4.2 for short- and long-term guideline values for each water sample.

Parameters	Units	Ultrapure Water + 50 g/L CBR (1)	Ultrapure Water + 50 g/L Raw Bauxite Residue (2)	Pre-treatment Neutralization (3)	Post-treatment Neutralization (4)
<b>Dissolved Metal Ions</b>					
Dissolved Cadmium (Cd)	ug/L	<0.020	<0.020	0.027	0.040
Dissolved Aluminum (Al)	mg/L	190	63	16	0.037
Dissolved Antimony (Sb)	mg/L	0.0070 (1)	<0.00060	0.0068	0.0079
Dissolved Arsenic (As)	mg/L	0.0070	0.061	0.0018	0.016
Dissolved Barium (Ba)	mg/L	0.065	0.13	0.15	0.14
Dissolved Beryllium (Be)	mg/L	<0.0010	<0.0010	<0.0010	<0.0010
Dissolved Boron (B)	mg/L	0.37	0.028	0.69	0.85
Dissolved Calcium (Ca)	mg/L	50	1.6	240	300
Dissolved Chromium (Cr)	mg/L	<0.0010	0.16	<0.0010	<0.0010
Dissolved Cobalt (Co)	mg/L	<0.00030	<0.00030	<0.00030	<0.00030
Dissolved Copper (Cu)	mg/L	<0.0010	0.017	<0.0010	0.015
Dissolved Iron (Fe)	mg/L	<0.060	0.57	<0.060	<0.060
Dissolved Lead (Pb)	mg/L	<0.00020	<0.00020	<0.00020	<0.00020
Dissolved Lithium (Li)	mg/L	<0.020	<0.020	<0.020	<0.020
Dissolved Magnesium (Mg)	mg/L	<0.20	<0.20	0.48	0.85
Dissolved Manganese (Mn)	mg/L	<0.0040	<0.0040	<0.0040	0.016
Dissolved Molybdenum (Mo)	mg/L	0.096	0.028	0.086	0.040
Dissolved Nickel (Ni)	mg/L	<0.00050	<0.00050	<0.00050	0.0018
Dissolved Phosphorus (P)	mg/L	<0.10	0.15	<0.10	<0.10
Dissolved Potassium (K)	mg/L	0.93	6.1	1.1	1.3
Dissolved Selenium (Se)	mg/L	0.021	0.0073	0.011	0.0084
Dissolved Silicon (Si)	mg/L	<0.50	1.1	<0.50	5.2
Dissolved Silver (Ag)	mg/L	<0.00010	<0.00010	<0.00010	<0.00010
Dissolved Sodium (Na)	mg/L	190	350	400	370
Dissolved Strontium (Sr)	mg/L	0.029	<0.020	0.12	0.23
Dissolved Sulphur (S)	mg/L	69	34	44	41
Dissolved Thallium (Tl)	mg/L	<0.00020	<0.00020	<0.00020	<0.00020
Dissolved Tin (Sn)	mg/L	<0.0010	<0.0010	<0.0010	<0.0010
Dissolved Titanium (Ti)	mg/L	<0.0010	0.028	<0.0010	<0.0010
Dissolved Uranium (U)	mg/L	<0.00010	0.0012	<0.00010	0.00012
Dissolved Vanadium (V)	mg/L	0.12	1.1	0.021	0.013
Dissolved Zinc (Zn)	mg/L	<0.0030	0.0073	<0.0030	0.055
<b>Anions</b>					
Fluoride (F)	mg/L	1.2	43	9.6	1.2
Chloride (Cl)	mg/L	30	34	31	27
Sulphate (SO4)	mg/L	85	100	84	70
<b>General Parameters</b>					
Hardness Estimated*	mg/L	1182	355	690	749
pH**		11	11	8.5	6.5

### 3.4.3. Comparison Between Pre-treatment and Post-treatment Neutralization

Two approaches were explored for the neutralization process via acetic acid: (1) pre-treatment and (2) post-treatment neutralization. The results (Table 12 Samples [3] and [4]) showed both pre-treatment and post-treatment neutralization effectively mitigated the leaching of the most concerning metals. For pre-treatment neutralization, the concentration of dissolved Al was reduced from 190 mg/L to 16 mg/L, yet still exceeded the guideline by 160 times. By comparison, for post-treatment neutralization, Al was further reduced to 0.037 mg/L which is below the guideline of 100 µg/L. Similarly, for Mo, its concentration decreased in both neutralization methods, but the post-treatment neutralization was more effective and brought the concentration of Mo further down below the guideline. The pre-treatment neutralization method exhibited a slightly higher reduction in the release of some metal elements such as As, Cu, and Se. It was difficult to determine the release of which metal ions would have a more significant impact on the overall toxicities of the water sample. In terms of operation, when applying pre-treatment neutralization, the pH of the final CBR-treated effluent might be more difficult to control, and additional neutralization of the effluent after CBR treatment might still be required. As described earlier in Section 2.9, though the pH of the CBR slurry was lowered to 6 during the pre-treatment, after 24 hours, the pH of the supernatant raised to around 8.5, potentially due to the continuous release of alkalinity overtime from the alkaline minerals in bauxite residue [43].

Assuming that the leaching of Al is more concerning and considering the ease of operation, post-treatment neutralization was regarded as the better approach and thus employed for the subsequent treatment experiments with OSPW and undiluted municipal WWTP effluents. The effect of post-treatment neutralization in OSPW (Section 3.5.1) and 100% tertiary municipal

WWTP effluent (Section 3.6.1) on further evaluated using a battery of *in-vitro* bioassays, accounting for the difference in metals leaching from CBR in different water matrices.

### **3.5. Treatment of OSPW**

#### **3.5.1. Removal of AEOs and Toxicities on Cells After Post-Treatment Neutralization**

The treatment of OSPW with post-treatment neutralization was assessed and compared with the treatment performance without neutralization (Figure 13a). The concentrations of acetic acid added were ~0.07 mg/L for 20 g/L, 0.42 mg/L for 50 g/L, and 1.33 mg/L for 100 g/L CBR-treated OSPW. For AEOs, the removal slightly decreased after post-treatment neutralization, with 100 g/L dosage showing a 10% drop in removal (55% to 45%). This result might be due to acetic acid influencing the chemical analysis of AEOs via FTIR which measures oxy-NAs and other organic acids [103]. Nevertheless, the removal of AEOs by CBR after post-treatment neutralization was still considered to be effective and a promising approach moving forward. Bauxite residue has not been applied at a pilot- or full-scale setup to date hence, the applicability of this approach in different reactor setups would be required to upscale the treatment process.

Similar to prior experiments, a battery of bioassays was used to assess the removal of toxicities after CBR treatment and post-treatment neutralization. Notable removal of estrogenicity and mutagenicity was observed with the application of post-treatment neutralization (Figure 13c, d). At all doses tested, the estrogenicity and mutagenicity after post-treatment neutralization were all lower than the untreated OSPW, likely because of a combination of (1) the removal of estrogenic and mutagenic substances such as NAs by CBR and (2) the successful alleviation of estrogenic and mutagenic substances leaching and by-products forming by the addition of acetic acid. Specifically, the dosage of 100 g/L produced the

best removal of estrogenicity (reduced from 0.14 REF to 56.5 REF) and mutagenicity (reduced from 6.7 REF to above 12.5 REF).

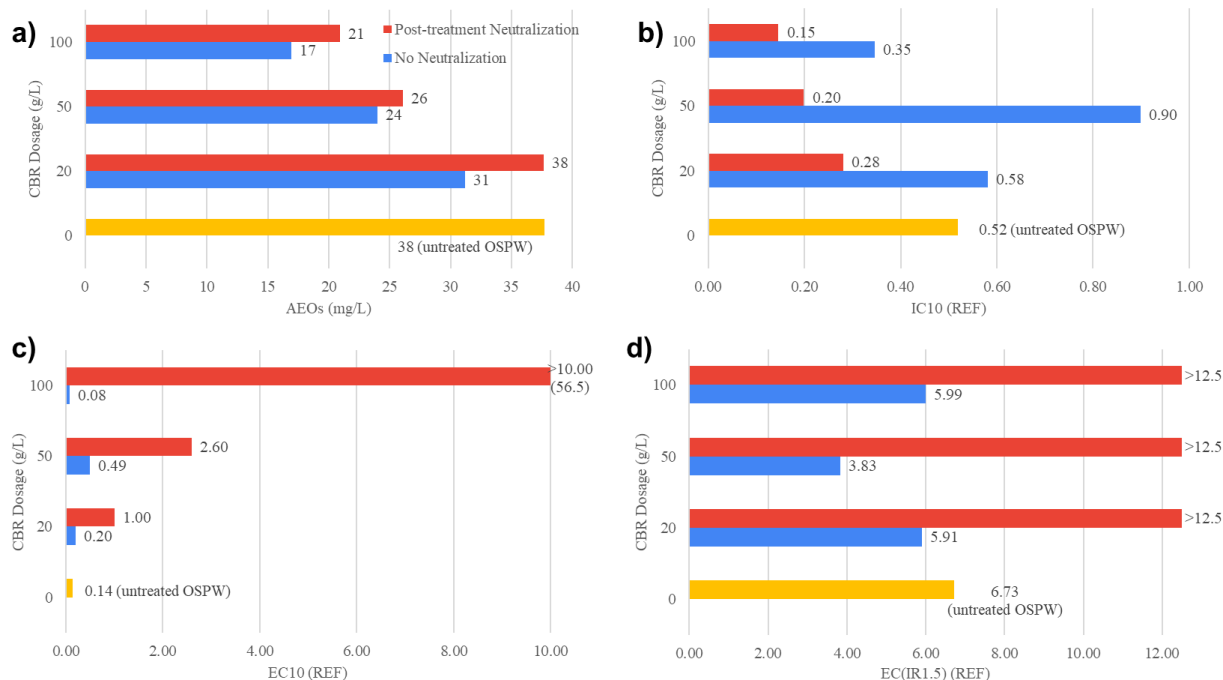


**Figure 13.** Quality of the CBR-treated oil sands process-affected water (OSPW) with post-treatment neutralization and without neutralization. (a) the removal of acid-extractable organics (AEOs) with different doses of CBR; (b) cytotoxicity, (c) estrogenicity, and (d) mutagenicity of the OSPW after the treatment with different CBR doses.

Although estrogenicity and mutagenicity removals were promising in terms of the potential for CBR to be utilized in water treatment, post-treatment neutralization increased the cytotoxicity of OSPW at all dosages tested (Figure 13b), suggesting that acetic acid might have resulted in the formation of more cytotoxic compounds through reactions with the contaminants in OSPW or from CBR. Additionally, after post-treatment neutralization was applied, it appeared that cytotoxicity increased with a higher dosage of CBR, which was not the original trend observed for non-neutralized batch test. This indicates that the potential generation of cytotoxic compounds might be related to the amount of acetic acid added (higher volume needed for

neutralization for a higher dosage of CBR) or the decrease in pH by the acetic acid added. It is currently difficult to assess which compounds might be cytotoxic (need to do an effect-directed analysis for this), but the result suggests that for future optimization, cytotoxicity is a good *in vitro* bioassay to use as it exhibits good sensitivity in detecting the change caused by the treatment with CBR. Although the IC10s of all CBR-treated OSPW samples observed were all less than 1.0 REF, meaning that the bacteria were inhibited by exposure to low concentrations of the sample, as the bacteria used (*Aliivibrio fischeri*) in this experiment is a marine species, the IC10 values obtained might not be representative of the effect on freshwater organisms [22]. Additionally, the toxicity effect might be different in more complicated biological systems than in the single cell used in this experiment [22]. Therefore, further exposure to other cell lines (e.g., mammalian cell lines) or whole organisms is necessary to understand the toxicity of CBR-treated waters (the toxicity with *Daphnia Magma* is ongoing).

### 3.5.2. Adsorption kinetics and isotherm for AEOs

The adsorption of AEOs by 50 g/L CBR reached equilibrium after approximately 8 h and the maximum removal achieved was about 50% (Figure 14a); the adsorption capacity of CBR also reached a maximum at ~0.25 mg/g after 8 h (Figure 14b). The adsorption of AEOs did not follow the pseudo-first-order kinetic (Figure 14c) but fitted well to the pseudo-second-order kinetic model with  $R^2=99.2\%$  (Figure 14d), indicating that chemisorption was the rate-limiting process for the uptake of AEOs [23]. The corresponding pseudo-second-kinetic parameters were determined to be 0.244 mg/g ( $q_e$ ) and 0.153 g/mg/min ( $k_2$ ). This result was similar to MB removal (Section 3.2) suggesting similar kinetic mechanisms for the adsorption by CBR. However, the adsorption capacity for AEOs obtained was lower than that for MB (~1 mg/g), suggesting that the surface of CBR might have a weaker attraction to AEOs compared to MB. To

explore the removal mechanisms for methylene and AEOs, it might be helpful in future studies to employ additional characterization tools (e.g., FTIR and zeta potential analysis) for a better understanding of the surface chemistry of CBR [82].

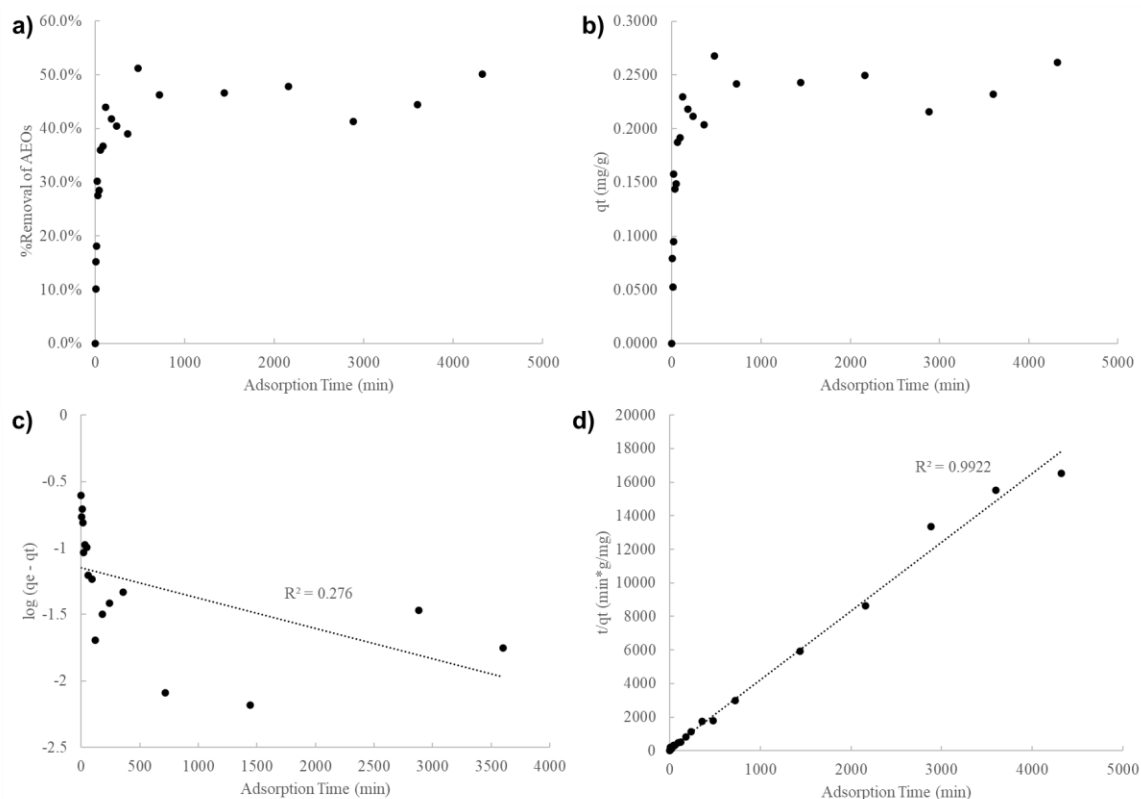


**Figure 14.** The adsorption kinetics for acid-extractable organics (AEOs) from oil sands process-affected water (OSPW) by 50 g/L calcined bauxite residue (CBR) (no neutralization). (a) %Removal of AEOs with time; (b) adsorption capacity ( $q_t$ ) at time  $t$ ; (c) Fitting of the data to pseudo-first-order kinetic model; (d) Fitting of the data to pseudo-second-order kinetic model.

The adsorption capacity/removal efficiency of CBR is lower than the granular activated carbon and carbon xerogel adsorbents (Table 13) but is comparable to the petroleum coke and biochar adsorbents, which were both derived from carbon-rich solid wastes and are currently assessed as a potential treatment for OSPW [104]–[107]. For example, the adsorption capacity (from the pseudo-second-order kinetic model) of petroleum coke is 0.16 mg/g (at a dosage of 23% by weight and an initial concentration of 68 mg AEOs/L), while CBR has an adsorption



capacity of 0.244 mg/g (at 50 g/L dosage and 38 mg AEOs/L). Considering that the application of petroleum coke has been field-piloted [108], it might also be worth assessing the treatment performance of CBR in OSPW beyond the current bench-scale experiments.

**Table 13.** The removal of AEOs from OSPW by other studies and this work. \*: the %removal varied with the source used for biochar generation. \*\*: CBR = calcined bauxite residue.

Adsorbent	Initial AEOs (mg/L)	Dosage (g/L)	Removal of AEOs (%)	Pseudo-second-order Kinetic			Reference
				$q_e$ (mg/g)	$k_2$ (g/mg/min)	$R^2$	
Granular Activated Carbon	67.5	0.4	62.8	-	-	-	[104]
Petroleum Coke	68	23 w.t%	-	0.16	0.657	0.99	[105]
Biochar	60	20	1.4-21*	-	-	-	[106]
Carbon Xerogel	~60	3	74.6	15.6	0.002	1.00	[107]
CBR**	38	50	50	0.244	0.153	0.99	This Work

Furthermore, the removal of AEOs increased almost linearly with CBR dosage until after 85 g/L (Figure 15a), suggesting that the maximum removal of AEOs that can be accomplished by increasing CBR dosage was ~69% (the remaining fraction of AEOs might be recalcitrant to the removal by CBR). At  $C_e \geq 21$  mg/L, the adsorption capacity at equilibrium appeared to increase with the concentration of AEOs (Figure 15b) until above 27 mg/L where the available binding sites on CBR might be saturated. On the contrary, at  $C_e \leq 21$  mg/L, decreasing the concentration of AEOs appeared to improve the adsorption capacity for AEOs. This might be due to the increase in CBR dosage (corresponding to the decreasing AEOs) led to an increase in the pH and significant release of metal ions (Section 3.4), and the metals released might enhance the removal of AEOs via coagulation, precipitation, or other mechanisms.

For CBR dose that  $\leq 65$  g/L, the adsorption of AEOs followed the Langmuir isotherm model ( $R^2 = 0.8415$ ) slightly better than the Freundlich isotherm model ( $R^2 = 0.8285$ ) (Figure 15c,d). This relationship is relatively weak again potentially because: (1) the CBR is a heterogenous material consisting of two types of particles (inorganic and carbonaceous) and they likely have different mechanisms for adsorption; (2) the pH of OSPW increased with the dosage of CBR applied, and this pH change likely also influenced the removal of AEOs.

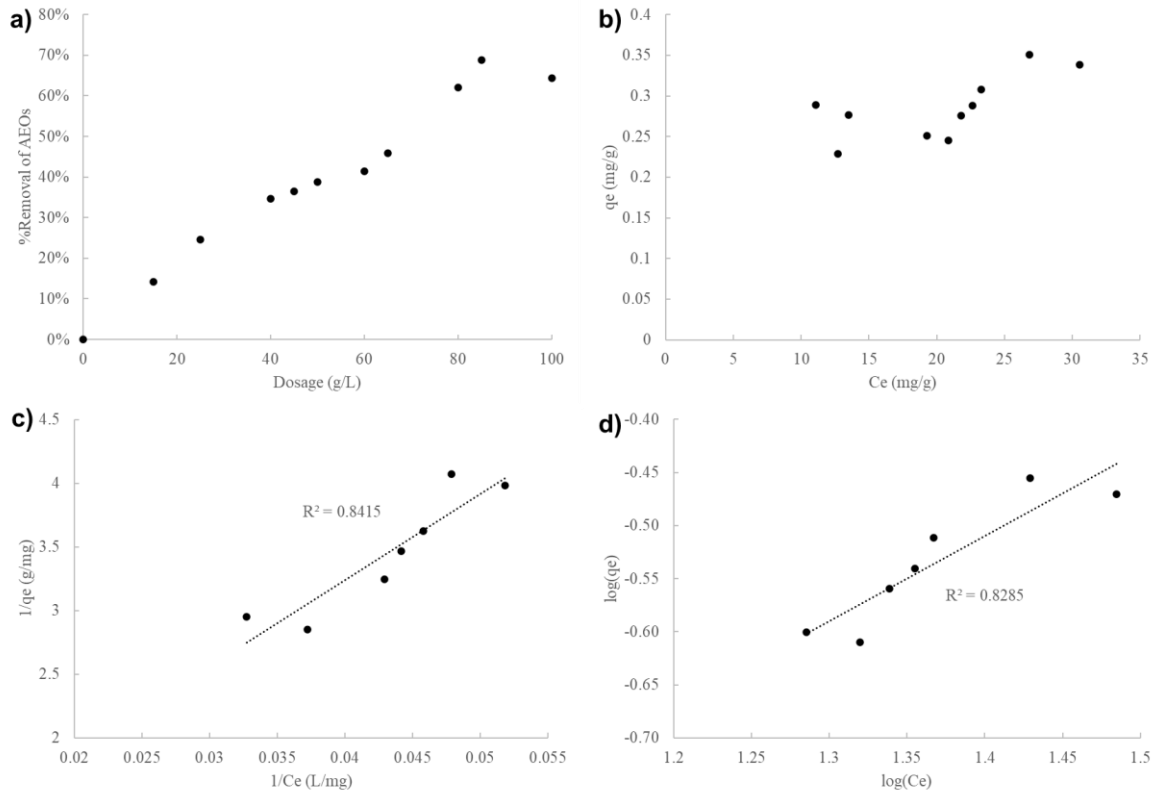


**Figure 15.** The adsorption isotherms for acid-extractable organics (AEOs) from OSPW using different dosages of calcined bauxite residue (CBR) (no neutralization). (a) %Removal of AEOs with different CBR doses. (b) Adsorption capacity at equilibrium,  $q_e$ , at different equilibrium concentrations of AEOs,  $C_e$ . (c) Fitting of data to Langmuir adsorption isotherm model for CBR doses  $\leq 65$  g/L. (d) Fitting of data to Freundlich adsorption isotherm model for CBR  $\leq 65$  g/L.

For doses  $\leq 65$  g/L, the adsorption isotherm parameters of AEOs by CBR are similar to that obtained by the petroleum coke adsorbent, but less effective than that obtained by the carbon xerogel adsorbent (Table 14). The Langmuir maximum adsorption capacity for CBR is 1.84 mg/g higher than that of the petroleum coke (0.39 mg/g). Though the operational parameters and initial concentrations were different between the petroleum coke study and this work, and the isotherm parameters were expected to change in different experiment settings, this preliminary comparison suggests that it might be valuable to compare the adsorption capacity between petroleum coke and CBR in future studies under same experimental conditions. It might also be beneficial to perform a cost-benefit analysis to compare petroleum coke and CBR to determine if there is potential market value with the use of CBR in OSPW treatment. Nonetheless, the results here suggest the future potential of CBR as a water/wastewater treatment material and it is worth investigating several avenues for optimization effectively given that this material is relatively inexpensive and is present in large quantities.

**Table 14.** The adsorption isotherm parameters for the removal of AEOs from OSPW in literature.

Adsorbent	Petroleum Coke	Carbon Xerogel	CBR (This Work)
Initial AEOs (mg/L)	68	~60	38
Langmuir Adsorption Isotherm Parameters			
$K_L$ (L/mg)	0.040	0.058	0.0081
$Q_m$ (mg/g)	0.39	30.77	1.836
$R^2$	0.91	0.971	0.8415
Freundlich Adsorption Isotherm Parameters			
$K_F$ (mg/g) $\cdot$ (L/mg) $^{1/n}$	0.028	3.41	0.0231
$n$	1.63	1.95	1.242
$R^2$	0.87	0.982	0.8285
Reference	[105]	[107]	-

### **3.6. Treatment of Municipal WWTP Wastewaters**

#### **3.6.1. Removal and Effect of Post-treatment Neutralization on Tertiary Effluent**

Effective removal in cytotoxicity, estrogenicity, mutagenicity, and total coliform was observed for the CBR treatment of municipal WWTP tertiary effluent (Plant A), regardless of whether post-treatment neutralization was applied (Figure 16). Although the removal of specific chemical compounds was not analyzed in this experiment, improved clarity of the CBR-treated effluent was observed, suggesting a reduction in organic contaminant concentration after treatment (Appendix B.5 Figures B.5.1 and B.5.2).

At 100 g/L CBR without neutralization and 50 g/L and 100 g/L with post-treatment neutralization, cytotoxicity of the tertiary effluent was reduced from 8.4 REF to above 20 REF, meaning the concentration after treatment is less likely to impose an adverse impact on the receiving aquatic environment [109]. For estrogenicity, post-treatment neutralization resulted in a higher removal at the dosages of 100 g/L (from 3.3 REF prior to treatment to >66 REF after treatment), whereas no neutralization produced slightly better removal at 20 and 50 g/L (from 3.3 REF before treatment to >128 REF and >109 REF after treatment). Mutagenicity was reduced to negligible levels both without and with post-treatment neutralization. It is clear, therefore, that post-treatment neutralization does not have a significant effect on the cell toxicity pathways for the treatment of municipal WWTP tertiary effluent in comparison to the OSPW treatment as previously discussed (Section 3.5.1). Nonetheless, the implementation of post-treatment neutralization is still necessary for the neutral pH often required for discharge - the non-neutralized CBR-treated effluent shows a pH of 10.3-12.3 depending on the dosage of CBR applied (from 20 g/L to 100 g/L).

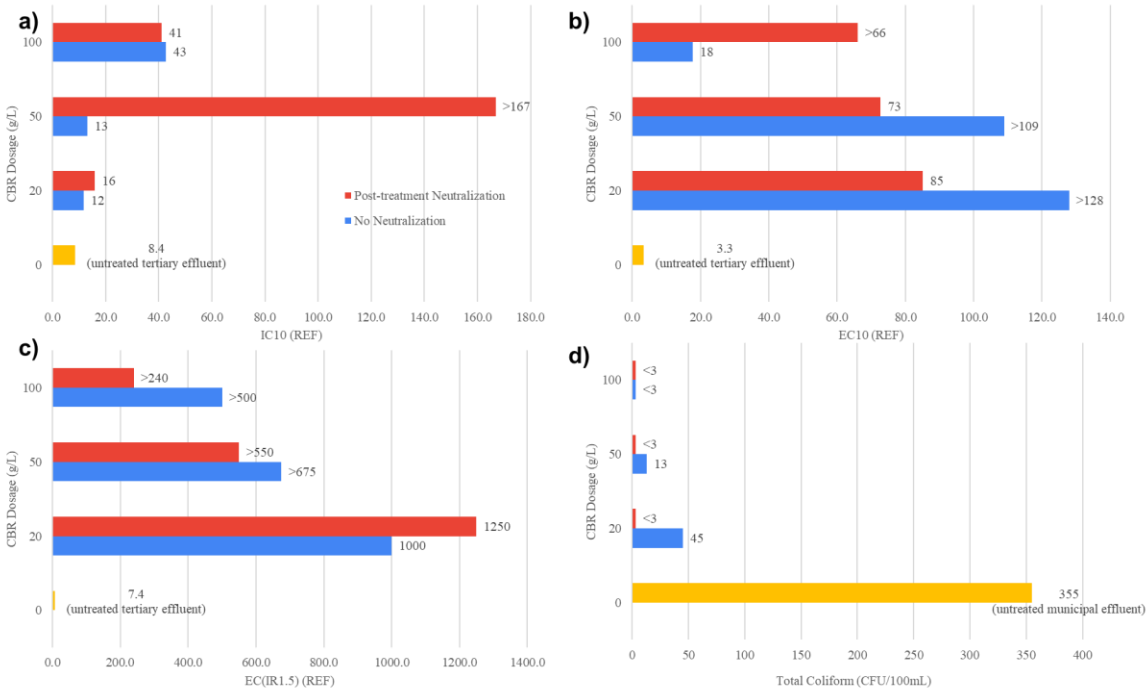


**Figure 16.** The effect of calcined bauxite residue (CBR) treatment and post-treatment neutralization on municipal WWTP (Plant A) tertiary effluent. (a) cytotoxicity, (b) estrogenicity, (c) mutagenicity, and (d) total coliform concentration of the untreated and treated tertiary effluent without neutralization and with post-treatment neutralization. Notes:  $IC_{10_{15min}}$  = the concentration that causes 10% inhibition at 15min; REF = relative enrichment factor;  $EC_{10}$ : the concentration that causes 10% effect;  $EC_{IR1.5}$  = the concentration that causes an induction ratio of 1.5; CFU = colony forming unit.

Moreover, excellent removals of total coliform bacteria were observed after CBR treatment. In the case where no neutralization was applied, CBR reduced total coliform from 355 CFU/100mL to 45 CFU/100mL at 20 g/L (87% removal), 13 CFU/100mL at 50g/L (96% removal), and less than 3 CFU/100mL at 100 g/L (>99% removal). After post-treatment neutralization was applied, the removal was further improved and the concentrations of total coliform at all three dosages tested were below 3 CFU/100mL after treatment. (>99% removal for all dosages) This high removal efficiency of total coliform bacteria was achieved possibly because: (1) the coliform bacteria were killed due to the high alkalinity and salinity released by CBR – the die-off rate of fecal coliforms increases significantly at pH greater than 9 and at

increased salinity [110]; (2) the bacteria were trapped and removed together with the CBR slurry; the leaching of polyvalent cations such as Al from CBR likely promoted destabilization and aggregation of the colloidal particles.

Overall, this experiment showed that CBR was effective in the treatment of municipal WWTP tertiary effluent – cytotoxicity, estrogenicity, mutagenicity, and the concentration of total coliform bacteria was greatly reduced at all three dosages tested (20, 50, and 100 g/L) for both un-neutralized and neutralized CBR-treated effluents. For the treatment of municipal WWTP tertiary effluent, the application of post-treatment neutralization did not significantly alter the toxicities of CBR-treated effluent samples compared to that without neutralization, but the removal of total coliform bacteria was enhanced after post-treatment neutralization. Overall, this experiment suggests a good potential for the application of CBR in municipal WWTPs, the section following explored which part of the conventional municipal WWTP processes CBR can be best utilized/supplemented.

### 3.6.2. Treatment Performance in Primary, Secondary, and Tertiary Effluents

Based on the previous finding that CBR is effective in the remediation of toxicities and the elimination of total coliform bacteria from tertiary effluent, a more comprehensive assessment was conducted to assess the potential implementation of CBR as a supplementary treatment during wastewater treatment. Here, the efficacy of CBR for treating effluents that have undergone different levels of treatment at an operational municipal WWTP (Plant B), including primary (after the biological nutrient removal [BNR]), secondary (after the secondary clarifier), and tertiary (after UV disinfection) effluents were evaluated (results shown in Table 15).

The pH values of the CBR-treated effluents were all within the neutral range for discharge to natural water bodies due to post-treatment neutralization. As expected, the alkalinity measured after CBR treatment increased substantially due to the release from CBR. The concentration of BOD also increased after treatment because of the addition of acetic acid. Acetic acid is a simple, carbon-based molecule and can act as a food source for bacteria (considered as assimilable organic carbon), driving their growth and subsequent oxygen needs. Although the batch testing here shows an elevated increase of BOD, it is unclear what the maximum increase would be to push BOD levels above permit limits when operated at operational/full-scale. The increase in BOD might be addressed by exploring alternative neutralization methods without the use of organic acids (e.g., hydrochloric acid) or by incorporating the CBR treatment process with the biological process (BNR in this case), such that the excess BOD supplied will be consumed by microorganisms. Again, this approach was outside the scope of this thesis and will have to be performed separately to assess the effectiveness of this approach.

**Table 15.** A summary of water quality parameters of untreated, 50 g/L CBR-treated, and 100 g/L CBR-treated primary effluent (after biological nutrient removal), secondary effluent (after secondary clarification), and tertiary effluent (after UV disinfection) from Plant B. The values boxed with a red outline exceeded the discharge limits by AEP (see Appendix B.4 Table B.4.3) [84]. \*: BNR = biological nutrient removal. \*\*: BOD here is 5-day carbonaceous BOD at 20°C. \*\*\*: NA = the data is not available due to the loss of the sample. More water quality parameters that were tested but not discussed were shown in Appendix B.3 Tables B.3.4 to B.3.9.

Category	Parameter	Unit	Primary Effluent (Post-BNR*)			Secondary Effluent (Post-Secondary Clarifier)			Tertiary Effluent (Post-UV)		
			Untreated	50 g/L	100 g/L	Untreated	50 g/L	100 g/L	Untreated	50 g/L	100 g/L
General	pH		7.42	7.76	8.39	7.15	8.11	8.17	7.36	8.22	8.04
	Alkalinity (total)	mg/L	230	440	890	140	420	1000	140	430	1000
	BOD**	mg/L	130	>390	>410	4.4	570	410	<2.0	590	>82
Solid	Total Suspended Solids	mg/L	69	51	44	49	27	85	5.7	35	100
Microorganism	Fecal Coliform	MPN/100mL	>2400	9	<1	1600	<1	<1	47	<1	<1
Cell Toxicity Pathway	Cytotoxicity IC10	REF	2	11	12	15	3.1	25	15	4.7	19
	Estrogenicity EC10	REF	1.6	9.2	>3.9	2.3	>63	>3.9	6.1	>31	>3.9
	Mutagenicity EC(IR1.5)	REF	17	>63	>125	52	>250	>250	30	>125	>250
Nutrient	Total Ammonia (N)	mg/L	26	8	9.5	0.16	0.12	0.13	NA**	0.12	0.15
	Total Phosphorus (P)	mg/L	4.7	0.097	0.13	1.1	0.038	0.047	0.18	0.025	0.051



Total suspended solids (TSS) concentration also increased as a result of CBR introduction (powdered form). The experiments were conducted in batch tests and although the particles were allowed to settle for 30 min, it has been proven insufficient in reducing solids concentration. Again, it would be worthwhile to assess the operational conditions needed to reduce the TSS concentrations such that it is below the effluent discharge limits of an operation WWTP.

Consistent with the results from previous experiments, excellent elimination of fecal coliforms was obtained for all three effluents at both dosages (50 g/L and 100 g/L) tested. The concentrations of fecal coliforms after 50 g/L and 100 g/L CBR treatment were all well below the discharge requirement. For primary effluent, 50 g/L CBR led to the removal of fecal coliform by >99.6% and 100 g/L CBR led to close to 100% removal. For secondary and tertiary effluents, after treatment, the concentration of fecal coliform was <1 MPN/100mL for both dosages. For primary effluent, cytotoxicity was reduced from 2 REF to 11 and 12 REF after the treatment of 50 g/L and 100 g/L CBR respectively. For secondary and tertiary-treated effluents, however, cytotoxicity increased for the treatment with 50 g/L CBR but decreased for 100 g/L CBR. Efficient removals of estrogenicity and mutagenicity were achieved at 50 g/L for all three effluents. Hence, it might be optimal to utilize a dosage of 100 g/L CBR as it produces the best removal in cytotoxicity, estrogenicity, mutagenicity, and fecal coliforms (disinfection). This finding is consistent with that obtained previously from the treatment of OSPW that CBR treatment paired with post-treatment neutralization with acetic acid is an effective approach for the elimination of estrogenic and mutagenic compounds. The toxicity would be further tested using the whole organism *Daphnia Magna* (ongoing) for a better understanding of the toxicity of the CBR-treated wastewater in complex biological systems.

In addition to fecal coliforms, estrogenicity, and mutagenicity, CBR also resulted in good removal of nutrients. For primary effluent, total ammonia was reduced greatly from 26 to 8 mg/L (69% removal) at the dosage of 50 g/L CBR and to 9.5 mg/L at 100 g/L (63% removal), though still above the 5 mg/L discharge limit (noted that discharge limits vary from plant to plant depending on the receiving environment. The Alberta government assesses this and provides the limits for their operation that they need to comply). The reason that smaller removal of total ammonia was observed at the higher CBR dosage might be due to the further increase in pH. At high pH, ammonia is converted from  $\text{NH}_4^+$  to  $\text{NH}_3\cdot\text{H}_2\text{O}$ , which is unfavorable for removal via adsorption [111]. Furthermore, total phosphorus in primary effluent decreased from 4.7 mg/L to 0.097 mg/L (98% removal) after treatment by 50 g/L CBR and to 0.13 mg/L (97% removal) after treatment by 100 g/L CBR, both meeting the discharge requirement successfully after CBR treatment. This observation was consistent with the finding by Huang et al. [41]. It was suggested that the surface of bauxite residue becomes more negative with increasing pH, resulting in stronger repulsion between the adsorbent and the negatively charged phosphate species [41].

For secondary effluents, total ammonia was reduced from 0.16 mg/L to 0.12 mg/L (25% removal) at 50 g/L and to 0.13 mg/L (19% removal) at 100 g/L, showing smaller removal efficiencies compared to that for the primary effluent potentially due to the lower initial concentration. Total phosphorous was reduced from 1.1 mg/L to 0.038 mg/L (97% removal) at 50 g/L and 0.047 mg/L (96% removal) at 100 g/L. Though the concentration of total phosphorus for tertiary effluent was already below the discharge limit to begin with, further removal was observed after the treatment of both 50 g/L (86% removal) and 100 g/L CBR (72% removal). In conclusion, CBR exhibits the highest removal efficiency in total ammonia and total phosphorus

for the treatment of primary effluent. However, for secondary and tertiary effluents, CBR can also enhance the removal of nutrients though at smaller rates. For the purpose of nutrient removal, 50 g/L was determined to be a better dosage to use for CBR than 100 g/L.

Barca et al. [112] examined the potential application of bauxite residue as filter bed material for the improvement of phosphorus removal in constructed wetlands using synthetic wastewater. As a result, they found that the implementation of bauxite residue produced excellent total phosphorus removal under both aerobic condition (98.5% removal) through Ca-P precipitation and anoxic condition (91.6% removal) through Fe-P precipitation [112]. Similarly, besides the direct addition in powdered form, CBR might also be compacted into a filter bed for application in WWTP. For incorporation into microbial processes, however, the dosage and pretreatment of CBR might require further consideration and optimization as microbial activities can be inhibited by the basic pH and the release of other hazardous chemicals of CBR. For example, in the study by Barca et al. [112], the bauxite residue was carbonated and neutralized by mixing with gypsum before being used as a filter substrate.

The effect of CBR treatment paired with post-treatment neutralization with acetic acid on dissolved metals concentration was shown in Tables 16 and 17 (concentrations in untreated effluents were shown in Appendix B.3 Table B.3.3). For untreated wastewaters, the concentration of dissolved Cu in the untreated primary effluent (0.005 mg/L) was slightly above the CCME guidelines for long-term effect protection (0.004 mg/L), and the concentrations of dissolved phosphorus in all untreated primary, secondary, and tertiary effluent were above the limit which hyper-eutrophic conditions can be triggered (without considering the dilution by the receiving water bodies). After treatment, the concentration of dissolved Cu in the primary effluent was reduced by 63% for 50 g/L CBR and by more than 80% for 100 g/L CBR, both

were below the CCME guidelines. The concentrations of phosphorus in all three effluents treated with CBR were reduced to below the detection limit of 0.1 mg/L (the trigger value for hyper-eutrophic conditions) for both 50 g/L and 100 g/L dosages. This result indicates that CBR treatment paired with post-treatment neutralization is effective for the removal of dissolved Cu and phosphorus for primary, secondary, and tertiary effluents from municipal WWTP.

On the other hand, the concentrations of dissolved Al, As, Mo, and Se increased and exceeded the CCME guidelines for long-term effects after CBR treatment (noted that this is not the discharge requirement, which will normally take into consideration the dilution capacity of the receiving water bodies). More specifically, the concentrations of dissolved Al ranged from about 15 to 76 times higher than the CCME guideline, 1.1 to 1.9 times higher for As, 1.2 to 1.9 times for Mo, and 12 to 23 times for Se. Based on this comparison, it appeared that the amount of Al and Se leached might be more concerning, and further optimization of the current treatment process should take into consideration the leaching of Al and Se from CBR. Burke et al. [102] studied the effect of three different neutralization methods on bauxite residue leachate from the Hungary dam failure accident and they found that all three methods tested effectively reduced the concentration of dissolved Al and As: (1) neutralization with HCl removed Al by precipitation and As by adsorption onto the Al precipitates; (2) neutralization with gypsum led to calcite precipitation, which in turn led to the removal of Al and As possibly through rapid scavenging; (3) neutralization with seawater produced carbonate precipitation which then removed Al and As by surface adsorption [102]. These neutralization methods might also be applicable for mitigating the leaching from CBR during water treatment, and they will be considered in future experiments.

Furthermore, the leaching of metals (Al, As Mo, and Se) increased with the CBR dosage applied from 50 g/L to 100 g/L. For Al, the leaching was less severe in primary effluent compared to that in secondary and tertiary effluents. This result may be due to the primary effluent containing more colloidal particles before treatment, therefore the chances for particle aggregation by the formation of different Al complexes were also higher. A similar trend was observed for the leaching of Mo and Se that their concentrations in primary effluents after treatment are slightly lower than or equal to that in secondary and tertiary effluents after treatment. Therefore, to minimize the leaching of metals from CBR, the dosage of 50 g/L is preferred, and treatment by CBR in high turbidity water is more favourable.

Conversely, as mentioned previously, the cytotoxicity of secondary and tertiary effluents treated with 50 g/L CBR was increased compared to the untreated effluents, but the cytotoxicity was reduced with 100 g/L CBR. This indicates the increase in the release of metals from CBR might not have directly contributed to the cytotoxicity of the effluent sample; it is also possible that the metal complexes formed might be less toxic compared to the original organic pollutants [101]. Based on the results obtained, it is difficult to elucidate the cause of the higher cytotoxicity observed at the lower dosage of CBR. The effect of metals released from CBR and the presence of other cytotoxic compounds from CBR might need to be examined further. For primary effluent, however, the cytotoxicity after 50 g/L CBR treatment was very close to that obtained after 100 g/L treatment, and they were both reduced compared to the untreated wastewater, meaning that using the CBR dosage of 50 g/L for primary effluent treatment would produce the similar cytotoxicity removal as the dosage of 100 g/L.

Combining the results obtained for the removal of nutrients, fecal coliform bacteria, cytotoxicity, estrogenicity, mutagenicity, and metal leaching, it appeared that 50 g/L would be

the more optimal dose to use and applying the CBR adsorbent to the treatment of primary effluent (after the biological removal unit) would maximize the removal efficiency while minimizing potential harmful biological effects. However, further optimization of the water treatment process by CBR is required as the concentrations of TSS and BOD exceeded the effluent discharge limits. Lastly, it is essential to control the CBR/wastewater pH during treatment and the CBR dosage when integrating the use of CBR into the BNR process as the basic pH and the release of polyvalent cations from CBR might inactivate or remove the microorganisms via coagulation and precipitation.

**Table 16.** The concentrations of dissolved metals in municipal WWTP (Plant B) primary (after biological nutrient removal), secondary (after secondary clarifier), and tertiary (after UV disinfection) effluents after treatment with 50 g/L CBR and post-treatment neutralization with acetic acid. The values **highlighted in green** exceeded the **long-term** guideline for the protection of freshwater aquatic life by CCME [44]. Results were not compared with the guidelines if not available. \*: Hardness was not measured but estimated based on the concentrations of dissolved calcium, magnesium, and aluminum. Refer to Appendix B.4 Table B.4.5 for short- and long-term guideline values for each sample. The concentration of total metals in the unfiltered supernatant was also measured and displayed in Appendix B.3 Table B.3.6.

Metal Ions	Units	Primary Effluent + 50 g/L CBR	Secondary Effluent + 50 g/L CBR	Tertiary Effluent + 50 g/L CBR
Dissolved Cadmium (Cd)	ug/L	0.040	0.043	0.037
Dissolved Aluminum (Al)	mg/L	1.5	3.8	3.3
Dissolved Antimony (Sb)	mg/L	0.0099	0.0077	0.0078
Dissolved Arsenic (As)	mg/L	0.0080	0.0062	0.0055
Dissolved Barium (Ba)	mg/L	<0.010	<0.010	<0.010
Dissolved Beryllium (Be)	mg/L	<0.0010	<0.0010	<0.0010
Dissolved Boron (B)	mg/L	0.86	0.76	0.74
Dissolved Calcium (Ca)	mg/L	150	170	170
Dissolved Chromium (Cr)	mg/L	<0.0010	<0.0010	<0.0010
Dissolved Cobalt (Co)	mg/L	0.00040	<0.00030	<0.00030
Dissolved Copper (Cu)	mg/L	0.0019	<0.0010	<0.0010
Dissolved Iron (Fe)	mg/L	<0.060	<0.060	<0.060
Dissolved Lead (Pb)	mg/L	0.00082	0.00068	0.00062
Dissolved Lithium (Li)	mg/L	<0.020	<0.020	<0.020
Dissolved Magnesium (Mg)	mg/L	1.4	0.53	0.53
Dissolved Manganese (Mn)	mg/L	<0.0040	<0.0040	<0.0040
Dissolved Molybdenum (Mo)	mg/L	0.087	0.095	0.088
Dissolved Nickel (Ni)	mg/L	0.0030	0.0014	0.0012
Dissolved Phosphorus (P)	mg/L	<0.10	<0.10	<0.10
Dissolved Potassium (K)	mg/L	5.6	6.2	6.0
Dissolved Selenium (Se)	mg/L	0.012	0.017	0.013
Dissolved Silicon (Si)	mg/L	0.58	<0.50	<0.50
Dissolved Silver (Ag)	mg/L	<0.00010	<0.00010	<0.00010
Dissolved Sodium (Na)	mg/L	260	260	260
Dissolved Strontium (Sr)	mg/L	0.16	0.18	0.18
Dissolved Sulphur (S)	mg/L	97	86	83
Dissolved Thallium (Tl)	mg/L	<0.00020	<0.00020	<0.00020
Dissolved Tin (Sn)	mg/L	<0.0010	<0.0010	<0.0010
Dissolved Titanium (Ti)	mg/L	<0.0010	<0.0010	<0.0010
Dissolved Uranium (U)	mg/L	0.00026	0.00013	0.00015
Dissolved Vanadium (V)	mg/L	0.023	0.018	0.017
Dissolved Zinc (Zn)	mg/L	0.0034	0.0037	<0.0030
Hardness Estimated*	mg/L	389	448	445

**Table 17.** The concentrations of dissolved metals in municipal WWTP (Plant B) primary (after biological nutrient removal), secondary (after secondary clarifier), and tertiary (after UV disinfection) effluents after treatment with 100 g/L CBR and post-treatment neutralization with acetic acid. The values **highlighted in green** exceeded the **long-term** guideline for the protection of freshwater aquatic life by CCME [44]. Results were not compared with the guidelines if not available. \*: Hardness was not measured but estimated based on the concentrations of dissolved calcium, magnesium, and aluminum. Refer to Appendix B.4 Table B.4.6 for short- and long-term guideline values for each sample –some guidelines were calculated based on the sample hardness, pH, and DOC. The concentration of total metals in the unfiltered supernatant was also measured and displayed in Appendix B.3 Table B.3.8.

Metal Ions	Units	Primary Effluent + 100 g/L CBR	Secondary Effluent + 100 g/L CBR	Tertiary Effluent + 100 g/L CBR
Dissolved Cadmium (Cd)	ug/L	0.021	0.024	0.025
Dissolved Aluminum (Al)	mg/L	3.2	7.6	5.1
Dissolved Antimony (Sb)	mg/L	0.0062	0.0048	0.0052
Dissolved Arsenic (As)	mg/L	0.0096	0.0063	0.0062
Dissolved Barium (Ba)	mg/L	0.015	0.012	0.014
Dissolved Beryllium (Be)	mg/L	<0.0010	<0.0010	<0.0010
Dissolved Boron (B)	mg/L	1.2	0.95	0.97
Dissolved Calcium (Ca)	mg/L	360	330	350
Dissolved Chromium (Cr)	mg/L	<0.0010	<0.0010	<0.0010
Dissolved Cobalt (Co)	mg/L	<0.00030	<0.00030	<0.00030
Dissolved Copper (Cu)	mg/L	<0.0010	<0.0010	<0.0010
Dissolved Iron (Fe)	mg/L	<0.060	<0.060	<0.060
Dissolved Lead (Pb)	mg/L	0.00032	0.00055	0.00043
Dissolved Lithium (Li)	mg/L	<0.020	<0.020	<0.020
Dissolved Magnesium (Mg)	mg/L	1.2	0.65	0.77
Dissolved Manganese (Mn)	mg/L	<0.0040	<0.0040	<0.0040
Dissolved Molybdenum (Mo)	mg/L	0.13	0.14	0.13
Dissolved Nickel (Ni)	mg/L	0.0018	0.00078	0.00083
Dissolved Phosphorus (P)	mg/L	<0.10	<0.10	<0.10
Dissolved Potassium (K)	mg/L	6.1	6.0	5.9
Dissolved Selenium (Se)	mg/L	0.021	0.023	0.023
Dissolved Silicon (Si)	mg/L	<0.50	<0.50	<0.50
Dissolved Silver (Ag)	mg/L	<0.00010	<0.00010	<0.00010
Dissolved Sodium (Na)	mg/L	470	440	440
Dissolved Strontium (Sr)	mg/L	0.30	0.27	0.29
Dissolved Sulphur (S)	mg/L	140	120	120
Dissolved Thallium (Tl)	mg/L	<0.00020	<0.00020	<0.00020
Dissolved Tin (Sn)	mg/L	<0.0010	<0.0010	<0.0010
Dissolved Titanium (Ti)	mg/L	<0.0010	<0.0010	<0.0010
Dissolved Uranium (U)	mg/L	<0.00010	<0.00010	<0.00010
Dissolved Vanadium (V)	mg/L	0.019	0.020	0.018
Dissolved Zinc (Zn)	mg/L	<0.0030	<0.0030	<0.0030
Hardness Estimated*	mg/L	922	869	905



#### 4. Study Limitations

Although the results from this study suggest that CBR is a promising wastewater treatment approach, the findings presented in this thesis have several limitations as outlined subsequently below:

- (1) Most of the treatment experiments were only run once and the raw and CBR-treated water samples were only analyzed once for each bioanalytical/chemical test due to limited sample volume and time constraints. Although positive and negative controls were included for validation of the assays, repeatability of the treatment and variation caused by the overall experimental design was not assessed.
- (2) Most of the removal/leaching experiments were conducted with a contact time of 24 h to allow for maximum adsorption or leaching. Real-life applications of CBR would likely have a different contact time and different operational parameters compared to this study. Additionally, the leaching/removal performance of CBR would likely change depending on the wastewater matrix. The effect of CBR treatment needs to be assessed again before it can be applied to any real-life scenario.
- (3) The *in vitro* bioassays (cell lines) used in this study were selected mainly based on their good sensitivity in detecting the effect of CBR treatment on wastewater. Whole effluent toxicity testing was not completed and can therefore show different results than the *in vitro* bioassay.
- (4) For *in vitro* bioassays, the samples were enriched by SPE prior to analysis, and some of the inorganic fraction and particulate fraction might have been removed during

process. It is unclear whether this portion eliminated what would have a positive or negative influence on the toxicity of the intact sample.

- (5) The CCME guidelines used for the determination of the significance of metals concentration leached from CBR were based on the receiving environment, they are not for end-of-pipe discharge compliance, which generally takes into consideration the capacity and sensitivity of the receiving water bodies. Thus, the significance of the metals released might need to be re-evaluated depending on local regulations and environments.
- (6) The knowledge of the pre-treatment process for the CBR material was patented and thus was restricted to the researchers. Although the comparison between the raw bauxite residue and CBR was attempted and removal/leaching efficiencies were obtained in this study, it is still difficult to assess the removal/leaching mechanisms by CBR.

## 5. Conclusions and Recommendations

This study assessed the potential application of CBR in the treatment of a variety of wastewaters (OSPW, municipal WWTP effluents, sewage-polluted water bodies, and dye-polluted wastewaters) and demonstrated the effectiveness of post-treatment neutralization in remediating the release of metals and potential toxic effects from CBR. The characterization results showed that CBR is a semi-crystalline and heterogenous material that consists of two types of particles: (1) carbonaceous and (2) inorganic. CBR has a BET surface area of 25.1 m<sup>2</sup>/g and a total pore volume of 0.137 cm<sup>3</sup>/g. By comparison with other bauxite residues, it was shown that the pre-treatment process of CBR could be optimized further for higher specific surface area and porosity via composites with other types of materials (activated carbon) or treatment with ammonium hydroxide. However, as the main purpose of the CBR was initially set for the recovery of valuable metals, material synthesis and further enhancement of the CBR material were not considered in this thesis.

Preliminary results showed CBR can remove synthetic OSPW prepared with commercial NAs – Sigma NAs (33.4%) and cyclohexanecarboxylic acid (48.8%) from the solution using 20 g/L CBR. Furthermore, the cytotoxicity (IC<sub>10</sub><sub>15min</sub>) of the synthetic OSPW made of cyclohexanecarboxylic acid was reduced from 2.5 REF to 4.9 REF after treatment, showing its potential as an adsorbent material. However, due to low recoveries and high inconsistencies observed for both Sigma NAs and cyclohexanecarboxylic acids (likely due to the loss in sample extraction in SPE) the removal of commercial NAs by CBR was not assessed further in this study. For future studies, it is recommended to evaluate alternative sample preparation methods

or alternative analytical methods that would not require extraction to improve the recovery of commercial NAs.

The adsorption of MB and AEOs by CBR was effective and both followed the pseudo-second-order kinetic model, suggesting that chemisorption is the rate-controlling process. The adsorption rate and adsorption capacity of MB varied both with the initial concentration of MB as well as the dosage of CBR applied. At equilibrium, approximately 1-1.1 g of CBR is required to completely remove 1 mg of MB, showing that CBR has a good potential to be used for the removal of organic dyes from textiles or other dye-polluted wastewaters. The maximum adsorption capacity of AEOs was determined to be  $\sim 0.25$  mg/g using real OSPW, comparable to the adsorption achieved by the pilot-scale petroleum coke and bench-scale biochar adsorbents, both were converted from waste material and applied for OSPW treatment. Considering that the treatment of OSPW by petroleum coke has been field-piloted, it might be beneficial to investigate the use of CBR for OSPW treatment further including cost-benefit analysis and optimization of the treatment process. Furthermore, the adsorption of MB and AEOs did not produce a good fit to the commonly used Freundlich nor the Langmuir isotherm model, potentially because (1) the different compositions of CBR exhibited different adsorption mechanisms, (2) the adsorption was affected by the increase in water pH, which increased with higher CBR dosage. It might be worth exploring other isotherm models that account for adsorption mechanisms different than the Freundlich and Langmuir models. Due to the complexity of CBR, it might also be desirable to optimize the use of CBR through direct experimentation with real wastewater than using the predictions from isotherm models.

Leaching experiments that utilize ultrapure water showed that CBR and raw bauxite residue both activated the cytotoxicity, estrogenicity, and mutagenicity bioassays, suggesting that without neutralization, the substances released from both CBR and raw bauxite residue could induce cell toxicity pathways. It was further observed that without neutralization, cytotoxicity, estrogenicity, and mutagenicity of OSPW were not reduced after the treatment with CBR, despite the removal in AEOs achieved. Chemical analysis results confirmed several metals were present at concentrations above the CCME guidelines for the protection of freshwater aquatic organisms from long-term effects after CBR treatment, and the exceedance of Al and pH appeared to be the most concerning. Note that CCME guidelines are not for end-of-pipe emission compliance but for evaluation of the quality of the water bodies. Nonetheless, neutralization is strongly recommended when using CBR for future treatment applications.

Post-treatment neutralization with acetic acid was further demonstrated to reduce the leaching of Al from CBR (from 190 mg/L without neutralization to 0.037 mg/L) in ultrapure water, more effective than pre-treatment neutralization (Al was reduced to 16 mg/L). The removals of estrogenicity and mutagenicity were also observed in CBR-treated OSPW after post-treatment neutralization. However, neutralization did not result in the removal of cytotoxicity, and it is difficult to assess which substances in the solution is causing this cytotoxicity. As a next step, it is recommended to investigate the toxicity of the treated OSPW using other cell lines or organisms that are more representative of the receiving environment (e.g., testing with daphnia is ongoing). These toxicity results will decide whether additional detoxification/treatment of CBR needs to be explored in future studies.

Excellent removals of fecal coliform bacteria, nutrients, cytotoxicity, estrogenicity, and mutagenicity were obtained after the treatment with CBR and post-treatment neutralization. Specifically, it appeared that applying CBR at the dosage of 50 g/L to primary effluent produced good removals of total ammonia (69%), total phosphorous (98%), fecal coliform (>99.6%), cytotoxicity IC<sub>10</sub><sub>15min</sub> (from 2 to 11 REF), estrogenicity EC<sub>10</sub> (from 1.6 to 9.2 REF), and mutagenicity EC<sub>IR1.5</sub> (from 17 to >63 REF), while resulting in the smallest concentration of Al (1.5 mg/L) released from CBR. However, at the bench-scale level, TSS and BOD in the CBR-treated effluents exceeded the discharge limits set for the local WWTP, and the concentrations of Al, As, Mo, and Se exceeded the CCME guidelines, prompting the need for further optimization of the CBR treatment process. In the next phase, it might be helpful to (1) optimize the settling process (e.g., sludge retention time and reactor size/shape) to improve the removal of TSS; (2) use alternative neutralization reagents to replace acetic acid to prevent the addition of BOD or incorporate the CBR treatment and post-neutralization process with the BNR process such that the BOD added will be consumed; (3) re-evaluate the significance of the metals released while taking into consideration the conditions of the prospective receiving water bodies and optimize the treatment process if necessary to reduce leaching.

For the treatment of diluted municipal WWTP tertiary effluent, employed to simulate surface water with sewage contamination (5% effluent, 95% river water), the application of CBR was deemed not cost-effective. After treatment with 50 g/L CBR (without neutralization), the concentration of dissolved Al increased from <0.003 mg/L to 110 mg/L and the water pH increased from 8 to 11, both exceeded the CCME guidelines. Meanwhile, insufficient removals (in some cases increases) were observed in cytotoxicity, estrogenicity, and mutagenicity of the

treated diluted effluent. Although the basic pH, the leaching of Al, and toxicities of the water samples might be mitigated by neutralization, the cost for implementing the CBR would likely surpass the benefit from the removal of pollutants by CBR. Thus, the improvement of sewage-polluted water bodies by CBR (using diluted municipal WWTP tertiary effluent) was not evaluated further.

Overall, the use of CBR for water treatment is a promising solution that encourages sustainable waste management practices. Treating waste from another waste material shows both environmental and economic benefits. Although there are still aspects of the CBR treatment that need to be optimized, this thesis suggests that CBR use can be explored at a larger-scale experiment (e.g., pilot-scale) to elucidate additional benefits and improvements for this material.

## References

- [1] M. A. Khairul, J. Zanganeh, and B. Moghtaderi, “The composition, recycling and utilisation of Bayer red mud,” *Resour Conserv Recycl*, vol. 141, pp. 483–498, Feb. 2019, doi: 10.1016/J.RESCONREC.2018.11.006.
- [2] L. J. Kirwan, A. Hartshorn, J. B. McMonagle, L. Fleming, and D. Funnell, “Chemistry of bauxite residue neutralisation and aspects to implementation,” *Int J Miner Process*, vol. 119, pp. 40–50, Mar. 2013, doi: 10.1016/J.MINPRO.2013.01.001.
- [3] W. Tang, M. Khavarian, and A. Yousefi, “Red Mud,” *Sustainable Concrete Made with Ashes and Dust from Different Sources: Materials, Properties and Applications*, pp. 577–606, Jan. 2022, doi: 10.1016/B978-0-12-824050-2.00013-9.
- [4] R. Khanna *et al.*, “Red Mud as a Secondary Resource of Low-Grade Iron: A Global Perspective,” *Sustainability 2022, Vol. 14, Page 1258*, vol. 14, no. 3, p. 1258, Jan. 2022, doi: 10.3390/SU14031258.
- [5] C. R. Borra, Y. Pontikes, K. Binnemans, and T. Van Gerven, “Leaching of rare earths from bauxite residue (red mud),” *Miner Eng*, vol. 76, pp. 20–27, May 2015, doi: 10.1016/J.MINENG.2015.01.005.
- [6] W. M. Mayes *et al.*, “Advances in Understanding Environmental Risks of Red Mud After the Ajka Spill, Hungary,” *Journal of Sustainable Metallurgy*, vol. 2, no. 4, pp. 332–343, Dec. 2016, doi: 10.1007/S40831-016-0050-Z/TABLES/4.
- [7] É. Ujaczki *et al.*, “The potential application of red mud and soil mixture as additive to the surface layer of a landfill cover system,” *Journal of Environmental Sciences*, vol. 44, pp. 189–196, Jun. 2016, doi: 10.1016/J.JES.2015.12.014.
- [8] A. Taylor, “A Flood of Red Sludge, One Year Later - The Atlantic,” *www.theatlantic.com*, Sep. 28, 2011. <https://www.theatlantic.com/photo/2011/09/a-flood-of-red-sludge-one-year-later/100158/> (accessed Apr. 03, 2023).
- [9] H. Zeng, F. Lyu, W. Sun, H. Zhang, L. Wang, and Y. Wang, “Progress on the Industrial Applications of Red Mud with a Focus on China,” *Minerals*, vol. 10, no. 9, p. 773, Aug. 2020, doi: 10.3390/min10090773.
- [10] E. Mukiza, L. Zhang, X. Liu, and N. Zhang, “Utilization of red mud in road base and subgrade materials: A review,” *Resour Conserv Recycl*, vol. 141, pp. 187–199, Feb. 2019, doi: 10.1016/j.resconrec.2018.10.031.
- [11] D. Rubinos, G. Spagnoli, and M. T. Barral, “Assessment of bauxite refining residue (red mud) as a liner for waste disposal facilities,” *Int J Min Reclam Environ*, vol. 29, no. 6, pp. 433–452, Nov. 2015, doi: 10.1080/17480930.2013.830906.



- [12] D. A. Rubinos and G. Spagnoli, "Assessment of red mud as sorptive landfill liner for the retention of arsenic (V)," *J Environ Manage*, vol. 232, pp. 271–285, Feb. 2019, doi: 10.1016/j.jenvman.2018.09.041.
- [13] D. D. Dimas, I. P. Giannopoulou, and D. Panias, "Utilization of alumina red mud for synthesis of inorganic polymeric materials," *Mineral Processing and Extractive Metallurgy Review*, vol. 30, no. 3, pp. 211–239, Jul. 2009, doi: 10.1080/08827500802498199.
- [14] M. Archambo and S. K. Kawatra, "Red Mud: Fundamentals and New Avenues for Utilization," *Mineral Processing and Extractive Metallurgy Review*, vol. 42, no. 7, pp. 427–450, Oct. 2021, doi: 10.1080/08827508.2020.1781109.
- [15] H. Tanvar and B. Mishra, "Comprehensive utilization of bauxite residue for simultaneous recovery of base metals and critical elements," *Sustainable Materials and Technologies*, vol. 33, p. e00466, Sep. 2022, doi: 10.1016/j.susmat.2022.e00466.
- [16] Y. Chen, T. an Zhang, G. Lv, X. Chao, and X. Yang, "Extraction and Utilization of Valuable Elements from Bauxite and Bauxite Residue: A Review," *Bull Environ Contam Toxicol*, vol. 109, no. 1, pp. 228–237, Jul. 2022, doi: 10.1007/S00128-022-03502-W/FIGURES/3.
- [17] X. Chao, T. Zhang, G. Lv, Y. Chen, X. Li, and X. Yang, "Comprehensive Application Technology of Bauxite Residue Treatment in the Ecological Environment: A Review," *Bull Environ Contam Toxicol*, vol. 109, no. 1, pp. 209–214, Jul. 2022, doi: 10.1007/s00128-022-03478-7.
- [18] M. Paradis, J. Duchesne, A. Lamontagne, and D. Isabel, "Long-term neutralisation potential of red mud bauxite with brine amendment for the neutralisation of acidic mine tailings," *Applied Geochemistry*, vol. 22, no. 11, pp. 2326–2333, Nov. 2007, doi: 10.1016/J.APGEOCHEM.2007.04.021.
- [19] E. Domingues *et al.*, "Catalytic Efficiency of Red Mud for the Degradation of Olive Mill Wastewater through Heterogeneous Fenton's Process," *Water 2019, Vol. 11, Page 1183*, vol. 11, no. 6, p. 1183, Jun. 2019, doi: 10.3390/W11061183.
- [20] J. Chen, Y. Wang, and Z. Liu, "Red mud-based catalysts for the catalytic removal of typical air pollutants: A review," *J Environ Sci (China)*, vol. 127, pp. 628–640, May 2023, doi: 10.1016/J.JES.2022.06.027.
- [21] S. Zhang, S. Guo, A. Li, D. Liu, H. Sun, and F. Zhao, "Low-cost bauxite residue-MoS<sub>2</sub> possessing adsorption and photocatalysis ability for removing organic pollutants in wastewater," *Sep Purif Technol*, vol. 283, Jan. 2022, doi: 10.1016/J.SEPPUR.2021.120144.

- [22] A. Katsoyiannis and C. Samara, “The fate of dissolved organic carbon (DOC) in the wastewater treatment process and its importance in the removal of wastewater contaminants,” *Environ Sci Pollut Res Int*, vol. 14, no. 5, pp. 284–292, Jul. 2007, doi: 10.1065/espr2006.05.302.
- [23] C. Li, L. Fu, J. Stafford, M. Belosevic, and M. Gamal El-Din, “The toxicity of oil sands process-affected water (OSPW): A critical review,” *Science of the Total Environment*, vol. 601–602, pp. 1785–1802, Dec. 2017, doi: 10.1016/J.SCITOTENV.2017.06.024.
- [24] T. R. Sahoo and B. Prelot, “Adsorption processes for the removal of contaminants from wastewater: the perspective role of nanomaterials and nanotechnology,” *Nanomaterials for the Detection and Removal of Wastewater Pollutants*, pp. 161–222, Jan. 2020, doi: 10.1016/B978-0-12-818489-9.00007-4.
- [25] I. Ali, M. Asim, and T. A. Khan, “Low cost adsorbents for the removal of organic pollutants from wastewater,” *J Environ Manage*, vol. 113, pp. 170–183, Dec. 2012, doi: 10.1016/J.JENVMAN.2012.08.028.
- [26] M. Campinas *et al.*, “Powdered activated carbon full-scale addition to the activated sludge reactor of a municipal wastewater treatment plant: Pharmaceutical compounds control and overall impact on the process,” *Journal of Water Process Engineering*, vol. 49, p. 102975, Oct. 2022, doi: 10.1016/j.jwpe.2022.102975.
- [27] J. E. Schollée, J. Hollender, and C. S. McArdell, “Characterization of advanced wastewater treatment with ozone and activated carbon using LC-HRMS based non-target screening with automated trend assignment,” *Water Res*, vol. 200, p. 117209, Jul. 2021, doi: 10.1016/j.watres.2021.117209.
- [28] Geomega Resources Inc., “Bauxite Residues Processing.” Accessed: May 10, 2023. [Online]. Available: <https://geomega.ca/bauxite-residues-processing/>
- [29] L. Wang *et al.*, “Application of Red Mud in Wastewater Treatment,” *Minerals 2019, Vol. 9, Page 281*, vol. 9, no. 5, p. 281, May 2019, doi: 10.3390/MIN9050281.
- [30] C. Namasivayam, R. T. Yamuna, and D. J. S. E. Arasi, “Separation Science and Technology Removal of procion orange from wastewater by adsorption on waste red mud REMOVAL OF PROCION ORANGE FROM WASTEWATER BY ADSORPTION ON WASTE RED MUD,” 2007, doi: 10.1081/SS-120003521.
- [31] C. Namasivayam and D. J. S. E. Arasi, “Removal of congo red from wastewater by adsorption onto waste red mud,” *Chemosphere*, vol. 34, no. 2, pp. 401–417, Jan. 1997, doi: 10.1016/S0045-6535(96)00385-2.
- [32] C. Namasivayam, R. T. Yamuna, and D. J. S. E. Arasi, “Removal of acid violet from wastewater by adsorption on waste red mud,” *Environmental Geology*, vol. 41, no. 3–4, pp. 269–273, Dec. 2001, doi: 10.1007/S002540100411/METRICS.

- [33] A. Naga Babu, D. Srinivasa Reddy, P. Sharma, G. Suresh Kumar, K. Ravindhranath, and G. V. Krishna Mohan, "Removal of Hazardous Indigo Carmine Dye from Waste Water Using Treated Red Mud," *Mater Today Proc*, vol. 17, pp. 198–208, Jan. 2019, doi: 10.1016/J.MATPR.2019.06.419.
- [34] V. K. Gupta, Suhas, I. Ali, and V. K. Saini, "Removal of Rhodamine B, Fast Green, and Methylene Blue from Wastewater Using Red Mud, an Aluminum Industry Waste," *Ind Eng Chem Res*, vol. 43, no. 7, pp. 1740–1747, Mar. 2004, doi: 10.1021/IE034218G/ASSET/IMAGES/LARGE/IE034218GF00009.JPEG.
- [35] V. K. Gupta, I. Ali, and V. K. Saini, "Removal of chlorophenols from wastewater using red mud: An aluminum industry waste," *Environ Sci Technol*, vol. 38, no. 14, pp. 4012–4018, Jul. 2004, doi: 10.1021/es049539d.
- [36] S. Aydın, F. Bedük, A. Ulvi, and M. E. Aydın, "Simple and effective removal of psychiatric pharmaceuticals from wastewater treatment plant effluents by magnetite red mud nanoparticles," *Science of the Total Environment*, vol. 784, Aug. 2021, doi: 10.1016/J.SCITOTENV.2021.147174.
- [37] H. Genç-Fuhrman, J. C. Tjell, and D. McConchie, "Adsorption of Arsenic from Water Using Activated Neutralized Red Mud," *Environ Sci Technol*, vol. 38, no. 8, pp. 2428–2434, Apr. 2004, doi: 10.1021/ES035207H.
- [38] Z. Zhao, B. Wang, Q. Feng, M. Chen, X. Zhang, and R. Zhao, "Recovery of nitrogen and phosphorus in wastewater by red mud-modified biochar and its potential application," *Science of The Total Environment*, vol. 860, p. 160289, Feb. 2023, doi: 10.1016/j.scitotenv.2022.160289.
- [39] R. Apak, E. Tütem, M. Hügül, and J. Hizal, "Heavy metal cation retention by unconventional sorbents (red muds and fly ashes)," *Water Res*, vol. 32, no. 2, pp. 430–440, Feb. 1998, doi: 10.1016/S0043-1354(97)00204-2.
- [40] A. I. Zouboulis and K. A. Kydros, "Use of red mud for toxic metals removal: The case of nickel," *Journal of Chemical Technology & Biotechnology*, vol. 58, no. 1, pp. 95–101, Apr. 2007, doi: 10.1002/jctb.280580114.
- [41] O. B. Akpor *et al.*, "Heavy metal pollutants in wastewater effluents: Sources, effects and remediation," *Heavy Metal Pollutants in Wastewater Effluents: Sources, Effects and Remediation. Advances in Bioscience and Bioengineering*, vol. 2, no. 4, pp. 37–43, 2014, doi: 10.11648/j.abb.20140204.11.
- [42] W. Huang *et al.*, "Phosphate removal from wastewater using red mud," *J Hazard Mater*, vol. 158, no. 1, pp. 35–42, Oct. 2008, doi: 10.1016/j.jhazmat.2008.01.061.

- [43] M. Wang and X. Liu, “Applications of red mud as an environmental remediation material: A review,” *J Hazard Mater*, vol. 408, p. 124420, Apr. 2021, doi: 10.1016/J.JHAZMAT.2020.124420.
- [44] J. Ren, J. Chen, W. Guo, B. Yang, X. peng Qin, and P. Du, “Physical, chemical, and surface charge properties of bauxite residue derived from a combined process,” *J Cent South Univ*, vol. 26, no. 2, pp. 373–382, Feb. 2019, doi: 10.1007/S11771-019-4009-7/METRICS.
- [45] Canadian Council of Ministers of the Environment (CCME), “Canadian Water Quality Guidelines for the Protection of Aquatic Life,” 2023. <https://ccme.ca/en/summary-table> (accessed Aug. 01, 2023).
- [46] H. Zeng, H. Tang, W. Sun, and L. Wang, “Strengthening Solid–liquid Separation of Bauxite Residue through the Synergy of Charge Neutralization and Flocculation,” *Sep Purif Technol*, vol. 285, p. 120296, Mar. 2022, doi: 10.1016/J.SEPPUR.2021.120296.
- [47] T. Tian *et al.*, “Effect of amendments on the leaching behavior of alkaline anions and metal ions in bauxite residue,” *Journal of Environmental Sciences*, vol. 85, pp. 74–81, Nov. 2019, doi: 10.1016/J.JES.2019.05.005.
- [48] P. B. Cusack *et al.*, “Enhancement of bauxite residue as a low-cost adsorbent for phosphorus in aqueous solution, using seawater and gypsum treatments,” *J Clean Prod*, vol. 179, pp. 217–224, Apr. 2018, doi: 10.1016/J.JCLEPRO.2018.01.092.
- [49] P. Kannan, F. Banat, S. W. Hasan, and M. Abu Haija, “Neutralization of Bayer bauxite residue (red mud) by various brines: A review of chemistry and engineering processes,” *Hydrometallurgy*, vol. 206, p. 105758, Dec. 2021, doi: 10.1016/J.HYDROMET.2021.105758.
- [50] Y. Li *et al.*, “Phosphate removal from aqueous solutions using raw and activated red mud and fly ash,” *J Hazard Mater*, vol. 137, no. 1, pp. 374–383, Sep. 2006, doi: 10.1016/j.jhazmat.2006.02.011.
- [51] N. Deihimi, M. Irannajad, and B. Rezai, “Characterization studies of red mud modification processes as adsorbent for enhancing ferricyanide removal,” *J Environ Manage*, vol. 206, pp. 266–275, Jan. 2018, doi: 10.1016/J.JENVMAN.2017.10.037.
- [52] N. Deihimi, M. Irannajad, and B. Rezai, “Removal of ferricyanide ions from aqueous solutions using modified red mud with cetyl trimethylammonium bromide,” *Environ Earth Sci*, vol. 78, no. 6, p. 187, Mar. 2019, doi: 10.1007/s12665-019-8173-8.
- [53] O. Kazak, Y. R. Eker, I. Akin, H. Bingol, and A. Tor, “A novel red mud@sucrose based carbon composite: Preparation, characterization and its adsorption performance toward methylene blue in aqueous solution,” *J Environ Chem Eng*, vol. 5, no. 3, pp. 2639–2647, Jun. 2017, doi: 10.1016/J.JECE.2017.05.018.

- [54] C. Z. Liao, L. Zeng, and K. Shih, “Quantitative X-ray Diffraction (QXRD) analysis for revealing thermal transformations of red mud,” *Chemosphere*, vol. 131, pp. 171–177, Jul. 2015, doi: 10.1016/J.CHEMOSPHERE.2015.03.034.
- [55] J. Cao, Y. Wang, Z. Yan, and G. Li, “Polystyrene microspheres-templated preparation of hierarchical porous modified red mud with high rhodamine B dye adsorption performance,” *Micro Nano Lett*, vol. 9, no. 4, pp. 229–231, 2014, doi: 10.1049/MNL.2014.0021.
- [56] E. Nazari, T. M. Roy, O. K. L. Strong, and A. J. Vreugdenhil, “Adsorption of Naphthenic Acids from Oil Sand Process-Affected Water (OSPW) Using Commercially Viable Petcoke-Sourced Activated Carbon,” *Proceedings of the 61st Conference of Metallurgists, COM 2022*, pp. 251–254, 2023, doi: 10.1007/978-3-031-17425-4\_35.
- [57] P. J. Quinlan and K. C. Tam, “Water treatment technologies for the remediation of naphthenic acids in oil sands process-affected water,” *Chemical Engineering Journal*, vol. 279, pp. 696–714, Nov. 2015, doi: 10.1016/J.CEJ.2015.05.062.
- [58] L. A. Pérez-Estrada, X. Han, P. Drzewicz, M. Gamal El-Din, P. M. Fedorak, and J. W. Martin, “Structure-reactivity of naphthenic acids in the ozonation process,” *Environ Sci Technol*, vol. 45, no. 17, pp. 7431–7437, Sep. 2011, doi: 10.1021/es201575h.
- [59] A. Afzal, P. Drzewicz, L. A. Pérez-Estrada, Y. Chen, J. W. Martin, and M. Gamal El-Din, “Effect of molecular structure on the relative reactivity of naphthenic acids in the UV/H<sub>2</sub>O<sub>2</sub> advanced oxidation process,” *Environ Sci Technol*, vol. 46, no. 19, pp. 10727–10734, Oct. 2012, doi: 10.1021/es302267a.
- [60] A. Afzal, P. Chelme-Ayala, P. Drzewicz, J. W. Martin, and M. Gamal El-Din, “Effects of Ozone and Ozone/Hydrogen Peroxide on the Degradation of Model and Real Oil-Sands-Process-Affected-Water Naphthenic Acids,” <http://dx.doi.org/10.1080/01919512.2014.967835>, vol. 37, no. 1, pp. 45–54, Jan. 2014, doi: 10.1080/01919512.2014.967835.
- [61] S. Mishra, V. Meda, A. K. Dalai, J. V. Headley, K. M. Peru, and D. W. McMartin, “Microwave treatment of naphthenic acids in water,” <https://doi.org/10.1080/10934529.2010.493801>, vol. 45, no. 10, pp. 1240–1247, 2010, doi: 10.1080/10934529.2010.493801.
- [62] Z. Shu, C. Li, M. Belosevic, J. R. Bolton, and M. G. El-Din, “Application of a solar UV/chlorine advanced oxidation process to oil sands process-affected water remediation,” *Environ Sci Technol*, vol. 48, no. 16, pp. 9692–9701, Aug. 2014, doi: 10.1021/ES5017558.
- [63] J. S. Clemente, M. D. Mackinnon, and P. M. Fedorak, “Aerobic Biodegradation of Two Commercial Naphthenic Acids Preparations,” *Environ Sci Technol*, vol. 38, no. 4, pp. 1009–1016, Feb. 2004, doi: 10.1021/ES030543J.

- [64] P. Pourrezaei *et al.*, “The impact of metallic coagulants on the removal of organic compounds from oil sands process-affected water,” *Environ Sci Technol*, vol. 45, no. 19, pp. 8452–8459, Oct. 2011, doi: 10.1021/ES201498V.
- [65] K. K. Bjornen, “Electrocoagulation for removal of dissolved naphthenic acids from water,” 8658014, Feb. 03, 2014
- [66] J. S. Taylor and S. J. Duranceau, “Membrane Case Studies, Past, Present and Future,” *Membrane Technology in Water and Wastewater Treatment*, pp. 3–24, Jan. 2000, doi: 10.1039/9781847551351-00003.
- [67] H. Peng, K. Volchek, M. MacKinnon, W. P. Wong, and C. E. Brown, “Application on to nanofiltration to water management options for oil sands operation,” *Desalination*, vol. 170, no. 2, pp. 137–150, Oct. 2004, doi: 10.1016/J.DESAL.2004.03.018.
- [68] M. H. Mohamed, L. D. Wilson, J. V. Headley, and K. M. Peru, “Novel materials for environmental remediation of tailing pond waters containing naphthenic acids,” *Process Safety and Environmental Protection*, vol. 86, no. 4, pp. 237–243, Jul. 2008, doi: 10.1016/J.PSEP.2008.04.001.
- [69] B. Sarkar, H. Fricska, Q. Gao, S. Tong, and C. Q. Jia, “Adsorption of single-ring model naphthenic acid from oil sands tailings pond water using physically activated petroleum coke,” *Can J Chem Eng*, 2022, doi: 10.1002/CJCE.24804.
- [70] S. Iranmanesh, T. Harding, J. Abedi, F. Seyedeyn-Azad, and D. B. Layzell, “Adsorption of naphthenic acids on high surface area activated carbons,” *J Environ Sci Health A Tox Hazard Subst Environ Eng*, vol. 49, no. 8, pp. 913–922, Mar. 2014, doi: 10.1080/10934529.2014.894790.
- [71] D. Prajapati, M. Shah, A. Yadav, and J. Panchal, “A critical review on emerging contaminants: origin, discernment, and remedies,” *Sustainable Water Resources Management 2023 9:3*, vol. 9, no. 3, pp. 1–11, Apr. 2023, doi: 10.1007/S40899-023-00853-Y.
- [72] V. S. Thomaidi, A. S. Stasinakis, V. L. Borova, and N. S. Thomaidis, “Is there a risk for the aquatic environment due to the existence of emerging organic contaminants in treated domestic wastewater? Greece as a case-study,” *J Hazard Mater*, vol. 283, pp. 740–747, Feb. 2015, doi: 10.1016/J.JHAZMAT.2014.10.023.
- [73] M. Kumar *et al.*, “Current research trends on emerging contaminants pharmaceutical and personal care products (PPCPs): A comprehensive review,” *Science of the Total Environment*, vol. 859, Feb. 2023, doi: 10.1016/J.SCITOTENV.2022.160031.
- [74] C. Sophia A. and E. C. Lima, “Removal of emerging contaminants from the environment by adsorption,” *Ecotoxicol Environ Saf*, vol. 150, pp. 1–17, Apr. 2018, doi: 10.1016/J.ECOENV.2017.12.026.

- [75] J. Y. Song, B. N. Bhadra, and S. H. Jhung, “Contribution of H-bond in adsorptive removal of pharmaceutical and personal care products from water using oxidized activated carbon,” *Microporous and Mesoporous Materials*, vol. 243, pp. 221–228, 2017, doi: 10.1016/J.MICROMESO.2017.02.024.
- [76] M. B. Ahmed, J. L. Zhou, H. H. Ngo, W. Guo, and M. Chen, “Progress in the preparation and application of modified biochar for improved contaminant removal from water and wastewater,” *Bioresour Technol*, vol. 214, pp. 836–851, Apr. 2016, doi: 10.1016/J.BIORTECH.2016.05.057.
- [77] M. C. Ncibi and M. Sillanpää, “Optimizing the removal of pharmaceutical drugs Carbamazepine and Dorzolamide from aqueous solutions using mesoporous activated carbons and multi-walled carbon nanotubes,” *J Mol Liq*, vol. 238, pp. 379–388, Jul. 2017, doi: 10.1016/J.MOLLIQ.2017.05.028.
- [78] M. Zambianchi *et al.*, “Graphene oxide doped polysulfone membrane adsorbers for the removal of organic contaminants from water,” *Chemical Engineering Journal*, vol. 326, pp. 130–140, 2017, doi: 10.1016/J.CEJ.2017.05.143.
- [79] Y. J. C. Martins, A. C. M. Almeida, B. M. Viegas, R. A. do Nascimento, and N. F. da P. Ribeiro, “Use of red mud from amazon region as an adsorbent for the removal of methylene blue: process optimization, isotherm and kinetic studies,” *International Journal of Environmental Science and Technology*, vol. 17, no. 10, pp. 4133–4148, Oct. 2020, doi: 10.1007/S13762-020-02757-2/TABLES/7.
- [80] Z. P. Hu, Z. M. Gao, X. Liu, and Z. Y. Yuan, “High-surface-area activated red mud for efficient removal of methylene blue from wastewater,” *Adsorption Science and Technology*, vol. 36, no. 1–2, pp. 62–79, Feb. 2018, doi: 10.1177/0263617416684348.
- [81] L. T. Hengdes *et al.*, “Adsorption and desorption of water-soluble naphthenic acid in simulated offshore oilfield produced water,” *Process Safety and Environmental Protection*, vol. 145, pp. 262–272, Jan. 2021, doi: 10.1016/J.PSEP.2020.08.018.
- [82] L. Pellenz *et al.*, “A comprehensive guide for characterization of adsorbent materials,” *Sep Purif Technol*, vol. 305, Jan. 2023, doi: 10.1016/J.SEPPUR.2022.122435.
- [83] J. Epp, “X-ray diffraction (XRD) techniques for materials characterization,” *Materials Characterization Using Nondestructive Evaluation (NDE) Methods*, pp. 81–124, Jan. 2016, doi: 10.1016/B978-0-08-100040-3.00004-3.
- [84] Alberta Environment and Parks (AEP), “Standards and Guidelines for Municipal Waterworks, Wastewater and Storm Drainage Systems Part 4 Wastewater Systems Guidelines for Design, Operating and Monitoring of a Total of 5 Parts,” 2021, Accessed: Aug. 14, 2023. [Online]. Available: <https://open.alberta.ca/publications/5668185>

- [85] Kia Barrow, B. I. Escher, K. A. Hicks, Maria König, Rita Schlichting, and M. J. Arlos, “Water quality monitoring with in vitro bioassays to compare untreated oil sands process-affected water with unimpacted rivers,” *Environ Sci (Camb)*, 2023, doi: 10.1039/D2EW00988A.
- [86] D. M. Grewer, R. F. Young, R. M. Whittal, and P. M. Fedorak, “Naphthenic acids and other acid-extractables in water samples from Alberta: What is being measured?,” *Science of The Total Environment*, vol. 408, no. 23, pp. 5997–6010, Nov. 2010, doi: 10.1016/J.SCITOTENV.2010.08.013.
- [87] B. Escher, P. Neale, and F. Leusch, “Bioanalytical Tools in Water Quality Assessment,” 2021, doi: 10.2166/9781789061987.
- [88] A. J. Bartlett, W. Norwood, J.-F. Féraud, and C. Blaise, “Mixture Effects in Ecotoxicology,” *Encyclopedia of Aquatic Ecotoxicology*, pp. 729–736, 2013, doi: 10.1007/978-94-007-5704-2\_67.
- [89] K. Barrow, “In vitro bioassay monitoring to assess baseline conditions prior to potential discharge of treated oil sands process water in receiving aquatic environments,” 2022, doi: 10.7939/R3-M09Y-ZB13.
- [90] “BioTox™ LumoPlate™ Ultimate Matrix Kit.” <https://www.biotoxicity.com/index.php/ebpi-toxicity-tests/aliivibrio-fischeri-toxicity-tests/biotox-lumoplate-ultimate-matrix-kit> (accessed May 19, 2023).
- [91] “UMU-ChromoTest™.” <https://biotoxicity.com/biotoxicity/index.php/ebpi-toxicity-tests/sos-genotoxicity-tests/umu-chromotest> (accessed May 30, 2023).
- [92] Alberta Environment and Parks, *Environmental quality guidelines for Alberta surface waters*. 2018. Accessed: May 14, 2023. [Online]. Available: <https://open.alberta.ca/publications/9781460138731>
- [93] Y. Liu, C. Lin, and Y. Wu, “Characterization of red mud derived from a combined Bayer Process and bauxite calcination method,” *J Hazard Mater*, vol. 146, no. 1–2, pp. 255–261, Jul. 2007, doi: 10.1016/j.jhazmat.2006.12.015.
- [94] K. S. P. Karunadasa, C. H. Manoratne, H. M. T. G. A. Pitawala, and R. M. G. Rajapakse, “Thermal decomposition of calcium carbonate (calcite polymorph) as examined by in-situ high-temperature X-ray powder diffraction,” *Journal of Physics and Chemistry of Solids*, vol. 134, pp. 21–28, Nov. 2019, doi: 10.1016/J.JPCS.2019.05.023.
- [95] T. Cornelius, “Variation of Physico-Chemical and Textural Properties of Laboratory Prepared Red Mud Through Acid and Thermal Activations,” *Advances in Materials*, vol. 6, no. 2, p. 11, 2017, doi: 10.11648/j.am.20170602.12.



- [96] M. H. M. Ahmed *et al.*, “Red-mud based porous nanocatalysts for valorisation of municipal solid waste,” *J Hazard Mater*, vol. 396, p. 122711, Sep. 2020, doi: 10.1016/j.jhazmat.2020.122711.
- [97] S. Wang, Y. Boyjoo, A. Choueib, and Z. H. Zhu, “Removal of dyes from aqueous solution using fly ash and red mud,” *Water Res*, vol. 39, no. 1, pp. 129–138, Jan. 2005, doi: 10.1016/j.watres.2004.09.011.
- [98] O. V. Petrov and I. Furó, “NMR cryoporometry: Principles, applications and potential,” *Prog Nucl Magn Reson Spectrosc*, vol. 54, no. 2, pp. 97–122, Feb. 2009, doi: 10.1016/j.pnmrs.2008.06.001.
- [99] M. Thommes *et al.*, “Physisorption of gases, with special reference to the evaluation of surface area and pore size distribution (IUPAC Technical Report),” *Pure and Applied Chemistry*, vol. 87, no. 9–10, pp. 1051–1069, Oct. 2015, doi: 10.1515/pac-2014-1117.
- [100] S. Samanipour, M. Hooshyari, J. A. Baz-Lomba, M. J. Reid, M. Casale, and K. V. Thomas, “The effect of extraction methodology on the recovery and distribution of naphthenic acids of oilfield produced water,” *Science of The Total Environment*, vol. 652, pp. 1416–1423, Feb. 2019, doi: 10.1016/j.scitotenv.2018.10.264.
- [101] R. Qin *et al.*, “Separation of oil sands process water organics and inorganics and examination of their acute toxicity using standard in-vitro bioassays,” *Science of the Total Environment*, vol. 695, Dec. 2019, doi: 10.1016/J.SCITOTENV.2019.07.338.
- [102] I. T. Burke *et al.*, “Behavior of aluminum, arsenic, and vanadium during the neutralization of red mud leachate by HCl, gypsum, or seawater,” *Environ Sci Technol*, vol. 47, no. 12, pp. 6527–6535, Jun. 2013, doi: 10.1021/ES4010834.
- [103] D. M. Grewer, R. F. Young, R. M. Whittal, and P. M. Fedorak, “Naphthenic acids and other acid-extractables in water samples from Alberta: What is being measured?,” *Science of The Total Environment*, vol. 408, no. 23, pp. 5997–6010, Nov. 2010, doi: 10.1016/j.scitotenv.2010.08.013.
- [104] Md. S. Islam, Y. Zhang, K. N. McPhedran, Y. Liu, and M. Gamal El-Din, “Granular activated carbon for simultaneous adsorption and biodegradation of toxic oil sands process-affected water organic compounds,” *J Environ Manage*, vol. 152, pp. 49–57, Apr. 2015, doi: 10.1016/j.jenvman.2015.01.020.
- [105] W. Zubot, M. D. MacKinnon, P. Chelme-Ayala, D. W. Smith, and M. Gamal El-Din, “Petroleum coke adsorption as a water management option for oil sands process-affected water,” *Science of The Total Environment*, vol. 427–428, pp. 364–372, Jun. 2012, doi: 10.1016/j.scitotenv.2012.04.024.
- [106] T. I. Bhuiyan, J. K. Tak, S. Sessarego, D. Harfield, and J. M. Hill, “Adsorption of acid-extractable organics from oil sands process-affected water onto biomass-based biochar:

- Metal content matters,” *Chemosphere*, vol. 168, pp. 1337–1344, Feb. 2017, doi: 10.1016/j.chemosphere.2016.11.126.
- [107] C. Benally, S. A. Messele, and M. Gamal El-Din, “Adsorption of organic matter in oil sands process water (OSPW) by carbon xerogel,” *Water Res*, vol. 154, pp. 402–411, May 2019, doi: 10.1016/j.watres.2019.01.053.
- [108] W. Zubot, Z. An, C. Benally, and M. Gamal El-Din, “Treatment of oil sands process water using petroleum coke: Field pilot,” *J Environ Manage*, vol. 289, p. 112407, Jul. 2021, doi: 10.1016/J.JENVMAN.2021.112407.
- [109] R. van der Oost, G. Sileno, M. Suárez-Muñoz, M. T. Nguyen, H. Besselink, and A. Brouwer, “SIMONI (smart integrated monitoring) as a novel bioanalytical strategy for water quality assessment: Part i—model design and effect-based trigger values,” *Environ Toxicol Chem*, vol. 36, no. 9, pp. 2385–2399, Sep. 2017, doi: 10.1002/ETC.3836.
- [110] W.-S. Lung, “Coliforms, Pathogens, and Viruses,” in *Water Quality Modeling That Works*, Cham: Springer International Publishing, 2022, pp. 203–230. doi: 10.1007/978-3-030-90483-8\_6.
- [111] P. Liang, H. Yu, J. Huang, Y. Zhang, and H. Cao, “The Review on Adsorption and Removing Ammonia Nitrogen with Biochar on its Mechanism,” *MATEC Web of Conferences*, vol. 67, p. 07006, Jul. 2016, doi: 10.1051/mateconf/20166707006.
- [112] C. Barca, D. Scanu, N. Podda, H. Miche, L. Poizat, and P. Hennebert, “Phosphorus removal from wastewater by carbonated bauxite residue under aerobic and anoxic conditions,” *Journal of Water Process Engineering*, vol. 39, p. 101757, Feb. 2021, doi: 10.1016/j.jwpe.2020.101757.

## Appendix A. Supplementary Material to Methodology

### Appendix A.1 Spectrum Scan and Calibration Curves for Methylene Blue (MB)

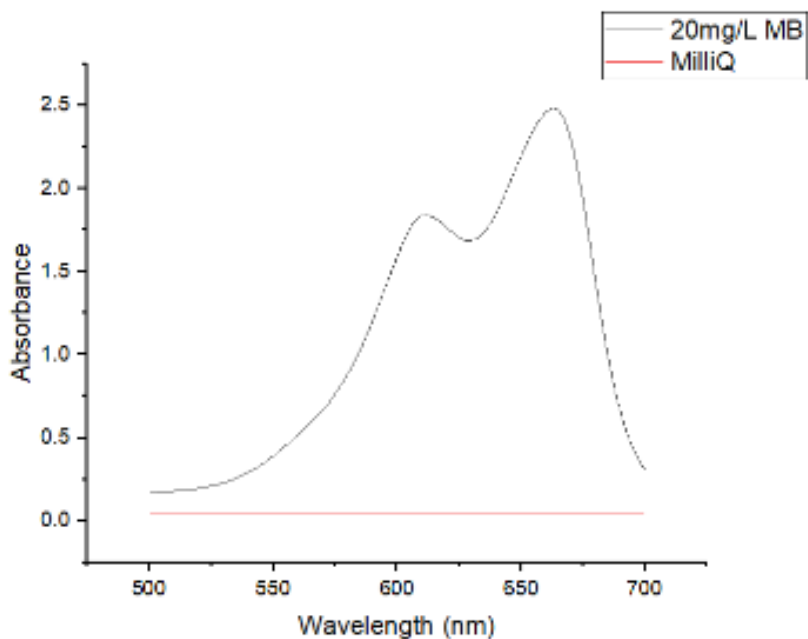


**Figure A.1.1.** Absorbance pattern for 20 mg/L methylene blue (MB). Peak absorbance was observed at 665nm.

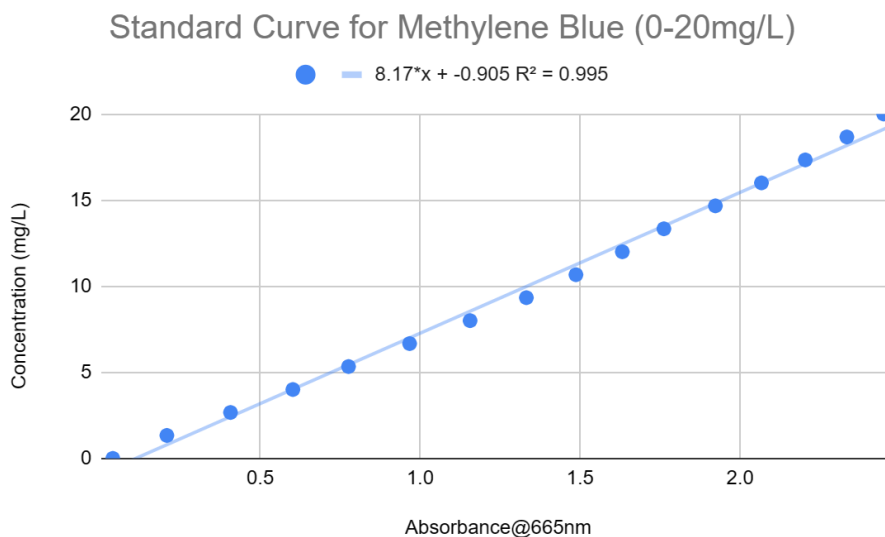


**Figure A.1.2.** Sample calibration curve for determining MB concentration in water samples. The calibration equation derived is applicable to samples with  $A_{665nm}$  values between 0 and 2.45 Au.

## Appendix A.2 Calibration Curves for Sigma NAs and Cyclohexanecarboxylic Acids

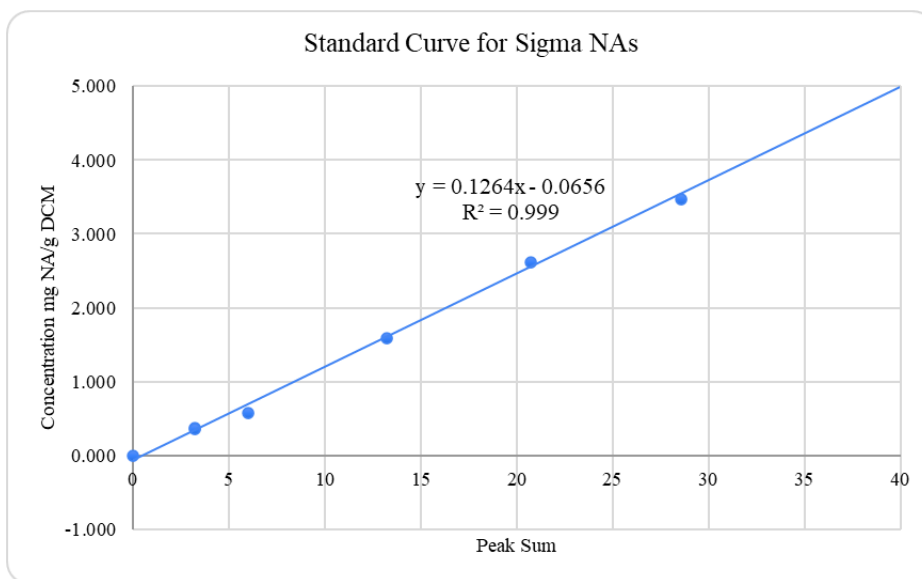


**Figure A.2.1.** Sample calibration curve for determining the concentration of Sigma NAs. DCM = dichloromethane. Peak Sum = sum of absorbances at  $\sim 1739$  and  $1701\text{ cm}^{-1}$ .

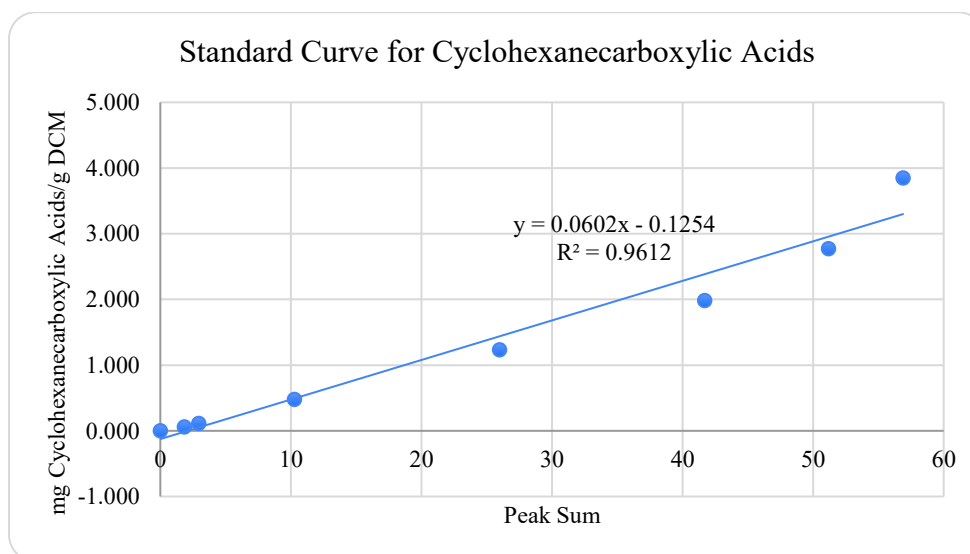


**Figure A.2.2.** Sample calibration curve for determining the concentration of cyclohexanecarboxylic acids. Peak Sum = sum of absorbances at  $\sim 1742$  and  $1704\text{ cm}^{-1}$ .

### Appendix A.3 YES Assay Stock Solution Preparation

**Table A.3.1.** Reagents for gold solution preparation adapted from Barrow et al. [85].

Compound	Concentration (g/L)	Preparation	Storage	Amount for Gold Solution (mL)
Adenine hydrochloride hydrate	1.2	Autoclave	RT*	75
L-Histidine-HCl	2.4	Autoclave	4°C	50
L-Arginine-HCl	2.4	Autoclave	4°C	25
L-Methionine	2.4	Autoclave	4°C	25
L-Tyrosine	0.9	Autoclave	RT	25
L-Isoleucine	3.6	Autoclave	4°C	25
L-Lysine-HCl	4	Autoclave	4°C	100
L-Phenylalanine	3	Autoclave	RT	25
L-Glutamic Acid	6	Autoclave	RT	25
L-Aspartic Acid	4	Autoclave	RT	25
L-Valine	18	Autoclave	4°C	25
L-Threonine	24	Autoclave	4°C	25
L-Serine	45	Autoclave	4°C	50
L-Leucine	3.6	Autoclave	RT	25
L-Tryptophan	4.8	Filter Sterilize	4°C	50
Uracil	2.4	Autoclave	RT	25

\*: room temperature

**Table A.3.2.** Other stock solutions preparation for YES following Barrow et al. [85].

Stock Solution	Ingredients	Preparation	Storage
10X YNB without Amino Acids	67g YNB Without Amino Acids 1L MilliQ	Filter Sterilize	4°C
20% Dextrose Stock	200g Dextrose 1L MilliQ	Filter Sterilize	4°C
CuSO <sub>4</sub> Pentahydrate	250mg CuSO <sub>4</sub> Pentahydrate 100mL MilliQ	Filter Sterilize	4°C
Gold Media	60mL 20% Dextrose 60mL 10X YNB 110mL GOLD Solution 370mL MilliQ	Filter Sterilize	4°C
Minimal Media	100mL 10X YNB 100mL 20% Dextrose 10mL L-Lysine 790mL MilliQ	Filter Sterilize	4°C
30% Glycerol	30mL Glycerol 70mL MilliQ	Autoclave	RT*

\*: room temperature

## Appendix B. Supplementary Material to Results and Discussions

### Appendix B.1. SEM Images of Higher Magnifications and Raw EDX Data

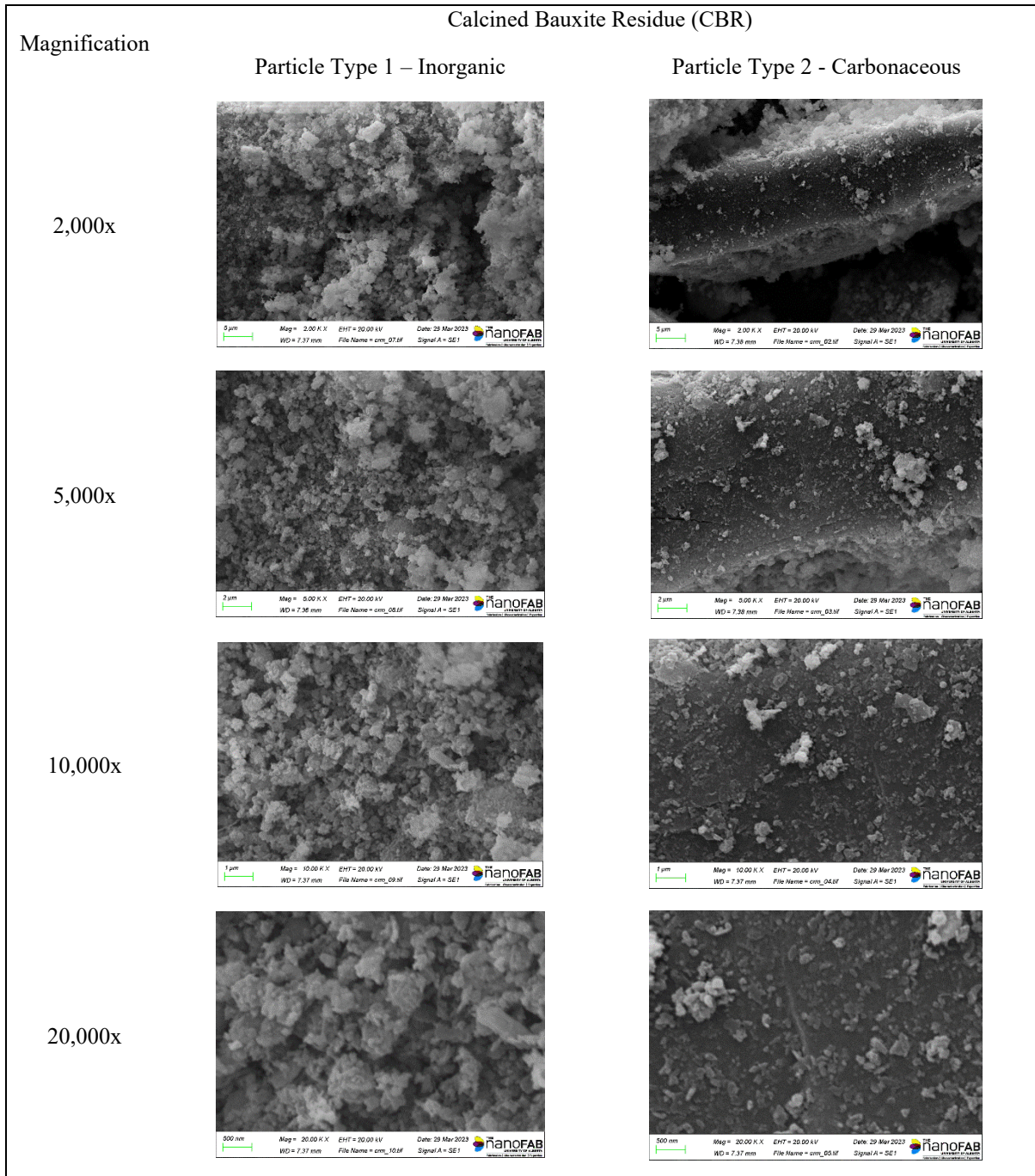


Figure B.1.1. SEM images of CBR at higher magnifications.

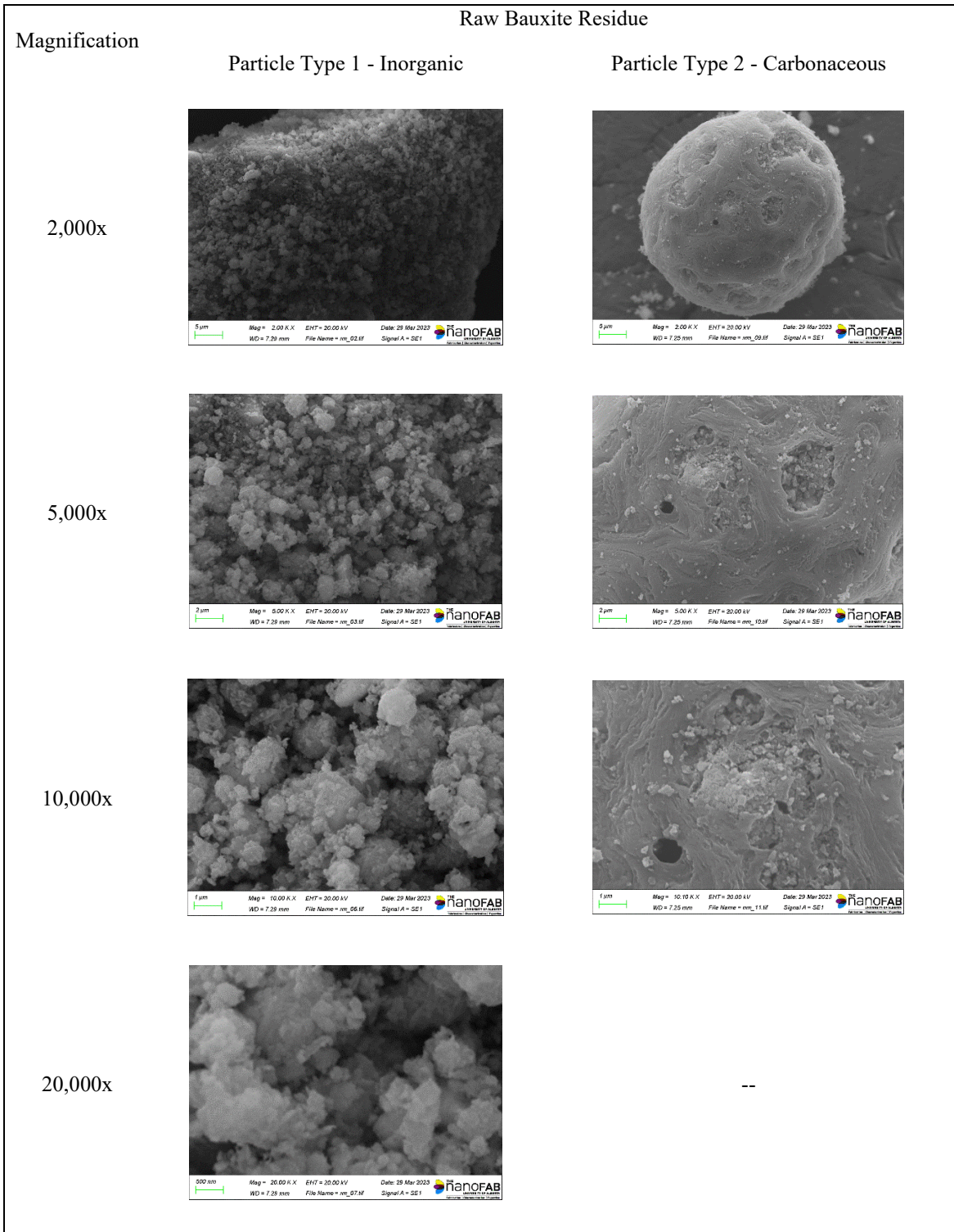
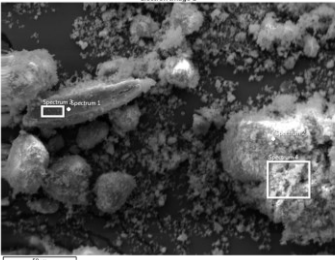
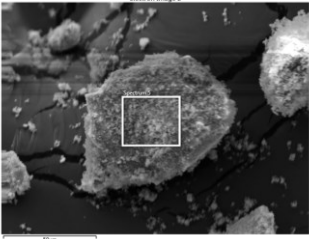


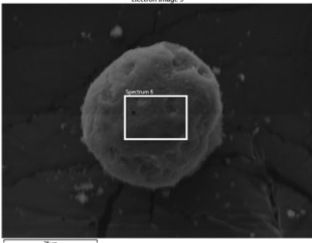
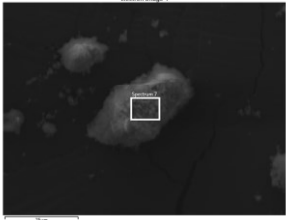
Figure B.1.2. SEM images of raw bauxite residue at higher magnifications.



**Table B.1.1.** Unaveraged energy-dispersive X-ray spectroscopy (EDX) results and the locations on CBR particles selected for analysis. Point 1 and Spectrum 3 were located on the carbonaceous particle, while Point 2, Spectrum 4, and Spectrum 5 were on the inorganic particle.

Spectrum Chosen	EDX Results (% by weight)				
	Spectrum Label	Spectrum 1	Spectrum 2	Spectrum 3	Spectrum 4
	C	77.93	18.62	76.86	15.50
	O	12.56	37.80	13.77	34.37
	Na	1.17	5.83	1.25	6.59
	Mg	0.25		0.20	
	Al	2.11	7.59	2.03	8.26
	Si	0.13	3.51	0.20	4.58
	S	1.74	0.21	1.60	0.24
	Cl		0.11		0.09
	K	0.07		0.07	
	Ca	0.73	0.60	0.70	0.73
	Ti	0.22	2.18	0.23	2.47
	Cr				0.13
	Fe	3.08	23.55	3.09	27.04
	Total	100.00	100.00	100.00	100.00
	Spectrum Label	Spectrum 5			
	C	17.00			
	O	39.14			
	Na	7.58			
	Al	8.95			
	Si	5.14			
	S	0.25			
	Cl	0.07			
	Ca	0.52			
	Ti	2.36			
Fe	18.99				
Total	100.00				

**Table B.1.2.** Energy-dispersive X-ray spectroscopy (EDX) results and the locations on raw bauxite residue particles selected for analysis. Spectrum 6 was located on the carbonaceous particle, while Spectrum 7 was located on the inorganic particle.

Spectrum Chosen	EDX Results (% by weight)	
	Spectrum Label	Spectrum 6
	C	74.34
	O	13.75
	Na	0.27
	Al	3.66
	Si	0.54
	S	2.40
	Ca	0.11
	Ti	0.66
	V	0.15
	Fe	4.11
	Total	100.00
	Spectrum Label	Spectrum 7
	C	19.53
	O	36.68
	Na	5.87
	Al	10.42
	Si	5.72
	S	0.37
	Cl	0.14
	Ca	0.56
	Ti	2.92
	Fe	17.79
Total	100.00	

## Appendix B.2. Experiment Designed to Improve the Recovery of AEOs

There are two goals of this experiment: (1) to determine if the ENV+/C8 cartridge (6cc/400mg, Biotage) can improve the recovery of AEOs; (2) to examine the effect of eluting the cartridges with dichloromethane (instead of methanol and ethyl acetate), and directly analyzing the eluent with FTIR without evaporation and reconstitution.

The results of the Oasis HLB and the ENV+/C8 cartridges were compared based on the recovery efficiencies of AEOs following the SPE extraction procedure described in Section 2.6 and the FTIR analysis procedure described in Section 2.7.2. A total volume of 300 mL of real OSPW, Sigma NAs (40 mg/L), and cyclohexanecarboxylic acid (60 mg/L) were prepared and then each divided into 6 smaller aliquots of 50 mL for separate extraction (n=3 for each cartridge type). Based on the results (Table B.2.1), the Oasis HLB cartridge produced better recoveries of AEOs at a higher consistency for all three water sample matrices tested. Thus, replacing Oasis HLB with ENV+/C8 for SPE likely would not improve the recovery of AEOs.

**Table B.2.1.** Recovery efficiencies of acid-extractable organics (AEOs) obtained using Oasis HLB and ENV+/C8 cartridges. OSPW = oil sands process-affected water.

Cartridge	40 mg/L Sigma NAs		60 mg/L Cyclohexanecarboxylic Acid		OSPW
	Measured (mg/L)	Average Recovery (%)	Measured (mg/L)	Average Recovery (%)	Measured (mg/L)
Oasis HLB	24.4 ± 0.3	61	14.6 ± 1.2	24	40.4 ± 0.2
ENV+/C8	19.7 ± 1.7	49	8.9 ± 2.6	15	36.2 ± 1.5

For the second test, 300 mL of 60 mg/L cyclohexanecarboxylic acid solution (from the same stock bottle as the one used for the first set of experiments above) was utilized and divided into 6 equal aliquots of 50 mL for extraction (n=3 for each cartridge type). The SPE extraction and FTIR analysis procedure were similar to the former, but without evaporation of the eluent.

After drying the cartridges under vacuum, they were eluted with 4-5 full Pasteur pipets of dichloromethane (about 3-6 mL in total) and immediately transferred to pre-weighed 15 mL amber vials. The amber vials were wrapped in parafilm and were stored at -20°C until analysis. On the day of the FTIR analysis, the vials were unwrapped and weighed, and the sample eluent was loaded to the FTIR cell two times (the first time for rinsing the cell and the second time for reading) for the measurement of AEOs. As dichloromethane is a strong solvent that might introduce background concentration by potentially dissolving some of the cartridge material during elution, 2 aliquots of 50 mL ultrapure water were used for background control for each cartridge type. The ultrapure water underwent the same extraction and direct elution with dichloromethane for FTIR analysis.

**Table B.2.2.** Recovery efficiencies of acid-extractable organics (AEOs) using dichloromethane for elution and directly analyzing the eluent with Fourier transform infrared spectroscopy (FTIR).

Cartridge	60 mg/L Cyclohexanecarboxylic Acid	
	Measured (mg/L)	Average Recovery (%)
Oasis HLB	19.4 ± 1.4	32
ENV+/C8	34.3 ± 2.1	57

The modified extraction and analytical procedure produced much higher recoveries for both cartridges. Especially for the ENV+/C8 cartridge, the recovery improved from 15% to 57%, as shown in Table B.2.2, indicating that both evaporation and the solvent used for elution likely contributed to the loss of AEOs in previous SPEs. Although the background control samples showed the dissolution of cartridge material (extracts were found to contain white powder), the cartridges did not contribute to the concentration of AEOs. However, after FTIR analysis, white stains were observed on the glass wall inside the FTIR cell (Figure B.2.1), and the stains were

not removed after rinsing with clean dichloromethane. Despite the improved recovery of cyclohexanecarboxylic acid, this method was not employed to protect the FTIR cell from damage.

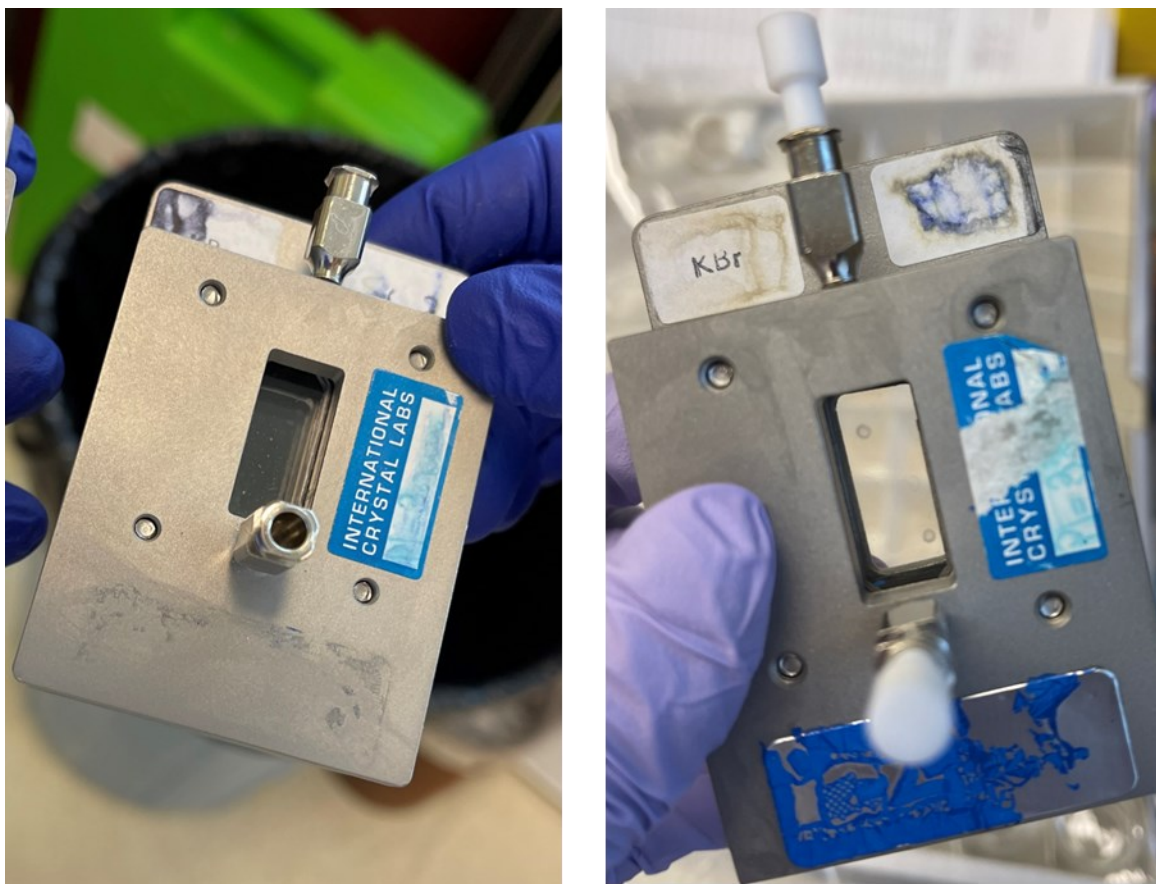


**Figure B.2.1.** Pictures of the FTIR cell before experiment (left) and after experiment (right). Before the cell wall was transparent but after the cell wall was less transparent due to the stains.

### Appendix B.3. More Chemical Analyses Results on Leaching/Removal of Pollutants

**Table B.3.1.** The effect of treatment with 50 g/L CBR on nitrogen parameters in OSPW and diluted municipal WWTP (Plant A) tertiary effluent (no neutralization).

Parameter	Unit	OSPW	OSPW + 50g/L CBR	Diluted Effluent	Diluted Effluent + 50g/L CBR
Nitrate (N)	mg/L	0.99	0.42	1.1	0.98
Nitrate (NO <sub>3</sub> )	mg/L	4.4	1.9	4.9	4.3
Nitrite (NO <sub>2</sub> )	mg/L	<0.033	0.046	<0.033	<0.033
Nitrite (N)	mg/L	<0.010	0.014	<0.010	<0.010
Nitrate plus Nitrite (N)	mg/L	0.99	0.44	1.1	0.98

**Table B.3.2.** The release of total metals and nutrients in ultrapure water by: (1) 50 g/L CBR (2) 50 g/L raw bauxite residue (3) 50 g/L CBR and pre-treatment neutralization with acetic acid (4) 50 g/L CBR and post-treatment neutralization with acetic acid.

Parameter	Unit	Ultrapure Water + 50 g/L CBR (1)	Ultrapure Water + 50 g/L Raw Bauxite Residue (2)	Pre-treatment Neutralization (3)	Post-treatment Neutralization (4)
Total Cadmium (Cd)	ug/L	0.022	<2.0	0.032	<0.020
Total Aluminum (Al)	mg/L	200	520	42	3.0
Total Antimony (Sb)	mg/L	0.0072	<0.060	0.0077	0.0084
Total Arsenic (As)	mg/L	0.025	0.043	0.012	0.019
Total Barium (Ba)	mg/L	<0.010	<0.20	0.022	0.041
Total Beryllium (Be)	mg/L	<0.0010	<0.10	<0.0010	<0.0010
Total Boron (B)	mg/L	0.35	0.42	0.56	0.80
Total Calcium (Ca)	mg/L	82	150	240	320
Total Chromium (Cr)	mg/L	0.042	1.9	0.11	0.017
Total Cobalt (Co)	mg/L	<0.00030	<0.030	0.00042	<0.00030
Total Copper (Cu)	mg/L	0.0046	0.12	0.0075	0.0044
Total Iron (Fe)	mg/L	17	160	47	6.2
Total Lead (Pb)	mg/L	0.0029	0.11	0.0071	0.0012
Total Lithium (Li)	mg/L	<0.020	<0.40	<0.020	<0.020
Total Magnesium (Mg)	mg/L	<0.20	<4.0	0.58	0.87
Total Manganese (Mn)	mg/L	0.0040	0.15	0.011	0.017
Total Molybdenum (Mo)	mg/L	0.099	<0.020	0.10	0.043
Total Nickel (Ni)	mg/L	0.0028	<0.050	0.0091	0.0042
Total Phosphorus (P)	mg/L	<0.10	<2.0	0.11	<0.10
Total Potassium (K)	mg/L	0.83	12	1.0	1.3
Total Selenium (Se)	mg/L	0.057	0.025	0.014	0.0083
Total Silicon (Si)	mg/L	4.4	350	12	6.6
Total Silver (Ag)	mg/L	<0.00010	<0.010	0.00014	<0.00010
Total Sodium (Na)	mg/L	190	730	410	380
Total Strontium (Sr)	mg/L	0.031	<0.40	0.14	0.24
Total Sulphur (S)	mg/L	32	51	38	30
Total Thallium (Tl)	mg/L	<0.00020	<0.020	<0.00020	<0.00020
Total Tin (Sn)	mg/L	0.0019	<0.10	0.0031	<0.0010
Total Titanium (Ti)	mg/L	0.94	11	1.4	0.34
Total Uranium (U)	mg/L	0.00033	0.014	0.00080	0.00023
Total Vanadium (V)	mg/L	0.16	1.4	0.17	0.034
Total Zinc (Zn)	mg/L	<0.0030	3.2	0.044	<0.0030
Nitrate (N)	mg/L	<0.010	0.11	<0.010	<0.050
Nitrate (NO3)	mg/L	<0.044	0.49	<0.044	<0.22
Nitrite (NO2)	mg/L	0.041	0.82	0.034	0.053
Orthophosphate (P)	mg/L	0.0041	0.11	<0.0030	0.0036
Nitrite (N)	mg/L	0.012	0.25	0.010	0.016
Nitrate plus Nitrite (N)	mg/L	<0.010	0.36	<0.010	<0.050

**Table B.3.3.** The concentrations of dissolved metals in untreated municipal WWTP (Plant B) primary (after biological nutrient removal), secondary (after secondary clarifier), and tertiary (after UV disinfection) effluents. The values **highlighted in green** exceeded the **long-term** guideline for the protection of freshwater aquatic life by CCME [44]. Results were not compared with the guidelines where the guideline values were not available. \*: Hardness was not measured but estimated based on the concentrations of dissolved calcium, magnesium, and aluminum. Refer to Appendix B.4 Table B.4.4 for short- and long-term guideline values for each sample.

Metal Ions	Units	Primary Effluent (Post-BNR)	Secondary Effluent (Post-Secondary Clarifier)	Tertiary Effluent (Post-UV)
Dissolved Cadmium (Cd)	ug/L	0.035	0.033	<0.020
Dissolved Aluminum (Al)	mg/L	0.053	0.029	0.031
Dissolved Antimony (Sb)	mg/L	0.0017	<0.00060	0.00084
Dissolved Arsenic (As)	mg/L	0.00070	0.00064	0.00054
Dissolved Barium (Ba)	mg/L	0.035	0.041	0.039
Dissolved Beryllium (Be)	mg/L	<0.0010	<0.0010	<0.0010
Dissolved Boron (B)	mg/L	0.26	0.19	0.18
Dissolved Calcium (Ca)	mg/L	49	61	61
Dissolved Chromium (Cr)	mg/L	<0.0010	<0.0010	<0.0010
Dissolved Cobalt (Co)	mg/L	0.00077	0.00066	0.00073
Dissolved Copper (Cu)	mg/L	0.0051	<0.0010	<0.0010
Dissolved Iron (Fe)	mg/L	0.17	<0.060	<0.060
Dissolved Lead (Pb)	mg/L	0.00030	0.00025	0.00022
Dissolved Lithium (Li)	mg/L	0.024	0.023	0.026
Dissolved Magnesium (Mg)	mg/L	17	18	18
Dissolved Manganese (Mn)	mg/L	0.091	0.085	0.082
Dissolved Molybdenum (Mo)	mg/L	0.013	0.018	0.017
Dissolved Nickel (Ni)	mg/L	0.0051	0.0036	0.0037
Dissolved Phosphorus (P)	mg/L	3.6	0.15	0.10
Dissolved Potassium (K)	mg/L	14	14	14
Dissolved Selenium (Se)	mg/L	0.00045	0.00038	0.00025
Dissolved Silicon (Si)	mg/L	2.4	2.6	2.5
Dissolved Silver (Ag)	mg/L	<0.00010	<0.00010	<0.00010
Dissolved Sodium (Na)	mg/L	63	71	70
Dissolved Strontium (Sr)	mg/L	0.38	0.44	0.43
Dissolved Sulphur (S)	mg/L	36	42	40
Dissolved Thallium (Tl)	mg/L	<0.00020	<0.00020	<0.00020
Dissolved Tin (Sn)	mg/L	<0.0010	<0.0010	<0.0010
Dissolved Titanium (Ti)	mg/L	<0.0010	<0.0010	<0.0010
Dissolved Uranium (U)	mg/L	0.00063	0.00033	0.00031
Dissolved Vanadium (V)	mg/L	<0.0010	<0.0010	<0.0010
Dissolved Zinc (Zn)	mg/L	0.034	0.041	0.035
Hardness Estimated*	mg/L	193	227	227



**Table B.3.4.** The concentrations of total metals in untreated municipal WWTP (Plant B) primary (after biological nutrient removal [BNR]), secondary (after secondary clarifier), and tertiary (after UV disinfection) effluents.

Parameter	Unit	Primary Effluent (Post-BNR)	Secondary Effluent (Post-Secondary Clarifier)	Tertiary Effluent (Post-UV)
Total Cadmium (Cd)	ug/L	0.15	0.089	0.026
Total Aluminum (Al)	mg/L	0.82	0.17	0.044
Total Antimony (Sb)	mg/L	0.00067	<0.00060	0.00063
Total Arsenic (As)	mg/L	0.0011	0.00073	0.00051
Total Barium (Ba)	mg/L	0.059	0.049	0.042
Total Beryllium (Be)	mg/L	<0.0010	<0.0010	<0.0010
Total Boron (B)	mg/L	0.24	0.20	0.19
Total Calcium (Ca)	mg/L	51	54	61
Total Chromium (Cr)	mg/L	0.0022	0.0020	<0.0010
Total Cobalt (Co)	mg/L	0.0013	0.00095	0.00092
Total Copper (Cu)	mg/L	0.032	0.012	0.0027
Total Iron (Fe)	mg/L	1.0	0.39	0.093
Total Lead (Pb)	mg/L	0.0029	0.00065	0.00028
Total Lithium (Li)	mg/L	<0.020	0.023	0.024
Total Magnesium (Mg)	mg/L	16	17	19
Total Manganese (Mn)	mg/L	0.11	0.14	0.10
Total Molybdenum (Mo)	mg/L	0.015	0.017	0.018
Total Nickel (Ni)	mg/L	0.0086	0.0049	0.0045
Total Phosphorus (P)	mg/L	4.9	1.5	0.27
Total Potassium (K)	mg/L	14	14	15
Total Selenium (Se)	mg/L	0.00092	0.00058	<0.00020
Total Silicon (Si)	mg/L	3.5	2.9	2.8
Total Silver (Ag)	mg/L	0.00019	0.00016	<0.00010
Total Sodium (Na)	mg/L	63	71	75
Total Strontium (Sr)	mg/L	0.39	0.43	0.46
Total Sulphur (S)	mg/L	31	39	39
Total Thallium (Tl)	mg/L	<0.00020	<0.00020	<0.00020
Total Tin (Sn)	mg/L	0.0013	0.0013	<0.0010
Total Titanium (Ti)	mg/L	0.026	0.0051	<0.0010
Total Uranium (U)	mg/L	0.00084	0.00070	0.00034
Total Vanadium (V)	mg/L	0.0013	<0.0010	<0.0010
Total Zinc (Zn)	mg/L	0.089	0.054	0.038

**Table B.3.5.** Additional water quality parameters measured in untreated municipal WWTP (Plant B) primary (after biological nutrient removal [BNR]), secondary (after secondary clarifier), and tertiary (after UV disinfection) effluents.

Parameter	Unit	Primary Effluent (Post-BNR)	Secondary Effluent (Post-Secondary Clarifier)	Tertiary Effluent (Post-UV)
Total Organic Carbon (C)	mg/L	44	11	9.4
Dissolved Organic Carbon (C)	mg/L	22	11	8.3
Alkalinity (PP as CaCO <sub>3</sub> )	mg/L	<1.0	<1.0	<1.0
Bicarbonate (HCO <sub>3</sub> )	mg/L	290	170	170
Carbonate (CO <sub>3</sub> )	mg/L	<1.0	<1.0	<1.0
Dissolved Fluoride (F)	mg/L	0.68	0.58	0.55
Hydroxide (OH)	mg/L	<1.0	<1.0	<1.0
Chloride (Cl)	mg/L	74	87	78
Sulphate (SO <sub>4</sub> )	mg/L	120	130	130
Orthophosphate (P)	mg/L	3.2	0.064	0.025
Nitrite (N)	mg/L	<0.010	0.083	0.11
Nitrate plus Nitrite (N)	mg/L	0.023	7.0	6.0
Total Kjeldahl Nitrogen (Calc)	mg/L	0.690	2.6	NA
Total Nitrogen (N)	mg/L	6.600	9.6	NA
Nitrate (N)	mg/L	0.023	6.9	5.8
Nitrate (NO <sub>3</sub> )	mg/L	0.10	31	26
Nitrite (NO <sub>2</sub> )	mg/L	<0.033	0.27	0.36
Dissolved Phosphorus (P)	mg/L	3	0.14	0.073
Total Coliform	CFU/100mL	2.7·10 <sup>7</sup>	2.8·10 <sup>4</sup>	2400

**Table B.3.6.** The concentrations of total metals in municipal WWTP (Plant B) primary (after biological nutrient removal), secondary (after secondary clarifier), and tertiary (after UV disinfection) effluents after treatment with 50 g/L CBR and post-treatment neutralization with acetic acid.

Parameter	Unit	Primary Effluent + 50 g/L CBR	Secondary Effluent + 50 g/L CBR	Tertiary Effluent + 50 g/L CBR
Total Cadmium (Cd)	ug/L	0.021	0.026	0.024
Total Aluminum (Al)	mg/L	4.9	6.1	7.3
Total Antimony (Sb)	mg/L	0.0095	0.0070	0.0071
Total Arsenic (As)	mg/L	0.0089	0.0066	0.0076
Total Barium (Ba)	mg/L	<0.010	<0.010	<0.010
Total Beryllium (Be)	mg/L	<0.0010	<0.0010	<0.0010
Total Boron (B)	mg/L	0.88	0.74	0.75
Total Calcium (Ca)	mg/L	160	180	180
Total Chromium (Cr)	mg/L	0.018	0.010	0.019
Total Cobalt (Co)	mg/L	0.00030	<0.00030	<0.00030
Total Copper (Cu)	mg/L	0.0021	<0.0010	0.0016
Total Iron (Fe)	mg/L	8.7	4.2	7.9
Total Lead (Pb)	mg/L	0.0020	0.0014	0.0019
Total Lithium (Li)	mg/L	<0.020	<0.020	<0.020
Total Magnesium (Mg)	mg/L	1.6	0.56	0.56
Total Manganese (Mn)	mg/L	<0.0040	<0.0040	<0.0040
Total Molybdenum (Mo)	mg/L	0.093	0.098	0.097
Total Nickel (Ni)	mg/L	0.0030	0.0016	0.0018
Total Phosphorus (P)	mg/L	0.12	<0.10	<0.10
Total Potassium (K)	mg/L	5.8	6.2	6.1
Total Selenium (Se)	mg/L	0.011	0.016	0.017
Total Silicon (Si)	mg/L	3.4	2.1	3.2
Total Silver (Ag)	mg/L	<0.00010	<0.00010	<0.00010
Total Sodium (Na)	mg/L	270	260	260
Total Strontium (Sr)	mg/L	0.15	0.17	0.18
Total Sulphur (S)	mg/L	70	70	71
Total Thallium (Tl)	mg/L	<0.00020	<0.00020	<0.00020
Total Tin (Sn)	mg/L	<0.0010	<0.0010	0.0010
Total Titanium (Ti)	mg/L	0.47	0.19	0.40
Total Uranium (U)	mg/L	0.00040	0.00025	0.00031
Total Vanadium (V)	mg/L	0.046	0.031	0.040
Total Zinc (Zn)	mg/L	<0.0030	<0.0030	<0.0030

**Table B.3.7.** Additional water quality parameters measured in municipal WWTP (Plant B) primary (after biological nutrient removal), secondary (after secondary clarifier), and tertiary (after UV disinfection) effluents after treatment with 50 g/L CBR and post-treatment neutralization with acetic acid.

Parameter	Unit	Primary Effluent + 50 g/L CBR	Secondary Effluent + 50 g/L CBR	Tertiary Effluent + 50 g/L CBR
Total Organic Carbon (C)	mg/L	350	340	42
Dissolved Organic Carbon (C)	mg/L	350	66	330
Alkalinity (PP as CaCO <sub>3</sub> )	mg/L	<1.0	<1.0	<1.0
Bicarbonate (HCO <sub>3</sub> )	mg/L	540	510	530
Carbonate (CO <sub>3</sub> )	mg/L	<1.0	<1.0	<1.0
Dissolved Fluoride (F)	mg/L	3.9	4.6	4.6
Hydroxide (OH)	mg/L	<1.0	<1.0	<1.0
Chloride (Cl)	mg/L	100	100	110
Sulphate (SO <sub>4</sub> )	mg/L	170	180	180
Orthophosphate (P)	mg/L	0.0032	<0.0030	<0.0030
Nitrite (N)	mg/L	<0.010	0.061	0.069
Nitrate plus Nitrite (N)	mg/L	0.014	5.7	4.6
Total Total Kjeldahl Nitrogen (Calc)	mg/L	1.42	0.21	0.94
Total Nitrogen (N)	mg/L	1.4	5.9	5.6
Nitrate (N)	mg/L	0.014	5.7	4.6
Nitrate (NO <sub>3</sub> )	mg/L	0.061	25	20
Nitrite (NO <sub>2</sub> )	mg/L	<0.033	0.20	0.23
Dissolved Phosphorus (P)	mg/L	0.032	0.013	0.0035
Total Coliform	CFU/100mL	52	<10	<10

**Table B.3.8.** The concentrations of total metals in municipal WWTP (Plant B) primary (after biological nutrient removal), secondary (after secondary clarifier), and tertiary (after UV disinfection) effluents after treatment with 100 g/L CBR and post-treatment neutralization with acetic acid.

Parameter	Unit	Primary Effluent + 100 g/L CBR	Secondary Effluent + 100 g/L CBR	Tertiary Effluent + 100 g/L CBR
Total Cadmium (Cd)	ug/L	0.035	0.040	0.036
Total Aluminum (Al)	mg/L	7.5	14	13
Total Antimony (Sb)	mg/L	0.0071	0.0040	0.0060
Total Arsenic (As)	mg/L	0.013	0.012	0.012
Total Barium (Ba)	mg/L	0.019	0.015	0.017
Total Beryllium (Be)	mg/L	<0.0010	<0.0010	<0.0010
Total Boron (B)	mg/L	1.1	0.92	0.97
Total Calcium (Ca)	mg/L	350	370	350
Total Chromium (Cr)	mg/L	0.018	0.014	0.031
Total Cobalt (Co)	mg/L	0.00036	<0.00030	<0.00030
Total Copper (Cu)	mg/L	0.0011	<0.0010	<0.0010
Total Iron (Fe)	mg/L	8.2	6.1	15
Total Lead (Pb)	mg/L	0.0015	0.0018	0.0026
Total Lithium (Li)	mg/L	<0.020	<0.020	<0.020
Total Magnesium (Mg)	mg/L	0.99	0.54	0.57
Total Manganese (Mn)	mg/L	<0.0040	<0.0040	<0.0040
Total Molybdenum (Mo)	mg/L	0.16	0.18	0.16
Total Nickel (Ni)	mg/L	0.0023	0.0015	0.0015
Total Phosphorus (P)	mg/L	0.13	<0.10	<0.10
Total Potassium (K)	mg/L	5.9	6.4	5.7
Total Selenium (Se)	mg/L	0.027	0.018	0.023
Total Silicon (Si)	mg/L	3.2	3.0	4.9
Total Silver (Ag)	mg/L	<0.00010	<0.00010	<0.00010
Total Sodium (Na)	mg/L	430	450	410
Total Strontium (Sr)	mg/L	0.25	0.25	0.25
Total Sulphur (S)	mg/L	88	91	89
Total Thallium (Tl)	mg/L	<0.00020	<0.00020	<0.00020
Total Tin (Sn)	mg/L	<0.0010	<0.0010	0.0010
Total Titanium (Ti)	mg/L	0.34	0.30	0.75
Total Uranium (U)	mg/L	0.00017	0.00014	0.00029
Total Vanadium (V)	mg/L	0.044	0.045	0.061
Total Zinc (Zn)	mg/L	<0.0030	<0.0030	<0.0030

**Table B.3.9.** Additional water quality parameters measured in municipal WWTP (Plant B) primary (after biological nutrient removal), secondary (after secondary clarifier), and tertiary (after UV disinfection) effluents after treatment with 100 g/L CBR and post-treatment neutralization with acetic acid.

Parameter	Unit	Primary Effluent + 100 g/L CBR	Secondary Effluent + 100 g/L CBR	Tertiary Effluent + 100 g/L CBR
Total Organic Carbon (C)	mg/L	530	610	640
Dissolved Organic Carbon (C)	mg/L	620	65	810
Alkalinity (PP as CaCO <sub>3</sub> )	mg/L	2.4	<1.0	<1.0
Bicarbonate (HCO <sub>3</sub> )	mg/L	1100	1200	1300
Carbonate (CO <sub>3</sub> )	mg/L	2.9	<1.0	<1.0
Dissolved Fluoride (F)	mg/L	6.4	5.8	4.8
Hydroxide (OH)	mg/L	<1.0	<1.0	<1.0
Chloride (Cl)	mg/L	130	130	130
Sulphate (SO <sub>4</sub> )	mg/L	200	210	210
Orthophosphate (P)	mg/L	<0.0030	<0.0030	<0.0030
Nitrite (N)	mg/L	<0.010	0.053	0.067
Nitrate plus Nitrite (N)	mg/L	<0.010	4.5	4.2
Total Total Kjeldahl Nitrogen (Calc)	mg/L	0.33	1.44	0.84
Total Nitrogen (N)	mg/L	0.33	5.9	5
Nitrate (N)	mg/L	<0.010	4.4	4.1
Nitrate (NO <sub>3</sub> )	mg/L	<0.044	20	18
Nitrite (NO <sub>2</sub> )	mg/L	<0.033	0.17	0.22
Dissolved Phosphorus (P)	mg/L	0.091	0.011	0.0057
Total Coliform	CFU/100mL	<10	<10	<10

## Appendix B.4. CCME Guidelines and AEP Discharge Compliance for Different Samples

**Table B.4.1.** Long-term and short-term guidelines for the protection of freshwater aquatic life for OSPW and diluted municipal WWTP effluent (5% tertiary effluent + 95% river water) before and after the treatment with 50 g/L of CBR (without neutralization). The guidelines were either directly obtained or calculated based on the hardness, pH, DOC, and temperature (assuming at 20°C) of the sample following the equations provided [44]. NA = not available. NC = not calculated because the sample pH was outside the suggested applicable range of the equation. \*: above this concentration hyper-eutrophic conditions might be triggered [44].

CCME Guidelines	Units	OSPW		OSPW+50g/L CBR		Diluted Effluent		Diluted Effluent + 50g/L CBR	
		Long-term	Short-term	Long-term	Short-term	Long-term	Short-term	Long-term	Short-term
<b>Metals</b>									
Cadmium (Cd)	ug/L	0.3	4.6	0.37	7.7	0.23	3.3	0.37	7.7
Aluminum (Al)	ug/L	100	NA	100	NA	100	NA	100	NA
Antimony (Sb)	ug/L	NA	NA	NA	NA	NA	NA	NA	NA
Arsenic (As)	ug/L	5	NA	5	NA	5	NA	5	NA
Barium (Ba)	ug/L	NA	NA	NA	NA	NA	NA	NA	NA
Beryllium (Be)	ug/L	NA	NA	NA	NA	NA	NA	NA	NA
Boron (B)	ug/L	1500	29000	1500	29000	1500	29000	1500	29000
Calcium (Ca)	ug/L	NA	NA	NA	NA	NA	NA	NA	NA
Chromium (Cr)	ug/L	NA	NA	NA	NA	NA	NA	NA	NA
Cobalt (Co)	ug/L	NA	NA	NA	NA	NA	NA	NA	NA
Copper (Cu)	ug/L	4	NA	4	NA	3.5	NA	4	NA
Iron (Fe)	ug/L	300	NA	300	NA	300	NA	300	NA
Lead (Pb)	ug/L	7	NA	7	NA	5.71	NA	7	NA
Lithium (Li)	ug/L	NA	NA	NA	NA	NA	NA	NA	NA
Magnesium (Mg)	ug/L	NA	NA	NA	NA	NA	NA	NA	NA
Manganese (Mn)	ug/L	560	13089	140	14881	260	9962	150	14881
Molybdenum (Mo)	ug/L	73	NA	73	NA	73	NA	73	NA
Nickel (Ni)	ug/L	150	NA	150	NA	135.49	NA	150	NA
Phosphorus (P)	ug/L	100*	NA	100*	NA	100*	NA	100*	NA
Potassium (K)	ug/L	NA	NA	NA	NA	NA	NA	NA	NA
Selenium (Se)	ug/L	1	NA	1	NA	1	NA	1	NA
Silicon (Si)	ug/L	NA	NA	NA	NA	NA	NA	NA	NA
Silver (Ag)	ug/L	0.25	NA	0.25	NA	0.25	NA	0.25	NA
Sodium (Na)	ug/L	NA	NA	NA	NA	NA	NA	NA	NA
Strontium (Sr)	ug/L	NA	NA	NA	NA	NA	NA	NA	NA
Sulphur (S)	ug/L	NA	NA	NA	NA	NA	NA	NA	NA
Thallium (Tl)	ug/L	0.8	NA	0.8	NA	0.8	NA	0.8	NA
Tin (Sn)	ug/L	NA	NA	NA	NA	NA	NA	NA	NA
Titanium (Ti)	ug/L	NA	NA	NA	NA	NA	NA	NA	NA
Uranium (U)	ug/L	15	33	15	33	15	33	15	33
Vanadium (V)	ug/L	NA	NA	NA	NA	NA	NA	NA	NA
Zinc (Zn)	ug/L	106	306	NC	NC	21	132	NC	NC
<b>Anions</b>									
Fluoride (F)	ug/L	120	NA	120	NA	120	NA	120	NA
Chloride (Cl)	mg/L	120	640	120	640	120	640	120	640
Sulphate (SO4)	mg/L	NA	NA	NA	NA	NA	NA	NA	NA
<b>Organics</b>									
Dissolved Organic Carbon (DOC)	mg/L	NA	NA	NA	NA	NA	NA	NA	NA
<b>Nutrients</b>									
Dissolved Ammonia (N)	mg/L	0.499	NA	0.024	NA	0.499	NA	0.024	NA
Orthophosphate (P)	mg/L	NA	NA	NA	NA	NA	NA	NA	NA
<b>General Parameters</b>									
Hardness	mg/L	NA	NA	NA	NA	NA	NA	NA	NA
pH		6.5-9.0	NA	6.5-9.0	NA	6.5-9.0	NA	6.5-9.0	NA

**Table B.4.2.** Long-term and short-term guidelines for the protection of freshwater aquatic life for four Milli Q ultrapure water samples treated with (1) 50 g/L CBR (2) 50 g/L raw bauxite residue (3) 50 g/L CBR and pre-treatment neutralization with acetic acid (4) 50 g/L CBR and post-treatment neutralization with acetic acid. The guidelines were either directly obtained or calculated based on the hardness, pH, DOC, and temperature (assuming at 20°C) of the sample following the equations provided [44]. NA = not available. NC = not calculated because the sample pH was outside the suggested applicable range of the equation. \*: above this concentration hyper-eutrophic conditions might be triggered [44].

Parameters	Units	Ultrapure Water + 50 g/L CBR (1)		Ultrapure Water + 50 g/L Raw Bauxite Residue (2)		Pre-treatment Neutralization (3)		Post-treatment Neutralization (4)	
		Long-term	Short-term	Long-term	Short-term	Long-term	Short-term	Long-term	Short-term
<b>Metals</b>									
Cadmium (Cd)	ug/L	0.37	7.7	0.37	7.6	0.37	7.7	0.37	7.7
Aluminum (Al)	ug/L	100	NA	100	NA	100	NA	100	NA
Antimony (Sb)	ug/L	NA	NA	NA	NA	NA	NA	NA	NA
Arsenic (As)	ug/L	5	NA	5	NA	5	NA	5	NA
Barium (Ba)	ug/L	NA	NA	NA	NA	NA	NA	NA	NA
Beryllium (Be)	ug/L	NA	NA	NA	NA	NA	NA	NA	NA
Boron (B)	ug/L	1500	29000	1500	29000	1500	29000	1500	29000
Calcium (Ca)	ug/L	NA	NA	NA	NA	NA	NA	NA	NA
Chromium (Cr)	ug/L	NA	NA	NA	NA	NA	NA	NA	NA
Cobalt (Co)	ug/L	NA	NA	NA	NA	NA	NA	NA	NA
Copper (Cu)	ug/L	4	NA	4	NA	4	NA	4	NA
Iron (Fe)	ug/L	300	NA	300	NA	300	NA	300	NA
Lead (Pb)	ug/L	7	NA	7	NA	7	NA	7	NA
Lithium (Li)	ug/L	NA	NA	NA	NA	NA	NA	NA	NA
Magnesium (Mg)	ug/L	NA	NA	NA	NA	NA	NA	NA	NA
Manganese (Mn)	ug/L	150	14881	140	280	150	14881	1400	14881
Molybdenum (Mo)	ug/L	73	NA	73	NA	73	NA	73	NA
Nickel (Ni)	ug/L	150	NA	150	NA	150	NA	150	NA
Phosphorus (P)	ug/L	100*	NA	100*	NA	100*	NA	100*	NA
Potassium (K)	ug/L	NA	NA	NA	NA	NA	NA	NA	NA
Selenium (Se)	ug/L	1	NA	1	NA	1	NA	1	NA
Silicon (Si)	ug/L	NA	NA	NA	NA	NA	NA	NA	NA
Silver (Ag)	ug/L	0.25	NA	0.25	NA	0.25	NA	0.25	NA
Sodium (Na)	ug/L	NA	NA	NA	NA	NA	NA	NA	NA
Strontium (Sr)	ug/L	NA	NA	NA	NA	NA	NA	NA	NA
Sulphur (S)	ug/L	NA	NA	NA	NA	NA	NA	NA	NA
Thallium (Tl)	ug/L	0.8	NA	0.8	NA	0.8	NA	0.8	NA
Tin (Sn)	ug/L	NA	NA	NA	NA	NA	NA	NA	NA
Titanium (Ti)	ug/L	NA	NA	NA	NA	NA	NA	NA	NA
Uranium (U)	ug/L	15	33	15	33	15	33	15	33
Vanadium (V)	ug/L	NA	NA	NA	NA	NA	NA	NA	NA
Zinc (Zn)	ug/L	NC	NC	NC	NC	NC	NC	NC	NC
<b>Anions</b>									
Fluoride (F)	ug/L	120	NA	120	NA	120	NA	120	NA
Chloride (Cl)	mg/L	120	640	120	640	120	640	120	640
Sulphate (SO4)	mg/L	NA	NA	NA	NA	NA	NA	NA	NA
<b>General Parameters</b>									
Hardness	mg/L	NA	NA	NA	NA	NA	NA	NA	NA
pH		6.5-9.0	NA	6.5-9.0	NA	6.5-9.0	NA	6.5-9.0	NA



**Table B.4.3.** The requirement for continuous discharge, applicable to tertiary treatment with mechanical processes for a current population > 20,000 by AEP [84]. CBOD = carbonaceous biochemical oxygen demand at 5 days and 20°C. \*These limits were taken from the approval to operate from a local wastewater treatment plant with tertiary treatment processes. The ammonia-N was the limit for June to November.

Parameters	Requirement
CBOD	< 20 mg/L
Total Suspended Solids (TSS)	< 20 mg/L
Total Phosphorus (TP)	< 1 mg/L
Ammonia-N	<5 mg/L*
Fecal Coliform	<200/100mL
pH	6.5-8.5*

**Table B.4.4.** Long-term and short-term guidelines for the protection of freshwater aquatic life for untreated municipal WWTP primary (after biological nutrient removal), secondary (after secondary clarifier), and tertiary (after UV disinfection) effluents. The guidelines were either directly obtained or calculated based on the hardness, pH, DOC, and temperature (assuming at 20°C) of the sample following the equations provided [44]. NA = not available. NC = not calculated because the sample pH was outside the suggested applicable range of the equation. \*: above this concentration hyper-eutrophic conditions might be triggered [44].

Metals	Units	Primary Effluent		Secondary Effluent		Tertiary Effluent	
		Long-term	Short-term	Long-term	Short-term	Long-term	Short-term
Cadmium (Cd)	ug/L	0.27	4.1	0.31	4.8	0.31	4.8
Aluminum (Al)	ug/L	100	NA	100	NA	100	NA
Antimony (Sb)	ug/L	NA	NA	NA	NA	NA	NA
Arsenic (As)	ug/L	5	NA	5	NA	5	NA
Barium (Ba)	ug/L	NA	NA	NA	NA	NA	NA
Beryllium (Be)	ug/L	NA	NA	NA	NA	NA	NA
Boron (B)	ug/L	1500	29000	1500	29000	1500	29000
Calcium (Ca)	ug/L	NA	NA	NA	NA	NA	NA
Chromium (Cr)	ug/L	NA	NA	NA	NA	NA	NA
Cobalt (Co)	ug/L	NA	NA	NA	NA	NA	NA
Copper (Cu)	ug/L	4	NA	4	NA	4	NA
Iron (Fe)	ug/L	300	NA	300	NA	300	NA
Lead (Pb)	ug/L	7	NA	7	NA	7	NA
Lithium (Li)	ug/L	NA	NA	NA	NA	NA	NA
Magnesium (Mg)	ug/L	NA	NA	NA	NA	NA	NA
Manganese (Mn)	ug/L	620	11857	760	13672	640	13672
Molybdenum (Mo)	ug/L	73	NA	73	NA	73	NA
Nickel (Ni)	ug/L	150	NA	150	NA	150	NA
Phosphorus (P)	ug/L	100*	NA	100*	NA	100*	NA
Potassium (K)	ug/L	NA	NA	NA	NA	NA	NA
Selenium (Se)	ug/L	1	NA	1	NA	1	NA
Silicon (Si)	ug/L	NA	NA	NA	NA	NA	NA
Silver (Ag)	ug/L	0.25	NA	0.25	NA	0.25	NA
Sodium (Na)	ug/L	NA	NA	NA	NA	NA	NA
Strontium (Sr)	ug/L	NA	NA	NA	NA	NA	NA
Sulphur (S)	ug/L	NA	NA	NA	NA	NA	NA
Thallium (Tl)	ug/L	0.8	NA	0.8	NA	0.8	NA
Tin (Sn)	ug/L	NA	NA	NA	NA	NA	NA
Titanium (Ti)	ug/L	NA	NA	NA	NA	NA	NA
Uranium (U)	ug/L	15	33	15	33	15	33
Vanadium (V)	ug/L	NA	NA	NA	NA	NA	NA
Zinc (Zn)	ug/L	120	NC	133	275	100	257

**Table B.4.5.** Long-term and short-term guidelines for the protection of freshwater aquatic life for municipal WWTP primary (after biological nutrient removal), secondary (after secondary clarifier), and tertiary (after UV disinfection) effluents after treatment with 50 g/L CBR and post-treatment neutralization with acetic acid. The guidelines were either directly obtained or calculated based on the hardness, pH, DOC, and temperature (assuming at 20°C) of the sample following the equations provided [44]. NA = not available. NC = not calculated because the sample pH was outside the suggested applicable range of the equation. \*: above this concentration hyper-eutrophic conditions might be triggered [44].

Metals	Units	Primary Effluent + 50g/L CBR		Secondary Effluent + 50 g/L CBR		Tertiary Effluent + 50 g/L CBR	
		Long-term	Short-term	Long-term	Short-term	Long-term	Short-term
Cadmium (Cd)	ug/L	0.37	7.7	0.37	7.7	0.37	7.7
Aluminum (Al)	ug/L	100	NA	100	NA	100	NA
Antimony (Sb)	ug/L	NA	NA	NA	NA	NA	NA
Arsenic (As)	ug/L	5	NA	5	NA	5	NA
Barium (Ba)	ug/L	NA	NA	NA	NA	NA	NA
Beryllium (Be)	ug/L	NA	NA	NA	NA	NA	NA
Boron (B)	ug/L	1500	29000	1500	29000	1500	29000
Calcium (Ca)	ug/L	NA	NA	NA	NA	NA	NA
Chromium (Cr)	ug/L	NA	NA	NA	NA	NA	NA
Cobalt (Co)	ug/L	NA	NA	NA	NA	NA	NA
Copper (Cu)	ug/L	4	NA	4	NA	4	NA
Iron (Fe)	ug/L	300	NA	300	NA	300	NA
Lead (Pb)	ug/L	7	NA	7	NA	7	NA
Lithium (Li)	ug/L	NA	NA	NA	NA	NA	NA
Magnesium (Mg)	ug/L	NA	NA	NA	NA	NA	NA
Manganese (Mn)	ug/L	460	14881	300	14881	300	14881
Molybdenum (Mo)	ug/L	73	NA	73	NA	73	NA
Nickel (Ni)	ug/L	150	NA	150	NA	150	NA
Phosphorus (P)	ug/L	100*	NA	100*	NA	100*	NA
Potassium (K)	ug/L	NA	NA	NA	NA	NA	NA
Selenium (Se)	ug/L	1	NA	1	NA	1	NA
Silicon (Si)	ug/L	NA	NA	NA	NA	NA	NA
Silver (Ag)	ug/L	0.25	NA	0.25	NA	0.25	NA
Sodium (Na)	ug/L	NA	NA	NA	NA	NA	NA
Strontium (Sr)	ug/L	NA	NA	NA	NA	NA	NA
Sulphur (S)	ug/L	NA	NA	NA	NA	NA	NA
Thallium (Tl)	ug/L	0.8	NA	0.8	NA	0.8	NA
Tin (Sn)	ug/L	NA	NA	NA	NA	NA	NA
Titanium (Ti)	ug/L	NA	NA	NA	NA	NA	NA
Uranium (U)	ug/L	15	33	15	33	15	33
Vanadium (V)	ug/L	NA	NA	NA	NA	NA	NA
Zinc (Zn)	ug/L	NC	NC	NC	NC	NC	NC

**Table B.4.6.** Long-term and short-term guidelines for the protection of freshwater aquatic life for untreated municipal WWTP primary (after biological nutrient removal), secondary (after secondary clarifier), and tertiary (after UV disinfection) effluents after the treatment with 100 g/L CBR and post-treatment neutralization with acetic acid. The guidelines were either directly obtained or calculated based on the hardness, pH, DOC, and temperature (assuming at 20°C) of the sample following the equations provided [44]. NA = not available. NC = not calculated because the sample pH was outside the suggested applicable range of the equation. \*: above this concentration hyper-eutrophic conditions might be triggered [44].

Metals	Units	Primary Effluent + 100 g/L CBR		Secondary Effluent + 100 g/L CBR		Tertiary Effluent + 100 g/L CBR	
		Long-term	Short-term	Long-term	Short-term	Long-term	Short-term
Cadmium (Cd)	ug/L	0.37	7.7	0.37	7.7	0.37	7.7
Aluminum (Al)	ug/L	100	NA	100	NA	100	NA
Antimony (Sb)	ug/L	NA	NA	NA	NA	NA	NA
Arsenic (As)	ug/L	5	NA	5	NA	5	NA
Barium (Ba)	ug/L	NA	NA	NA	NA	NA	NA
Beryllium (Be)	ug/L	NA	NA	NA	NA	NA	NA
Boron (B)	ug/L	1500	29000	1500	29000	1500	29000
Calcium (Ca)	ug/L	NA	NA	NA	NA	NA	NA
Chromium (Cr)	ug/L	NA	NA	NA	NA	NA	NA
Cobalt (Co)	ug/L	NA	NA	NA	NA	NA	NA
Copper (Cu)	ug/L	4	NA	4	NA	4	NA
Iron (Fe)	ug/L	300	NA	300	NA	300	NA
Lead (Pb)	ug/L	7	NA	7	NA	7	NA
Lithium (Li)	ug/L	NA	NA	NA	NA	NA	NA
Magnesium (Mg)	ug/L	NA	NA	NA	NA	NA	NA
Manganese (Mn)	ug/L	320	14881	320	14881	520	14881
Molybdenum (Mo)	ug/L	73	NA	73	NA	73	NA
Nickel (Ni)	ug/L	150	NA	150	NA	150	NA
Phosphorus (P)	ug/L	100*	NA	100*	NA	100*	NA
Potassium (K)	ug/L	NA	NA	NA	NA	NA	NA
Selenium (Se)	ug/L	1	NA	1	NA	1	NA
Silicon (Si)	ug/L	NA	NA	NA	NA	NA	NA
Silver (Ag)	ug/L	0.25	NA	0.25	NA	0.25	NA
Sodium (Na)	ug/L	NA	NA	NA	NA	NA	NA
Strontium (Sr)	ug/L	NA	NA	NA	NA	NA	NA
Sulphur (S)	ug/L	NA	NA	NA	NA	NA	NA
Thallium (Tl)	ug/L	0.8	NA	0.8	NA	0.8	NA
Tin (Sn)	ug/L	NA	NA	NA	NA	NA	NA
Titanium (Ti)	ug/L	NA	NA	NA	NA	NA	NA
Uranium (U)	ug/L	15	33	15	33	15	33
Vanadium (V)	ug/L	NA	NA	NA	NA	NA	NA
Zinc (Zn)	ug/L	NC	NC	NC	NC	NC	NC

## Appendix B.5 Visual Quality of the Treatment of Tertiary Effluent by CBR

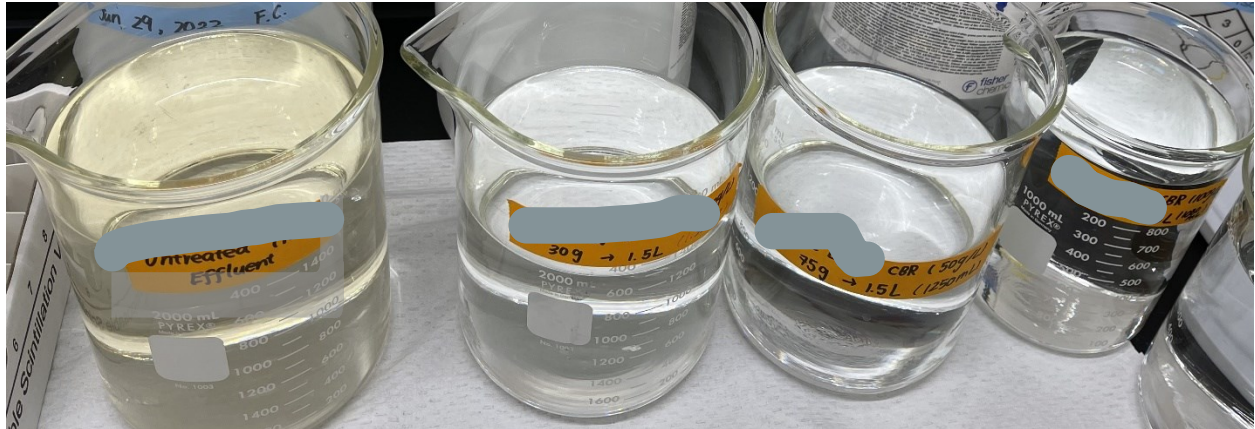


**Figure B.5.1.** From left to right: filtered untreated municipal WWTP tertiary effluent, filtered 20g/L-, 50g/L-, and 100g/L-CBR-treated municipal WWTP tertiary effluent.

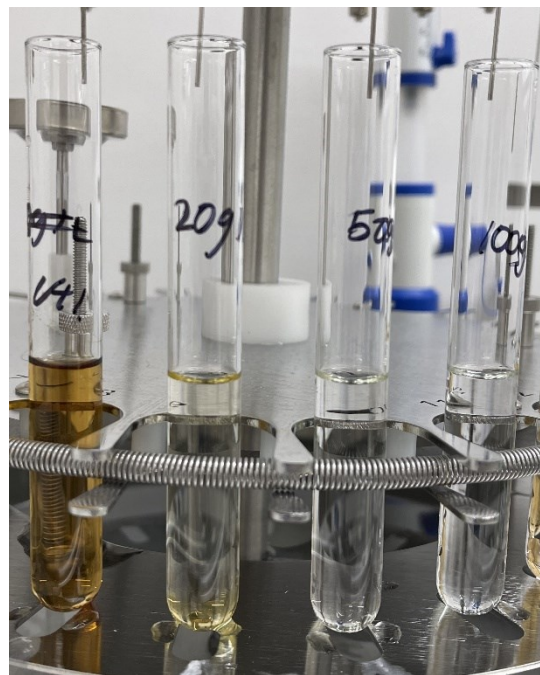


**Figure B.5.2.** From left to right: the SPE extracts of untreated, 20g/L-CBR-treated, 50g/L-CBR-treated, and 100g/L-CBR-treated municipal WWTP effluents.